



UNIVERSITÀ
DEGLI STUDI
DI PADOVA

Sede Amministrativa: Università degli Studi di Padova

Dipartimento di Dipartimento di Medicina animale, produzioni e salute (MAPS)

CORSO DI DOTTORATO DI RICERCA IN SCIENZE VETERINARIE
E SICUREZZA ALIMENTARE

CICLO XXXVI

Challenges in veterinary molecular diagnosis

Tesi redatta con il contributo finanziario dell'Istituto Zooprofilattico Sperimentale delle Venezie

Coordinatore: Ch.mo Prof. Mattia Cecchinato

Supervisore: Ch.mo Prof. Mattia Cecchinato

Dottorando: Fortin Andrea

Summary

CHAPTER 1:	3
INTRODUCTION	
CHAPTER 2:	9
AIM OF THE THESIS	
CHAPTER 3:	11
REDESIGN AND VALIDATION OF A REAL-TIME RT-PCR TO IMPROVE SURVEILLANCE FOR AVIAN INFLUENZA VIRUSES OF THE H9 SUBTYPE	
CHAPTER 4:	26
EFFECT OF ASSAY CHOICE, VIRAL CONCENTRATION AND OPERATOR INTERPRETATION ON INFECTIOUS BRONCHITIS VIRUS DETECTION AND CHARACTERIZATION	
CHAPTER 5:	36
A NOVEL ARRAY OF REAL-TIME RT-PCR ASSAYS FOR THE RAPID PATHOTYPING OF TYPE I AVIAN PARAMYXOVIRUS (APMV-1)	
CHAPTER 6:	56
GENERAL CONCLUSIONS	
CHAPTER 7:	60
REFERENCES	

CHAPTER 1:

INTRODUCTION

The poultry industry has experienced significant growth in the past decade, making it one of the world's major protein suppliers (European Parliament. Directorate General for Parliamentary Research Services., 2019; “FAOSTAT,” 2023). This expansion has resulted in an increased number of farms and higher animal density, which raise the likelihood of interactions between poultry and wild birds. Such interactions can lead to the spillover of pathogens from wild birds to poultry and vice versa (Plowright et al., 2017; Rohaim et al., 2017).

The elevated density and close proximity of susceptible hosts in these settings create favourable conditions for the transmission of pathogens, contributing to the spread of diseases (Hochachka and Dhondt, 2000; Gilbert et al., 2017).

Indeed, recent years have seen an increase in the incidence and distribution of World Organisation for Animal Health (WOAH) reportable pathogens.

To effectively monitor the circulation trends of these pathogens, veterinary health authorities have embraced advanced and efficient systems, aiming to enhance productivity and poultry health for enabling a precise and accurate monitoring, which provides timely information on pathogen prevalence and distribution. By adopting faster and more efficient technologies, authorities can promptly respond to emerging challenges and take proactive measures to safeguard poultry health and welfare.

To help this process of reliable method sharing, WOAH groups in part 3 of its Manual of Diagnostic Tests and Vaccines for Terrestrial Animals all the listed diseases, i.e. very serious and rapidly spreading diseases to which every state should pay attention. For each disease, the manual collects all the most robust and widespread methods for diagnosis divided by purpose, including both classical virology methods (e.g. viral isolation, serum neutralisation) and molecular methods.

Indeed, for many years, pathogen screening and characterisation techniques heavily relied on live matrices. These methods included isolation in embryonated eggs or specific cell cultures, as well as immunological techniques like enzyme-linked immunosorbent assay (ELISA) and haemagglutination inhibition (HI). These traditional approaches played a crucial role in the identification and categorization of various pathogens.

In the context of avian influenza virus or Newcastle disease virus, another commonly employed technique was the experimental infection of laboratory animals, followed by the observation of symptoms and disease progression over a specific period of time. This approach allowed researchers to assess the pathogenicity of these viruses and gain insights into their virulence and impact on the host.

The use of live matrices and animal experiments provided valuable data that contributed to a comprehensive understanding of different pathogens, enabling scientists to identify and classify various strains. These methods have been pivotal in building a foundation of knowledge about pathogens that has paved the way for further research and the development of more advanced diagnostic techniques.

Although valuable, they also had limitations. They often required considerable time, resources, and skilled personnel, making them less suitable for rapid and large-scale screening. Additionally, some of these techniques involved using animals for experimentation, which raised ethical concerns.

The systems that, at the current state of the art, have proven to be the most suitable for meeting demands for speed and accuracy are biotechnology-based methods. Indeed, these methods are faster than classical methods because they are based on the identification and characterisation of nucleic acids and do not require a live matrix, making them also more ethically sustainable.

The amplification of the pathogen target required for its identification or characterization does not take place within a living organism (eggs, cells, etc.), but rather through the principle of polymerase chain reaction (PCR), which allows exponential amplification of the target nucleotide material. This process involves the use of a DNA polymerase enzyme to carry out DNA replication *in vitro*; passing through the denaturation step that opens the double helix and makes the DNA accessible, the primer annealing step that circumscribes the target area of amplification, and the step of synthesizing the new DNA strand complementary to the previous one (Waters and Shapter, 2014).

The presence of the amplified fragment of interest can be detected in several ways, with the most commonly used methods being electrophoresis and fluorescence detection. Electrophoresis is based on the distinction of the amplified fragments according to their size, separated by a branched polymer (acrylamide, agarose) and made visible with the use of a fluorescent intercalating agent. On the other hand, fluorescence detection uses molecules (antibodies or oligo nucleotides) that specifically bind to the amplified zone and are visible because they are tagged by

fluorophores. In both cases, a signal will only be obtained if the target nucleic acid is present in the analysed sample.

This system is so efficient in amplifying the signal given by the target that it makes molecular methods extremely sensitive, allowing the identification of the pathogen even if there are a few dozen specimens, a quantity that is orders of magnitude less than traditional methods. By not requiring *in vivo* steps, molecular methods have also the advantage of reducing human effort compared to traditional methods.

For these reasons, diagnostics using bimolecular techniques has a higher throughput than traditional ones, and this feature can be further accentuated because these methods are very prone to automation at every stage, from nucleic acid extraction to its analysis with various available techniques (WOAH, 2021). This possibility of automation, such as the use of automated liquid handling in molecular methods, significantly reduces the probability of human error and cross-contamination, and also further reduces the time between the arrival of the samples at the laboratory and the issued result. The use of molecular diagnostic methods therefore allows laboratories to indicate the presence or absence of a given pathogen within a maximum of 24 hours from the time of the sample arrival. For traditional methods, this would be impossible due to the technical time required.

The most commonly used method is real-time PCR (rPCR). This technique involves the use of an area-specific oligo probe within the amplified fragment, in addition to the primers required for conventional PCR. The probe is usually labelled with a fluorophore at one end and a quencher at the other, different configurations are possible but in general, the fluorophore-quencher proximity prevents the probe from emitting fluorescence when it is intact. However, depending on the probe type, during the annealing and elongation phases of the PCR, the fluorophore and quencher are separated, or the DNA polymerase enzyme degrades the probe, while it binds to the target sequence. The degradation releases the fluorophore, which becomes unbound from the quencher and emits fluorescence when excited. The instrument detects the fluorescence in real time, allowing for continuous monitoring of the reaction's progress and the potential presence of the target pathogen.

The use of a fluorophore-labelled probe in real-time PCR eliminates the need for an additional detection step, as required by conventional PCR, making the process more streamlined. These characteristics allowed real-time PCR to become a very popular method for detecting pathogens, even in the veterinary field. The advantage of rapid and accurate identification of the target pathogen without the need for further manipulation after amplification, reduces the risk of contamination and reporting time,

increasing its value in diagnosing infections and monitoring disease outbreaks in the poultry industry and beyond (Hoffmann et al., 2009).

In addition to identifying the pathogen, these methods also allow its precise characterisation, because they target the genetic material of the pathogen, granting a high level of specificity. The most widespread method for obtaining the nucleotide sequences of pathogens is Sanger sequencing, which allows the nucleotide sequence of the target genetic zone to be determined following preliminary amplification by conventional PCR. Depending on how the PCR amplification is constructed, different information about the pathogen can be obtained:

- The sequence of variable zones of the pathogen's genome for detailed identification of its genotype by phylogenetic analysis of the obtained sequence (WOAH, 2023a);
- The sequence of a gene or a genetic region responsible for the degree of pathogenicity (e.g. cleavage site) (OFFLU, 2022) or embedding the peculiar characteristics of strains with known pathogenicity (WOAH, 2022a).

In both cases, the obtained sequence is compared with a database of already characterized reference sequences using specific software (e.g. BLAST), to identify the pathogen and eventually catalogue it according to its virulence characteristics, limiting the use of animals or eggs and also shortening the response time at this stage. (Crossley et al., 2020).

However, the use of nucleic acids as the target of biotechnology-based analysis methods also presents a significant risk. Nucleic acids, due to their inherent nature, are susceptible to mutation and recombination events. This variability can impact on the method's characteristics over time, especially if one of these events affects a binding site of primers or probes used for amplifying a target region, either for direct identification PCR (real-time or conventional) or for amplification before sequencing. Such an event can lead to alterations in the specificity or sensitivity of the involved methods.

For instance, the diagnosis of many avian viruses like Infectious Bronchitis (IBV), Newcastle Disease (NDV) and Avian Influenza (AI) relies on a diagnostic algorithm primarily composed of three steps: a screening method is applied first and it is often based on real-time PCR, targeting a conserved genetic segment shared among all subtypes of the same pathogen. Secondly, if the screening method detects the virus in the sample, it is followed by a conventional PCR designed on an informative segment capable of discriminating the detected virus based on pathotype or genotype (such as a

cleavage site or a hypervariable zone). Third, after verifying the successful amplification of the target segment through electrophoresis, Sanger sequencing is conducted to acquire the sequence of the target segment.

From this example, it is evident that even a seemingly concise procedure, commonly practiced in numerous laboratories, is subject to the two aforementioned challenges: During the design phase of the screening method, it is crucial to identify a well-conserved region among the subtypes to perform the screening without excessive divergence of the oligo nucleotides from the target sequences. Only a highly conserved region ensures that the method maintains consistent characteristics across different subtypes. Conversely, in the development of conventional typing PCR, the identification of a variable region among the subtypes, yet at certain extents conserved within them, is essential to obtain a uniquely identifying sequence through the sequencing of the amplified segment (WOAH, 2021).

During the implementation of this diagnostic algorithm, it becomes necessary to periodically monitor the absence of mutations in new strains in the paired regions of the used oligonucleotides. This is because two gene segments and several oligonucleotides are involved in the correct detection and identification. The use of different target genes and different oligo designs within the same diagnostic procedure, even within variable regions, increases the risk that mutations in the viral genome will alter the intended oligo-target binding. This alteration could compromise the ability of the diagnostic algorithm to accurately identify the virus for which it was designed (Kwok et al., 1990; Christopherson et al., 1997; Smith et al., 2002; Kim et al., 2006).

Another challenge with biotechnology-based methods is the requirement of trained personnel both during the test setup phase and the interpretation of obtained results, due to the need to combine multiple experiments involving different molecular techniques to achieve accurate outcomes. Furthermore, molecular diagnostic methods demand well-equipped laboratories housing costly instrumentation, such as real-time PCR platforms and Sanger sequencers (WOAH, 2023b).

The basic diagnostic algorithm described above provides a standard approach commonly used by laboratories to identify avian and non-avian pathogens. However, this procedure may not be effective for detecting simultaneous infections sustained by different subtypes of the same pathogen, since they might present a remarkable heterogeneity. While this feature is desirable and essential for highly specific methods, it also poses a major problem when it comes to the need for a broad-spectrum screening method inclusive of each type of strain belonging to a specific class of pathogens.

Within the same viral species, there can be a high nucleotide variability, as demonstrated by the 20 different genotypes in class II of Newcastle disease virus (NDV) (Dimitrov et al., 2019) or the 35 lineages of avian bronchitis virus (IBV) (Valastro et al., 2016; Houta et al., 2021).

The inclusivity of the diagnostic method is influenced by the sequence of the oligo nucleotides used for PCR protocol. Pathogens with genetic sequences that perfectly match the sequences of the oligos will be more easily identified compared to pathogens with genetic differences in the recognition zone of the oligos used in the protocol, resulting in mismatches. As a result, different methods may exhibit varying affinities for individual subtypes of the pathogen. Consequently, in cases of coexisting subtypes within the same sample, the identification of the most common or most similar subtype will be favoured.

This is especially problematic for viruses such as IBV and NDV, for which vaccination with an attenuated virus is required and routinely performed on the field. Indeed, the presence of the vaccine virus could flank a pathogenic virus that is not detected if screening and sequencing methods have a higher affinity for the attenuated vaccine virus.

Due to the potential ambivalence and limitations of biotechnology-based methods, the WOAHP manual advises diagnostic laboratories to adopt a two-pronged approach.

Firstly, the WOAHP manual recommends the preservation and continued use of well-established and stable traditional methods. These methods can serve as reliable reference standards in cases where there are doubts or uncertainties in the interpretation of results, thereby maintaining a multidisciplinary approach to pathogen identification.

Secondly, the WOAHP stresses the importance of constant monitoring, improvement and update of diagnostic techniques. This proactive approach is necessary to ensure accurate and efficient detection of various pathogens, especially in the context of highly variable viruses. Continuous research and updates in diagnostic methodologies are essential to meet the evolving challenges in the poultry industry and to promptly respond to potential disease outbreaks.

By combining the strengths of both traditional and biotechnology-based methods, while aware of their respective limitations, diagnostic laboratories can enhance their ability to effectively identify and manage infectious diseases in poultry populations. This comprehensive and adaptive approach contributes to safeguarding the welfare of the poultry industry and protecting public health.

CHAPTER 2:

AIM OF THE THESIS

This thesis presents a compilation of studies focusing on optimizing biotechnological methods for avian diagnostics. While these studies explore various avian viruses, their collective objective is to address three primary challenges inherent in biotechnology-based diagnostics.

One of these challenges involves optimizing existing methods for identifying highly prevalent and variable viruses, such as the avian influenza virus subtype H9, as addressed in the chapter 3. The continuously evolving nature of influenza viruses necessitates an ongoing monitoring process to assess the performance of current methods and requires to continually update diagnostic techniques for effectively identifying and tracking their spread.

Another critical challenge pertains to selecting the most efficient molecular biology-based method from the available options. This choice becomes more intricate for viruses that are widely distributed and are managed with various potential vaccination strategies, such as avian bronchitis virus (Chapter 4). The need for this selection of protocols is prompted by the widespread availability of biotechnology-based diagnostic methods and plays a pivotal role in minimizing the disease's impact on the poultry industry.

Furthermore, this thesis addresses the challenge of enhancing pathotyping methods for viruses of significant health importance, such as those on the WOAHA list. These methods aim to be more rapid, inclusive, and less susceptible to errors caused by co-infections. An example of such a pathogen is the Newcastle disease virus, and the paper “A novel array of real-time RT-PCR assays for the rapid pathotyping of type I avian paramyxovirus (APMV-1)” reported in chapter 5 proposes an alternative method for pathotyping to provide a more effective and timely response to outbreaks.

The thesis tackles three issues that affect all molecular biology-based methods used in avian diagnostics, using avian influenza, infectious bronchitis, and Newcastle disease viruses as recurring models. Indeed, these viruses are responsible for the three major livestock diseases worldwide.

In summary, this thesis aims to offer a comprehensive approach to address these three overarching topics concerning molecular biology-based methods and offer new tools and insights for their management, utilizing avian influenza, infectious bronchitis, and Newcastle disease viruses as illustrative models. These highly impacting viruses, serve as excellent examples of pathogens with genetic variability (AI H9), high rates of spread associated with large-scale vaccination activities resulting in long-term effects on the population (IBV), and pathogens exhibiting diverse and variable virulence (NDV).

CHAPTER 3:

REDESIGN AND VALIDATION OF A REAL-TIME RT-PCR TO IMPROVE SURVEILLANCE FOR AVIAN INFLUENZA VIRUSES OF THE H9 SUBTYPE

Panzarin, V.; Marciano, S.; Fortin, A.; Brian, I.; D'Amico, V.; Gobbo, F.;
Bonfante, F.; Palumbo, E.; Sakoda, Y.; Le, K.T.; et al.

Viruses, 2022

Article

Redesign and Validation of a Real-Time RT-PCR to Improve Surveillance for Avian Influenza Viruses of the H9 Subtype

Valentina Panzarin ^{1,*}, Sabrina Marciano ¹, Andrea Fortin ¹, Irene Brian ¹, Valeria D'Amico ¹, Federica Gobbo ¹, Francesco Bonfante ¹, Elisa Palumbo ¹, Yoshihiro Sakoda ², Kien Trung Le ², Duc-Huy Chu ³, Ismaila Shittu ⁴, Clement Meseko ⁴, Abdoul Malick Haido ⁵, Theophilus Odoom ⁶, Mame Nahé Diouf ⁷, Fidélia Djegui ⁸, Mieke Steensels ⁹, Calogero Terregino ¹ and Isabella Monne ¹

- ¹ EU/OIE/National Reference Laboratory for Avian Influenza and Newcastle Disease, FAO Reference Centre for Animal Influenza and Newcastle Disease, Division of Comparative Biomedical Sciences, Istituto Zooprofilattico Sperimentale delle Venezie (IZSVe), 35020 Legnaro, Italy; smarciano@izsvenezie.it (S.M.); afortin@izsvenezie.it (A.F.); ibrian@izsvenezie.it (I.B.); vdamico@izsvenezie.it (V.D.); fgobbo@izsvenezie.it (F.G.); fbonfante@izsvenezie.it (F.B.); epalumbo@izsvenezie.it (E.P.); cterregino@izsvenezie.it (C.T.); imonne@izsvenezie.it (I.M.)
 - ² OIE Reference Laboratory for Avian Influenza, Faculty of Veterinary Medicine, Hokkaido University, Sapporo 060-0818, Japan; sakoda@vetmed.hokudai.ac.jp (Y.S.); letrungkien16@gmail.com (K.T.L.)
 - ³ Department of Animal Health, Ministry of Agriculture and Rural Development (MARD), Hanoi 115-19, Vietnam; chuduchuy@gmail.com
 - ⁴ Regional Laboratory for Animal Influenzas and Other Transboundary Animal Diseases, National Veterinary Research Institute (NVRI), Vom 930010, Nigeria; ismaila.shittu@gmail.com (I.S.); cameseko@yahoo.com (C.M.)
 - ⁵ Laboratoire Central de l'Élevage (LABOCEL), Ministère de l'Agriculture et de l'Élevage, Niamey 485, Niger; haido.malick@yahoo.fr
 - ⁶ Accra Veterinary Laboratory, Veterinary Services Directorate, Ministry of Food & Agriculture, Accra M161, Ghana; theodoom@yahoo.com
 - ⁷ Laboratoire National de l'Élevage et de Recherches Vétérinaires (LNERV) de l'Institut Sénégalais de Recherches Agricoles (ISRA), Dakar-Hann 2057, Senegal; mamenaha.diouf@isra.sn
 - ⁸ Laboratoire de Diagnostic Vétérinaire et de Sérosurveillance (LADISERO), Parakou 23, Benin; djegui_fidelia@yahoo.fr
 - ⁹ AI/ND National Reference Laboratory, Sciensano, 1050 Brussels, Belgium; mieke.steensels@sciensano.be
- * Correspondence: vpanzarin@izsvenezie.it



Citation: Panzarin, V.; Marciano, S.; Fortin, A.; Brian, I.; D'Amico, V.; Gobbo, F.; Bonfante, F.; Palumbo, E.; Sakoda, Y.; Le, K.T.; et al. Redesign and Validation of a Real-Time RT-PCR to Improve Surveillance for Avian Influenza Viruses of the H9 Subtype. *Viruses* **2022**, *14*, 1263. <https://doi.org/10.3390/v14061263>

Academic Editor: Feng Li

Received: 20 April 2022

Accepted: 4 June 2022

Published: 10 June 2022

Publisher's Note: MDPI stays neutral with regard to jurisdictional claims in published maps and institutional affiliations.



Copyright: © 2022 by the authors. Licensee MDPI, Basel, Switzerland. This article is an open access article distributed under the terms and conditions of the Creative Commons Attribution (CC BY) license (<https://creativecommons.org/licenses/by/4.0/>).

Abstract: Avian influenza viruses of the H9 subtype cause significant losses to poultry production in endemic regions of Asia, Africa and the Middle East and pose a risk to human health. The availability of reliable and updated diagnostic tools for H9 surveillance is thus paramount to ensure the prompt identification of this subtype. The genetic variability of H9 represents a challenge for molecular-based diagnostic methods and was the cause for suboptimal detection and false negatives during routine diagnostic monitoring. Starting from a dataset of sequences related to viruses of different origins and clades (Y439, Y280, G1), a bioinformatics workflow was optimized to extract relevant sequence data preparatory for oligonucleotides design. Analytical and diagnostic performances were assessed according to the OIE standards. To facilitate assay deployment, amplification conditions were optimized with different nucleic extraction systems and amplification kits. Performance of the new real-time RT-PCR was also evaluated in comparison to existing H9-detection methods, highlighting a significant improvement of sensitivity and inclusivity, in particular for G1 viruses. Data obtained suggest that the new assay has the potential to be employed under different settings and geographic areas for a sensitive detection of H9 viruses.

Keywords: avian influenza; H9Nx; molecular diagnosis; real-time RT-PCR; validation

1. Introduction

The low pathogenicity avian influenza viruses (LPAIV) of the H9 subtype were described for the first time in the United States of America (Wisconsin, 1966) [1]. After

sporadic detections in Eurasia and North America, since the mid-1990s H9 viruses have expanded their geographic range to large territories of Asia, the Middle East and Africa [2–5] becoming endemic in domestic Galliformes [6–12]. The dissemination of H9 viruses in different continents resulted in the establishment of two distinct phylogeographic lineages: the American and the Eurasian. The latter gave origin to three main clades, i.e., Y439, Y280 (syn. BJ94) and G1, which includes G1-Western and G1-Eastern subclades [4,5]. Although the H9 hemagglutinin (HA) has been found associated with any of the nine neuraminidase (NA) subtypes, a noticeable preference for the N2 has been observed for the majority of the records [5].

In galliform poultry species, H9N2-induced clinical signs include diminished food and water intake, mild-to-severe respiratory syndromes and a drop in oviposition [13–22]. High morbidity and mortality can be observed upon secondary or concomitant infections [23–29]. Importantly, H9N2 viruses of the G1 and Y280 clades showed the ability to also infect mammals and humans as dead-end hosts [30]. Moreover, the cocirculation of zoonotic H9N2 with other AIV subtypes favors the occurrence of genetic reassortment and the emergence of novel viruses of public health concern, as demonstrated by the notorious cases of human infections caused by H5N1, H7N9 and H10N8 harboring the internal gene cassette donated by poultry-adapted H9N2 viruses [30–38].

Although H9N2 are non-notifiable, the economic damages and the public health risk posed by these viruses in endemic areas have prompted several countries to undertake vaccination campaigns [15,39,40]. However, the inability of inactivated vaccines to efficiently suppress shedding, suboptimal immunity levels and coverage in flocks, as well as a high heterogeneity in the immunization regimens across poultry production systems, are the most likely causes for increasing antigenic drift and genetic variability in endemic regions [41–43].

Because of the important implications on animal and human health, and the impact of vaccination and viral spread on genetic diversification, the development of universal tools for targeted H9 surveillance has clearly become a crucial task. So far, several real-time RT-PCR (rRT-PCR) assays have been developed to identify H9 viruses in birds and/or humans. However, most of these methods appear suboptimal for the universal recognition of all H9 clades, because they were validated with a sample collection under-representing the overall genetic variability of H9, or designed to detect only locally spread variants [44–47]. Monne and collaborators [48] have developed and validated one of the most widely used protocols for H9 detection that so far has been successfully applied in different contexts and geographic areas [27,49–51]. More recently, surveillance activities carried out at the Istituto Zooprofilattico Sperimentale delle Venezie (IZSVe) by employing this method revealed suboptimal detection of G1 strains from Africa and the Middle East, yielding flat amplification plots or false negatives. A subsequent NGS analysis has shown the occurrence of critical mismatches at the probe binding region, most likely being the cause for the observed diagnostic failures. In this study, we performed an in-depth bioinformatics analysis to redesign the assay originally developed by Monne et al., in order to detect H9Nx viruses of any of the Y439, Y280 and G1 clades. The new rRT-PCR was extensively validated and optimized with different reagents to facilitate its acquisition by third-party laboratories. Diagnostic sensitivity was also compared with existing broad-spectrum H9 assays successfully employed for the detection of this subtype [29,48,52]. The newly developed pan-H9 rRT-PCR showed good performances with all the clades and types of matrices tested, improved sensitivity and full restoration of inclusivity for G1 viruses and has the potential to be used in different areas and contexts.

2. Materials and Methods

2.1. *In Silico Update*

The complete HA nucleotide sequences of avian and human H9Nx collected since 2015 in Eurasia and Africa were downloaded from the GISAID (Global Initiative on Sharing

All Influenza Data) EpiFlu database [53] on 18 February 2021. The dataset includes H9Nx strains of the Y439, G1 and Y280 clades.

Sequences were aligned with MAFFT version 7 (Multiple Alignment with Fast Fourier Transform) [54,55] using default parameters. Geneious Prime 2020.1.2 (Biomatters Ltd., Auckland, New Zealand) [56] was employed to remove truncated or low quality sequences from the multisequence alignment (MSA) and to concatenate the hybridization regions of primers and probe developed by Monne and colleagues [48]. The concatenated-MSA (5338 records) was condensed to identify unique haplotypes ($n = 480$), and traced to assess the sequences composition within each haplotype using the SequenceTracer tool available on the Alignment Explorer web platform v1.4.3 (provided by the National Institute of Public Health, Czech Republic) [57,58]. A scoring system was adopted to categorize haplotypes based on their frequency and spatiotemporal distribution. Clusters of identical sequences with higher frequency, intercontinental spread and extended circulation over recent years were prioritized for primers and probe renewal. To assess the level of nucleotide variability at oligonucleotides binding regions within the concatenated-MSA, the Shannon entropy value $H(i)$ was derived from the sequence logo generated with Geneious Prime 2020.1.2 (Biomatters Ltd., Auckland, New Zealand) [56]. Nucleotide positions with $H(i) > 0.05$ (corresponding to $<1\%$ sequences over the entire dataset) were carefully inspected for their polymorphisms. The occurrence of nucleotide signatures associated with priority haplotypes was adopted as a criterion for redesigning pan-H9 rRT-PCR oligonucleotides (Table 1). The IDT OligoAnalyzer online tool (Leuven, Belgium) [59] was employed to verify the physical properties of primers and probe.

Table 1. Primers and probe of the pan-H9 rRT-PCR assay. LNA-modified bases are in bold and underlined.

Oligonucleotide	Sequence 5' → 3'	Nt. Position ¹
Pan-H9 for	ATR GGG TTT GCT GCC	1615–1629
Pan-H9 rev1	TCA TAT ACA AAT GTT GCA YCT G	1662–1683
Pan-H9 rev2	TTA TAT ACA GAT GTT GCA YCT G	1662–1683
Pan-H9 probe	TTC TGG GCY <u>ATG TCH</u> AAY GG	1636–1655

¹ Nucleotide position refers to strain A/pheasant/Italy/21VIR2284-1/2021 (GISAID reference number EPI1947247).

After the completion of the validation pathway, assay inclusivity was verified *in silico* with newly released sequences (downloaded on 18 March 2022) using Geneious Prime 2020.1.2 (Biomatters Ltd., Auckland, New Zealand) [56].

2.2. rRT-PCR Assay Set Up

For the entire validation process, nucleic acids were isolated using the QIAasympyphony DSP Virus/Pathogen Midi kit (Qiagen, Hilden, Germany) on a QIAasympyphony SP instrument (Qiagen, Hilden, Germany) (sample volume 300 μ L; custom protocol), unless otherwise specified. During the lysis phase, all the samples were spiked with an exogenous internal control (intype IC-RNA, Indical Bioscience GmbH, Leipzig, Germany) to reproduce routine laboratory conditions as foreseen by the upstream AIV screening method adopted at the IZSve [60,61] that employs the same nucleic acids.

Amplification reaction was assembled with the AgPath-ID One-Step RT-PCR Reagents (Applied Biosystems, Waltham, MA, USA), 400 nM primer for, 200 nM each primer rev, 200 nM probe, 20 units RNase inhibitor and 5 μ L template, in a final volume of 25 μ L. Thermal cycling was performed on a CFX96 Deep Well Real-Time PCR System, C1000 Touch (Biorad, Hercules, CA, USA), as follows: 50 °C for 10 min, 95 °C for 10 min, followed by 45 cycles at 95 °C for 15 s, 54 °C for 30 s and 72 °C for 15 s. Data were analyzed using Bio-Rad CFX Manager software (Version 3.1) (Biorad, Hercules, CA, USA), with fluorescence drift correction for the baseline adjustment and single threshold manually set above the background noise (c.ca 50 RFU).

2.3. Analytical Specificity (Asp)

The capacity of the pan-H9 rRT-PCR to distinguish the target from other microorganisms and sample matrix components was assessed. In detail, exclusivity was verified by testing either AIV negative specimens from birds (swabs, organs homogenates) as well as avian nontarget bacteria and viruses, including different AIV HA subtypes. Inclusivity was confirmed on reference isolates available at the IZSve repository of different origins and clades. Finally, selectivity was evaluated by testing different types of sample matrices, derived from confirmed H9 clinical cases. The complete list of samples tested for analytical specificity is available as Supplementary Materials (Table S1).

2.4. Analytical Sensitivity (ASe) and Repeatability

Tracheal and cloacal swabs rehydrated in PBSa, and oviduct homogenate (1:10 *w/v* in PBS with antibiotics and antimycotics—PBSa) collected from SFP chickens were contaminated with a dilution series of titrated H9 isolates of the Y439, G1 and Y280 clades. Each dilution was tested by rRT-PCR in triplicate. The highest dilution at which all the replicates tested positive identified the limit of detection (LoD). Intra- and interassay repeatability, expressed as percent coefficient of variation (%CV), was estimated in tracheal swabs and oviduct homogenates artificially contaminated with different doses of Y439 and G1 viruses (i.e., LoD, LoD + 1 log, LoD + 3 log) by two operators, on three different days.

For the pan-H9 rRT-PCR application as a frontline method for targeted diagnosis of this subtype, the possibility to coamplify the exogenous internal control in a duplex format was also explored in tracheal swabs and oviduct homogenates spiked with Y280.

To evaluate pan-H9 rRT-PCR performance under challenging conditions, serial dilutions of synthetic RNA (Ultram RNA oligonucleotides, Integrated DNA Technologies, IDT, Leuven, Belgium) representing G1 and Y280 strains with multiple mismatches at the oligonucleotides binding regions, were also tested in triplicate. For comparison, a synthetic RNA with a perfect match (positive control) was also analyzed.

2.5. Diagnostic Sensitivity (DSe) and Specificity (DSp)

OIE guidelines [62] were followed to establish the number of field samples with known infectious status required to assess the diagnostic performances of the pan-H9 rRT-PCR, with the following estimates: 98% sensitivity and specificity, 5% error and 99% confidence. In total, 70 positive and 53 negative samples (including specimens positive for AIV subtypes other than H9) were tested (Table 2). More detailed information is available in Table S3. The AIV screening method in place at the IZSve was run in parallel [60,61].

Table 2. Clinical samples with known infectious status used to assess DSe and DSp.

	Origin	Collection Year	Matrix	Species	No.
H9-confirmed cases	Europe	2018–2022	Swabs, stool	Mallard, teal, pheasant, goose, other unspecified avian species	22
	Africa	2019–2021	Swabs, organs, FTA	Chicken, cockerel, other unspecified avian species	21
	Middle East	2019–2021	FTA	Chicken	17
	Asia	2012–2021	Organs, FTA	Chicken	10
H9-negative samples *	Europe	2018–2021	Swabs, organs	Chicken, turkey, mallard, teal, pheasant, goose, quail, magpie, partridge, shoveler, duck, swan, gull	53

* Comprise H1, H3, H5 and H6 AIV positive samples.

2.6. Reproducibility and Robustness

Two identical series of $n = 13$ oviduct homogenates, either negative or spiked with different loads of G1 or Y280 viruses, were analyzed in parallel with a territorial laboratory

of the IZSve (SCT1—Buttapietra, Verona). Nucleic acids were isolated with the MagMAX Pathogen RNA/DNA Kit (Applied Biosystems, Waltham, MA, USA) on a KingFisher Flex Processor (Thermo Fisher Scientific, Waltham, MA, USA) (sample volume 200 μ L; protocol “low-cell-content samples”). For each sample aliquot, rRT-PCR was run in duplicate. Reproducibility was assessed also by participating in the OFFLU proficiency testing program 2021 for avian influenza A virus, H5 and H7 subtyping [63] organized by the Australian National Science Agency—Commonwealth Scientific and Industrial Research Organisation (CSIRO). Nucleic acids’s extraction was performed both with automatic and manual systems (i.e., MagMAX Pathogen RNA/DNA Kit, Applied Biosystems, Waltham, MA, USA and QIAamp Viral RNA Mini Kit, Qiagen, Hilden, Germany). Although H9 subtyping was not part of the assessable parameters of the exercise, the organization provided decoding for H9N2 samples included in the panel to allow self-assessment.

2.7. Procedural Modifications for Pan-H9 rRT-PCR Deployment

To facilitate assay deployment and circumvent possible issues deriving from reagents depletion, different kits for nucleic acids purification and amplification were evaluated.

2.7.1. Automatic and Manual Nucleic Acids Isolation Kits

SPF tracheal and cloacal swabs rehydrated in PBSa and oviduct homogenate (1:10 *w/v* in PBSa) spiked with G1 were processed comparatively with: (i) QIA Symphony DSP Virus/Pathogen Midi kit (Qiagen, Hilden, Germany) as described above, (ii) MagMAX Pathogen RNA/DNA Kit (Applied Biosystems, Waltham, MA, USA) on a KingFisher Flex Processor (Thermo Fisher Scientific, Waltham, MA, USA) as described above, and (iii) NucleoSpin RNA (Macherey-Nagel, Dueren, Germany) (sample volume 100 μ L; protocol “RNA purification from cultured cells and tissue”). Samples were analyzed in triplicate from the nucleic acids’ extraction phase. Amplification was carried out with the AgPath-ID One-Step RT-PCR Reagents (Applied Biosystems, Waltham, MA, USA), as previously detailed.

2.7.2. One-Step Real-Time RT-PCR Kits

Nucleic acids isolated from tracheal and cloacal swabs ($n = 24$ positive samples) collected from G1 experimentally challenged chickens in the framework of a previous research project were used to evaluate the performance of different real-time RT-PCR kits. Amplification conditions were optimized for the QIAGEN OneStep RT-PCR Kit (Qiagen, Hilden, Germany) and the Quantitect Probe RT-PCR Kit (Qiagen, Hilden, Germany). Details of standardized protocols are available as Supplementary Materials. Performances were compared with the AgPath-ID One-Step RT-PCR Reagents (Applied Biosystems, Waltham, MA, USA), under the conditions described above.

2.8. Comparison with Existing Molecular Diagnostic Methods

A comprehensive literature review was carried out to identify available molecular methods for H9 diagnosis. rRT-PCR protocols fully validated and/or extensively used under field conditions, namely Saito et al. (2018) [52] and Hassan et al. (2019) [29] (later implemented in [64]), were selected to be compared with the new pan-H9 rRT-PCR and the original protocol by Monne et al. (2008) [48]. For this purpose, a subset of 46 H9-positive field samples employed for DSe were tested, applying the experimental conditions as per original papers. In parallel, the screening rRT-PCR targeting the AIV M-gene (Heine et al., 2015) [60,61] was also performed.

2.9. Statistical Analysis

Statistical analyses based on Ct values obtained for the (i) reproducibility, (ii) amplification kits comparison and (iii) evaluation of sensitivity for different real-time PCR assays (paragraphs 2.6, 2.7.2 and 2.8) were performed using Prism 9.3.1 (GraphPad, San Diego, CA, USA). Negative samples were arbitrarily assigned a value of 45. Student’s *t*-test (significance with $p < 0.05$) and Spearman’s rank correlation were estimated.

3. Results

3.1. Analytical Performance

3.1.1. Exclusivity, Inclusivity and Selectivity

The capacity of the pan-H9 rRT-PCR to specifically detect only the target was confirmed upon verification of the analytical specificity. No background hybridization was recorded when testing negative tracheal/cloacal swabs and oviduct homogenates. The absence of cross-reaction was verified also against a wide panel of avian microorganisms, and exclusivity with respect to non-H9 AIV subtypes was also demonstrated. In contrast, the pan-H9 rRT-PCR successfully recognized a panel of H9N2, H9N6, H9N7 and H9N8 reference strains of different origins that tested positive at low Ct values ($8 \leq Ct \leq 14.88$). All represented clades (Y439, Y280, G1) were detected. The absence of inhibition and/or interference phenomena referable to the different types of sample matrix analyzed was preliminarily demonstrated with a selection of H9 clinical samples, which were successfully recognized in all cases. Detailed information is reported in Table S1.

3.1.2. Analytical Sensitivity and Repeatability

In all cases but one, the LoD reached values close to 1 EID₅₀/100 µL, independently of the virus clade and sample matrix combination tested. Only for Y280 in the oviduct, the pan-H9 rRT-PCR was 1 log less sensitive (Table 3). The method showed to be repeatable at all the dilutions tested, including the LoD, with an agreement between Ct values above 96% (Table S2).

Table 3. Analytical sensitivity in tracheal swabs, cloacal swabs and oviduct homogenate for H9 Y439, G1 and Y280 clades. The LoD is expressed as EID₅₀/100 µL and mean Ct values. For each dilution series, the amplification efficiency *E* (%) and the coefficient of correlation *R*² are reported. n.t.: not tested.

Strain	Tracheal Swab			Cloacal Swab			Oviduct		
	LoD (Ct)	<i>E</i> (%)	<i>R</i> ²	LoD (Ct)	<i>E</i> (%)	<i>R</i> ²	LoD (Ct)	<i>E</i> (%)	<i>R</i> ²
A/pheasant/Italy/21VIR2284-22/2021/H9N2 (Y439 clade)	1.51 (33.85)	90.5	0.995	1.51 (33.48)	95.9	0.997	1.51 (34.80)	90.4	0.998
A/chicken/Nigeria/19VIR8424-15/2019/H9N2 (G1 clade)	3.16 (34.06)	99.9	0.996	3.16 (35.06)	94.8	0.998	3.16 (36.04)	99.4	0.998
A/chicken/Malaysia/2630-8/2012/H9N2 (Y280 clade)	1.41 (33.78)	95.6	0.998	1.41 (33.81)	98.0	0.997	14.12 (32.01)	97.8	0.996
A/chicken/Malaysia/2630-8/2012/H9N2 (Y280 clade) with intype IC-RNA *	1.41 (33.53)	97.2	0.998	n.t.	n.t.	n.t.	14.12 (32.13)	90.9	0.985

* rRT-PCR run in duplex format with the internal control.

Sensitivity tests were also run in duplex, coamplifying an exogenous internal control. Such experimental setting is required to assure the quality and conformity of analytical results and prevent issues deriving from an inhibition of the amplification reaction, in the event that the assay is employed as a frontline method for the targeted diagnosis of H9 viruses. Results for Y280 spiked into tracheal swabs and oviduct highlight that the LoDs of the simplex and duplex formats are the same, demonstrating that the coamplification of the internal control does not impair assay sensitivity (Table 3).

Finally, tolerance of the pan-H9 rRT-PCR to mismatches occurrence was evaluated by testing serial dilutions of synthetic RNAs representing G1 and Y280 viruses with different HA sequences. Overall, assay sensitivity was retained in the presence of two mismatches at the primers' hybridization regions, yielding performance similar to the positive control with a perfect match. A more severe impact on the LoD and reaction efficiency was observed for synthetic RNAs with ≥ 6 mismatches (Table 4).

Table 4. Analytical sensitivity of synthetic RNAs representing G1 and Y280 viruses. The LoD is expressed as copies/ μ L of RNA and mean Ct values. For each dilution series, the amplification efficiency E (%) and the coefficient of correlation R^2 are reported.

Synthetic RNA *	No. of Mismatches			Performance		
	For	Probe	Revs	LoD (Ct)	E (%)	R^2
MN038193 (G1)	2	0	0	10^1 (38.98)	85.6	0.998
MK553893 (Y280)	0	1	6	10^5 (37.56)	82.3	0.982
MN765147 (Y280)	0	0	2	10^2 (34.54)	91.7	0.998
MN765086 (Y280)	0	1 (3'-end)	5	10^4 (38.98)	78.5	0.973
Positive control \S	0	0	0	10^1 (37.56)	86.4	0.993

* The GenBank accession number of the HA sequences used to produce synthetic RNAs is reported for each sample. \S Synthetic RNA with perfect match with respect to primers and probe sequences.

3.2. Diagnostic Performance with Clinical Samples

DSe and DSp were used as indicators to establish the capacity of the assay to correctly identify true positive and true negative field samples. In detail, H9-confirmed cases from a plethora of geographic origins, sample matrices and hosts were successfully detected with the pan-H9 rRT-PCR, with Ct values comparable to the AIV screening method targeting the M gene. No false positives were observed when testing H9-negative samples (Table S3). Overall, the diagnostic sensitivity and specificity values totaled 100%. Based on the Ct values yielded for H9-positive samples, a diagnostic cut-off of 35 is proposed.

3.3. Interlaboratory Reproducibility

The simultaneous testing of positive and negative oviduct homogenates at two different facilities of the IZSvE revealed a high reproducibility of the pan-H9 rRT-PCR, ($p < 0.0001$; $r = 0.996$) (Table S4) and is indicative of assay robustness. Only one sample corresponding to the LoD of G1 clade was missed by one of the two laboratories.

Additionally, all the H9 positive samples included in the OFFLU proficiency testing program 2021 were successfully identified, resulting in a perfect agreement between the pan-H9 rRT-PCR and the expected values (Cohen's Kappa coefficient, $K = 1$).

3.4. Potential for Pan-H9 rRT-PCR Deployment

To facilitate the transferability of the pan-H9 rRT-PCR to third-party laboratories, the performance of different reagents was evaluated. First, three diverse nucleic acids purification systems were compared in terms of LoD, upon use of the same amplification kit (i.e., AgPath-ID One-Step RT-PCR Reagents, Applied Biosystems, Waltham, MA, USA). In all the sample matrices tested, the assay sensitivity was higher (3.16 EID₅₀/100 μ L) when using automatic extraction methods. In contrast, the NucleoSpin RNA (Macherey-Nagel, Dueren, Germany) appeared less efficient independently of the type of sample, with a LoD of 31.6 EID₅₀/100 μ L (Table 5).

Secondly, reaction conditions for two different amplification kits (i.e., the QIAGEN OneStep RT-PCR Kit and the Quantitect Probe RT-PCR Kit, Qiagen, Hilden, Germany) were optimized and compared to the standard protocol, using nucleic acids isolated from tracheal and cloacal swabs obtained from a previous H9 in vivo challenge (Figure 1). All the conditions allowed target detection and yielded similar Ct values with high correlation.

Table 5. Analytical sensitivity in tracheal swabs, cloacal swabs and oviduct homogenate spiked with H9 G1 (A/chicken/Nigeria/19VIR8424-15/2019/H9N2) using different nucleic acids extraction kits. The LoD is expressed as EID₅₀/100 µL and mean Ct values. For each dilution series, the amplification efficiency *E* (%) and the coefficient of correlation *R*² are reported.

Nucleic Acids' Purification Systems	Tracheal Swab			Cloacal Swab			Oviduct		
	LoD (Ct)	<i>E</i> (%)	<i>R</i> ²	LoD (Ct)	<i>E</i> (%)	<i>R</i> ²	LoD (Ct)	<i>E</i> (%)	<i>R</i> ²
QIASymphony DSP Virus/Pathogen Midi kit (Qiagen, Hilden, Germany)	3.16 (34.06)	99.9	0.996	3.16 (35.06)	94.8	0.998	3.16 (36.04)	99.4	0.998
MagMAX Pathogen RNA/DNA Kit (Applied Biosystems, Waltham, MA, USA)	3.16 (35.29)	93.8	0.993	3.16 (33.97)	98.7	0.999	3.16 (34.87)	98.8	0.994
NucleoSpin RNA (Macherey-Nagel, Dueren, Germany)	31.6 (35.47)	104.9	0.995	31.6 (34.38)	95.4	0.997	31.6 (34.68)	94.6	0.992

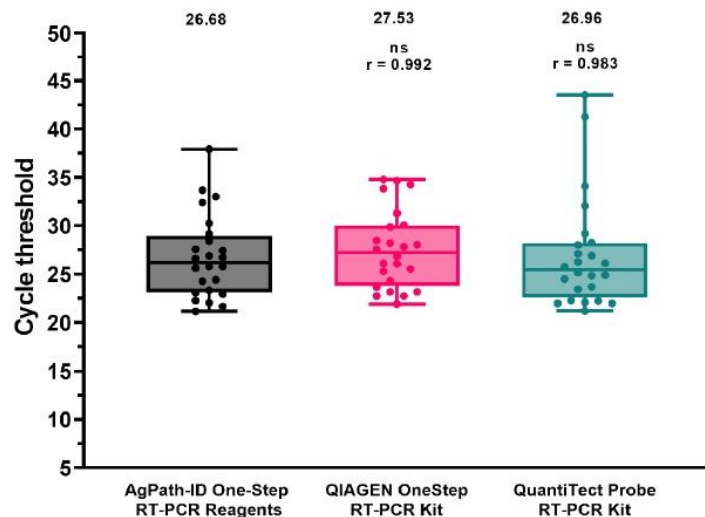


Figure 1. Performance comparison of different amplification kits. Dots represent individual Ct values. Mean Ct and Spearman's rank correlation coefficient (*r*) are reported. ns: not significant.

3.5. Comparison of the Pan-H9 rRT-PCRs with Other Assays

A selection of field samples ($n = 46$) employed for the assessment of DSe was also used to compare the sensitivity of the pan-H9 rRT-PCR with respect to existing rRT-PCR methods for the identification of the H9 subtype, as well as for AIV screening (Figure 2 and Table S3). Overall, the pan-H9 rRT-PCR showed a significantly higher detection rate and sensitivity compared to other assays targeting this subtype. In detail, G1 viruses from Africa and the Middle East missed by the rRT-PCR by Monne et al. (2008) were successfully recognized with the new method. The assay developed by Saito et al. (2019) yielded one false negative and significantly higher Ct values (mean value: 28.80 vs. 25.20). Dropouts were observed also for the assay developed by Hassan and collaborators (2019), which was unable to recognize eight samples. For 13 Asian and African specimens comprising several G1-confirmed viruses, flat amplification plots and a low fluorescence were noticeable. When considering positive samples with sharp fluorescence curves, the differences in Ct values between the assay by Hassan et al. (2019) and the pan-H9 rRT-PCR were not statistically significant ($r = 0.885$; $p = 0.538$).

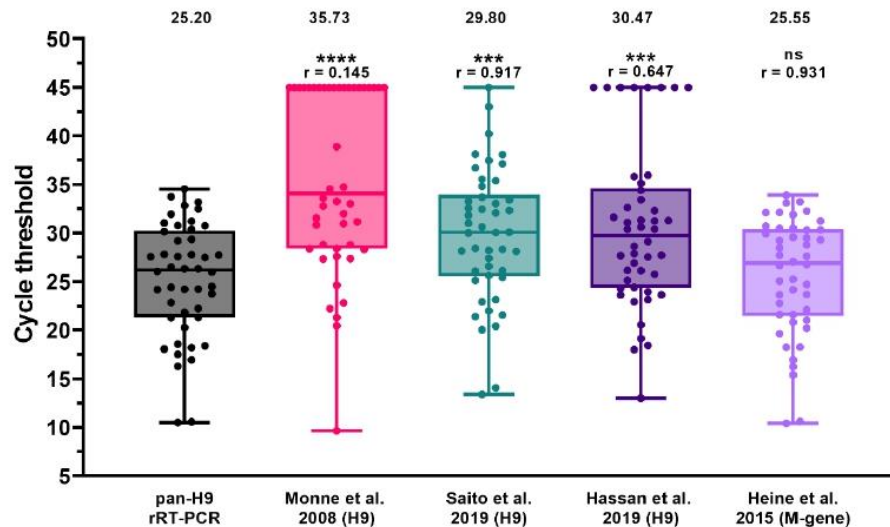


Figure 2. Diagnostic sensitivity of the pan-H9 rRT-PCR compared to M-gene screening rRT-PCR (Heine et al., 2015) [60] and three existing H9 detection methods [29,48,52]. Dots represent individual Ct values. Negative samples were arbitrarily assigned a value of 45. Mean Ct and Spearman's rank correlation coefficient (r) are reported. **** $p < 0.0001$; *** $p < 0.0002$; ns: not significant.

The pan-H9 rRT-PCR sensitivity was also compared with the screening rRT-PCR for AIV targeting the matrix (M) gene (Heine et al., 2015). All samples were identified by the new H9 assay, yielding Ct values comparable to that of the M-gene rRT-PCR ($r = 0.931$).

4. Discussion

The absence of notification obligations for H9Nx combined with insufficient surveillance for this subtype in countries with limited resources has led to an overall underestimation of its circulation [4,5]. This gap is worsened by the adverse effect of evolutionary drivers acting on viral diversification [41,65,66], which might result in diagnostic dropout for molecular-based methods. Nowadays, the resolution of such issues largely benefits from the constant increase of sequence data available that permits a timely update of diagnostic methods and improvement of laboratories responsiveness [67]. As a matter of fact, for clinical samples originating from Africa and the Middle East, we recently experienced failures in H9 identification by rRT-PCR [48] revealed by NGS analyses. This prompted us to undertake an in-depth update of the protocol originally designed by Monne and collaborators and widely used in different geographic areas and settings, with the aim of developing a pan-H9 rRT-PCR capable of recognizing the Y439, Y280 and G1 clades. To this end, a bioinformatics workflow was optimized to extract relevant data preparatory for the redesign of the oligonucleotides that account for the overall genetic variability of contemporary H9Nx. The new assay accommodates 95.3% of the entire dataset of sequences analyzed (5086 scores out of 5338) with ≤ 3 mismatches. The remaining sequences showed different degrees of variability at oligonucleotides binding regions and are mostly related to viral haplotypes that occurred only once, before 2018, and were extinct soon after. Although for the pan-H9 rRT-PCR design these sequences were considered negligible, assay inclusivity was verified in the presence of a high number of mismatches, confirming the potentiality of our method to identify even highly divergent viruses at high concentration, while avoiding unwanted cross-reaction with other AIV subtypes and common avian bacteria and viruses. In view of the frequent cocirculation of H9 viruses with other pathogens, assay specificity appears crucial in order to correctly identify disease etiology.

The newly designed pan-H9 rRT-PCR showed a high analytical sensitivity and repeatability in the sample matrices relevant for the tissue tropism of H9Nx viruses (i.e., tracheal and cloacal swabs and oviduct), reaching values between 1.51 and 14.12 EID₅₀/100 μ L

for representative strains of the Y439, G1 and Y280 clades. Evaluation of diagnostic sensitivity was extended to a wider variety of sample matrices, hosts, geographic origins and viral haplotypes, and was assessed comparatively with other methods. In particular, in the routine practice, a comparison with Ct values obtained with AIV screening tests designed to maximize sensitivity and inclusivity represents a useful source of information for diagnosticians to infer semiquantitative data on the approximate viral load for specific AIV subtypes. In our settings, the pan-H9 rRT-PCR showed a performance comparable to that of the AIV M-gene assay [60,61], as assessed by a significant correlation in terms of Ct values. Thus, any remarkable discrepancy between H9 and M-gene assays should be critically evaluated, as it might be indicative of the emergence of mutant strains that possibly imply assays' update. Notably, a comparison with existing H9 rRT-PCR protocols highlights that the new assay enables a significantly higher detection rate and lower Ct values, with restored capability to detect mutant viruses of the G1 clade. While limitations of the protocol by Monne and colleagues [48] were known for samples from Africa and the Middle East, drawbacks of the rRT-PCR by Hassan et al. [29] were unexpected due to its high inclusivity assessed *in silico*. A more careful analysis of false negatives and doubtful samples (i.e., flat amplification plots) from Benin and Nigeria for which sequence data are available, highlights the occurrence of one mismatch at the 9th position of the probe's binding region. The same mismatch was previously found to be responsible for diagnostic dropouts that affected the assay developed by Monne and collaborators [48] and most likely could explain these outcomes as well.

One of the strategies of diagnostic laboratories to reduce costs while preserving results quality relies on the standardization of material, prioritizing the procurement of reagents already in use for routine activities and thus taking advantage of economies of scale. In order to facilitate this process for third-party laboratories willing to acquire the pan-H9 rRT-PCR, experimental conditions were optimized for different extraction systems and amplification kits. Automatic purification systems showed a better performance while reducing turnaround time and personnel occupation. Amplification conditions were optimized for different reagents from Thermo Fisher Scientific (Waltham, MA, USA) and Qiagen (Hilden, Germany), yielding comparable results. Chemistry dependence was observed for the TaqMan Fast Virus 1-Step Master Mix (Applied Biosystems, Waltham, MA, USA) and the SuperScript III One-Step RT-PCR System with Platinum *Taq* DNA Polymerase (Invitrogen, Waltham, MA, USA), both yielding higher Ct values and a lower sensitivity (data not shown). Because of their performance, these kits were not considered further in the validation process. Another important feature implemented in the pan-H9 rRT-PCR, is the inclusion of an exogenous internal control while maintaining the overall sensitivity. This option appears useful in case of a documented circulation of H9 viruses, for which targeted surveillance without prior M-gene screening is required to speed up viral detection and identification. These data confirm an overall high resilience of the pan-H9 assay to procedural modifications, as well as satisfactory reproducibility and robustness as also assessed by interlaboratory exercises carried out during the validation process.

5. Conclusions and Perspectives

Avian influenza viruses of the H9N2 subtype maintain the attention of animal health authorities high because of their growing prevalence and adverse impact on local poultry production, despite the extensive use of inactivated vaccines in endemic areas. Another important reason for H9 monitoring relies on its zoonotic potential, *per se* or secondary to the effect of reassortment with other AIV subtypes and pathotypes circulating in avian and mammalian species. The availability of sensitive and performant methods for H9 diagnosis is thus crucial for an early detection and to support surveillance activities aiming to improve animal health and prevent zoonotic events. The new real-time RT-PCR protocol for H9 detection was conceived to maximize its inclusivity and sensitivity, and was extensively validated and optimized for its application in different areas and settings. While this work aims to provide a reliable tool for H9 detection based on the most recent sequence data

available, the genetic drift of AIV viruses, mostly involving the HA gene, imposes the periodical assessment of assay inclusivity with newly released sequences to verify whether the assay is still fit-for-purpose.

Supplementary Materials: The following supporting information can be downloaded at: <https://www.mdpi.com/article/10.3390/v14061263/s1>, Table S1: Analytical specificity; Table S2: Within-run and between-days repeatability; Table S3: Diagnostic sensitivity and specificity and assays comparison; Table S4: Reproducibility; File S1: Amplification conditions with different real-time PCR kits.

Author Contributions: Conceptualization, V.P., C.T. and I.M.; methodology, V.P.; software, V.P. and A.F.; validation, S.M., A.F., I.B. and V.D.; formal analysis, V.P. and I.B.; investigation, V.P. and S.M.; resources, F.G., F.B., I.M., E.P., Y.S., K.T.L., D.-H.C., I.S., C.M., A.M.H., T.O., M.N.D., F.D. and M.S.; data curation, V.P., F.G. and I.M.; writing—original draft preparation, V.P.; writing—review and editing, S.M., A.F., I.B., V.D., F.G., F.B., E.P., Y.S., K.T.L., D.-H.C., I.S., C.M., A.M.H., T.O., M.N.D., F.D., M.S., C.T. and I.M.; visualization, V.P. and I.B.; supervision, C.T. and I.M.; project administration, V.P.; funding acquisition, C.T. All authors have read and agreed to the published version of the manuscript.

Funding: This research was partially funded by the Italian Ministry of Health (grant number RC IZSVe 07/2018 and RC IZSVe 11/2019). Comparative tests with different H9 detection assays were supported by the European Commission, within the framework of the activities foreseen by the EURL for AI/ND.

Institutional Review Board Statement: Animal experiment procedures were conducted in strict accordance with the Decree of the Italian Ministry of Health no. 26 of 4 March 2014 on the protection of animals used for scientific purposes, implementing Directive 2010/63/EU, and approved by the Ethics Committee of IZSVe (authorization no 709/2020-PR).

Data Availability Statement: The data presented in this study are reported in the main text or are available as Supplementary Materials.

Acknowledgments: We are grateful to Alessandra Drago, Silvia Maniero, Luca Tassoni, Elena Bertoli, Silvia Ormelli, Viviana Valastro and Elisabetta Stefani for their technical support. Special thanks go to field veterinarians for their effort in submitting clinical samples. We thank the OIE for supporting training activities of the NVRI staff on the validation of molecular methods through the OIE Twinning Project (IZSVe/NVRI) entitled “Improving NVRI laboratory capacity for better control of the Avian Influenza virus at National and Regional level”. Francesca Ellero is acknowledged for her assistance in manuscript editing.

Conflicts of Interest: The authors declare no conflict of interest.

References

1. Homme, P.J.; Easterday, B.C. Avian Influenza Virus Infections. I. Characteristics of Influenza A-Turkey-Wisconsin-1966 Virus. *Avian Dis.* **1970**, *14*, 66–74. [[CrossRef](#)] [[PubMed](#)]
2. Capua, I.; Alexander, D.J. Ecology, Epidemiology and Human Health Implications of Avian Influenza Virus Infections. In *Avian Influenza and Newcastle Disease*; Springer: Milano, Italy, 2009; pp. 1–18. [[CrossRef](#)]
3. Nagy, A.; Mettenleiter, T.C.; Abdelwhab, E.M. A Brief Summary of the Epidemiology and Genetic Relatedness of Avian Influenza H9N2 Virus in Birds and Mammals in the Middle East and North Africa. *Epidemiol. Infect.* **2017**, *145*, 3320–3333. [[CrossRef](#)] [[PubMed](#)]
4. Peacock, T.H.P.; James, J.; Sealy, J.E.; Iqbal, M. A Global Perspective on H9N2 Avian Influenza Virus. *Viruses* **2019**, *11*, 620. [[CrossRef](#)] [[PubMed](#)]
5. Carnaccini, S.; Perez, D.R. H9 Influenza Viruses: An Emerging Challenge. *Cold Spring Harb. Perspect. Med.* **2020**, *10*, a038588. [[CrossRef](#)] [[PubMed](#)]
6. Channa, A.A.; Tariq, M.; Nizamani, Z.A.; Kalhor, N.H. Prevalence of Avian Influenza H5, H7 and H9 Viruses in Commercial Layers in Karachi, Pakistan. *Iran. J. Vet. Res.* **2021**, *22*, 352–355. [[CrossRef](#)]
7. Gupta, S.D.; Hoque, M.A.; Fournié, G.; Henning, J. Patterns of Avian Influenza A (H5) and A (H9) Virus Infection in Backyard, Commercial Broiler and Layer Chicken Farms in Bangladesh. *Transbound. Emerg. Dis.* **2021**, *68*, 137–151. [[CrossRef](#)]
8. Kim, Y.; Biswas, P.K.; Giasuddin, M.; Hasan, M.; Mahmud, R.; Chang, Y.-M.; Essen, S.; Samad, M.A.; Lewis, N.S.; Brown, I.H.; et al. Prevalence of Avian Influenza A (H5) and A (H9) Viruses in Live Bird Markets, Bangladesh. *Emerg. Infect. Dis.* **2018**, *24*, 2309–2316. [[CrossRef](#)]

9. Luo, S.; Xie, Z.; Li, M.; Li, D.; Xie, L.; Huang, J.; Zhang, M.; Zeng, T.; Wang, S.; Fan, Q.; et al. Survey of Low Pathogenic Avian Influenza Viruses in Live Poultry Markets in Guangxi Province, Southern China, 2016–2019. *Sci. Rep.* **2021**, *11*, 23223. [[CrossRef](#)]
10. Nugroho, C.; Silaen, O.; Kurnia, R.; Soejoedono, R.; Poetri, O.; Soebandrio, A. Isolation and Molecular Characterization of the Hemagglutinin Gene of H9N2 Avian Influenza Viruses from Poultry in Java, Indonesia. *J. Adv. Vet. Anim. Res.* **2021**, *8*, 423–434. [[CrossRef](#)]
11. Rahman, M.M.; Nooruzzaman, M.; Kabiraj, C.K.; Mumu, T.T.; Das, P.M.; Chowdhury, E.H.; Islam, M.R. Surveillance on Respiratory Diseases Reveals Enzootic Circulation of Both H5 and H9 Avian Influenza Viruses in Small-scale Commercial Layer Farms of Bangladesh. *Zoonoses Public Health* **2021**, *68*, 896–907. [[CrossRef](#)]
12. Shaban, S.; Kyei, F.; Awuni, J.; Danquah, A.; Odoom, T.; Yingar, D.N.Y.T.; Ababio, P.T.; Emikpe, B.O. Dynamics of Influenza A (Avian Influenza) Virus in Poultry in the Greater Accra Region of Ghana amongst the Production Levels. *J. Immunoass. Immunochem.* **2022**, *43*, 1952426. [[CrossRef](#)] [[PubMed](#)]
13. Nili, H.; Asasi, K. Natural Cases and an Experimental Study of H9N2 Avian Influenza in Commercial Broiler Chickens of Iran. *Avian Pathol.* **2002**, *31*, 247–252. [[CrossRef](#)] [[PubMed](#)]
14. Kim, J.A.; Cho, S.H.; Kim, H.S.; Seo, S.H. H9N2 Influenza Viruses Isolated from Poultry in Korean Live Bird Markets Continuously Evolve and Cause the Severe Clinical Signs in Layers. *Vet. Microbiol.* **2006**, *118*, 169–176. [[CrossRef](#)] [[PubMed](#)]
15. Banet-Noach, C.; Perk, S.; Simanov, L.; Grebenyuk, N.; Rozenblut, E.; Pokamunski, S.; Pirak, M.; Tendler, Y.; Panshin, A. H9N2 influenza viruses from Israeli poultry: A five-year outbreak. *Avian Dis.* **2007**, *51* (Suppl. S1), 290–296. [[CrossRef](#)] [[PubMed](#)]
16. Nili, H.; Mohammadi, A.; Habibi, H.; Firouzi, S. Pathogenesis of H9N2 Virus in Chukar Partridges. *Avian Pathol.* **2013**, *42*, 230–234. [[CrossRef](#)]
17. Jakhesara, S.J.; Bhatt, V.D.; Patel, N.V.; Prajapati, K.S.; Joshi, C.G. Isolation and Characterization of H9N2 Influenza Virus Isolates from Poultry Respiratory Disease Outbreak. *SpringerPlus* **2014**, *3*, 196. [[CrossRef](#)]
18. Bonfante, F.; Mazzetto, E.; Zanardello, C.; Fortin, A.; Gobbo, F.; Maniero, S.; Bigolaro, M.; Davidson, I.; Haddas, R.; Cattoli, G.; et al. A G1-Lineage H9N2 Virus with Oviduct Tropism Causes Chronic Pathological Changes in the Infundibulum and a Long-Lasting Drop in Egg Production. *Vet. Res.* **2018**, *49*, 83. [[CrossRef](#)]
19. Chuan, Z.Y.; Bin, Z.; Hui, S.Z.; Jing, W.X.; Hui, F.X.; Xi, G.L.; Ying, L.; Yan, C.X.; Feng, Z.Z. Replication and Pathology of Duck Influenza Virus Subtype H9N2 in Chukar. *Biomed. Environ. Sci.* **2018**, *31*, 306–310. [[CrossRef](#)]
20. Awuni, J.A.; Bianco, A.; Dogbey, O.J.; Fusaro, A.; Yingar, D.T.; Salviato, A.; Ababio, P.T.; Milani, A.; Bonfante, F.; Monne, I. Avian Influenza H9N2 Subtype in Ghana: Virus Characterization and Evidence of Co-Infection. *Avian Pathol.* **2019**, *48*, 470–476. [[CrossRef](#)]
21. Kariithi, H.M.; Welch, C.N.; Ferreira, H.L.; Pusch, E.A.; Ateya, L.O.; Binepal, Y.S.; Apopo, A.A.; Dulu, T.D.; Afonso, C.L.; Suarez, D.L. Genetic Characterization and Pathogenesis of the First H9N2 Low Pathogenic Avian Influenza Viruses Isolated from Chickens in Kenyan Live Bird Markets. *Infect. Genet. Evol.* **2020**, *78*, 104074. [[CrossRef](#)]
22. Kye, S.-J.; Park, M.-J.; Kim, N.-Y.; Lee, Y.-N.; Heo, G.-B.; Baek, Y.-K.; Shin, J.-I.; Lee, M.-H.; Lee, Y.-J. Pathogenicity of H9N2 Low Pathogenic Avian Influenza Viruses of Different Lineages Isolated from Live Bird Markets Tested in Three Animal Models: SPF Chickens, Korean Native Chickens, and Ducks. *Poult. Sci.* **2021**, *100*, 101318. [[CrossRef](#)] [[PubMed](#)]
23. Sei, S. Natural Co-Infection Caused by Avian Influenza H9 Subtype and Infectious Bronchitis Viruses in Broiler Chicken Farms. *Vet. Arhiv* **2010**, *80*, 269–281. Available online: <https://hrcak.srce.hr/56716> (accessed on 19 January 2019).
24. Pan, Q.; Liu, A.; Zhang, F.; Ling, Y.; Ou, C.; Hou, N.; He, C. Co-Infection of Broilers with *Ornithobacterium Rhinotracheale* and H9N2 Avian Influenza Virus. *BMC Vet. Res.* **2012**, *8*, 104. [[CrossRef](#)] [[PubMed](#)]
25. Śmietanka, K.; Minta, Z.; Świętoń, E.; Olszewska, M.; Józwiak, M.; Domańska-Blicharz, K.; Wyrostek, K.; Tomczyk, G.; Piłkuła, A. Avian Influenza H9N2 Subtype in Poland—Characterization of the Isolates and Evidence of Concomitant Infections. *Avian Pathol.* **2014**, *43*, 427–436. [[CrossRef](#)] [[PubMed](#)]
26. Bonfante, F.; Cattoli, G.; Leardini, S.; Salomoni, A.; Mazzetto, E.; Davidson, I.; Haddas, R.; Terregino, C. Synergy or Interference of a H9N2 Avian Influenza Virus with a Velogenic Newcastle Disease Virus in Chickens Is Dose Dependent. *Avian Pathol.* **2017**, *46*, 488–496. [[CrossRef](#)] [[PubMed](#)]
27. Naguib, M.M.; El-Kady, M.F.; Lüscho, D.; Hassan, K.E.; Arafa, A.-S.; El-Zanaty, A.; Hassan, M.K.; Hafez, H.M.; Grund, C.; Harder, T.C. New Real Time and Conventional RT-PCRs for Updated Molecular Diagnosis of Infectious Bronchitis Virus Infection (IBV) in Chickens in Egypt Associated with Frequent Co-Infections with Avian Influenza and Newcastle Disease Viruses. *J. Virol. Methods* **2017**, *245*, 19–27. [[CrossRef](#)]
28. Horwood, P.F.; Horm, S.V.; Suttie, A.; Thet, S.; Phalla, Y.; Rith, S.; Sorn, S.; Holl, D.; Tum, S.; Ly, S.; et al. Co-Circulation of Influenza A H5, H7, and H9 Viruses and Co-Infected Poultry in Live Bird Markets, Cambodia. *Emerg. Infect. Dis.* **2018**, *24*, 352–355. [[CrossRef](#)]
29. Hassan, K.E.; El-Kady, M.F.; El-Sawah, A.A.A.; Luttermann, C.; Parvin, R.; Shany, S.; Beer, M.; Harder, T. Respiratory Disease Due to Mixed Viral Infections in Poultry Flocks in Egypt between 2017 and 2018: Upsurge of Highly Pathogenic Avian Influenza Virus Subtype H5N8 since 2018. *Transbound. Emerg. Dis.* **2021**, *68*, 21–36. [[CrossRef](#)]
30. Pusch, E.; Suarez, D. The Multifaceted Zoonotic Risk of H9N2 Avian Influenza. *Vet. Sci.* **2018**, *5*, 82. [[CrossRef](#)]
31. Lam, T.T.-Y.; Wang, J.; Shen, Y.; Zhou, B.; Duan, L.; Cheung, C.-L.; Ma, C.; Lycett, S.J.; Leung, C.Y.-H.; Chen, X.; et al. The Genesis and Source of the H7N9 Influenza Viruses Causing Human Infections in China. *Nature* **2013**, *502*, 241–244. [[CrossRef](#)]

32. Chen, H.; Yuan, H.; Gao, R.; Zhang, J.; Wang, D.; Xiong, Y.; Fan, G.; Yang, F.; Li, X.; Zhou, J.; et al. Clinical and Epidemiological Characteristics of a Fatal Case of Avian Influenza A H10N8 Virus Infection: A Descriptive Study. *Lancet* **2014**, *383*, 714–721. [[CrossRef](#)]
33. Shanmuganatham, K.K.; Jones, J.C.; Marathe, B.M.; Feeroz, M.M.; Jones-Engel, L.; Walker, D.; Turner, J.; Rabiul Alam, S.M.; Kamrul Hasan, M.; Akhtar, S.; et al. The Replication of Bangladeshi H9N2 Avian Influenza Viruses Carrying Genes from H7N3 in Mammals. *Emerg. Microbes Infect.* **2016**, *5*, e35. [[CrossRef](#)] [[PubMed](#)]
34. Shen, Y.-Y.; Ke, C.-W.; Li, Q.; Yuan, R.-Y.; Xiang, D.; Jia, W.-X.; Yu, Y.-D.; Liu, L.; Huang, C.; Qi, W.-B.; et al. Novel Reassortant Influenza A (H5N6) Viruses in Humans, Guangdong, China, 2015. *Emerg. Infect. Dis.* **2016**, *22*, 1507–1509. [[CrossRef](#)] [[PubMed](#)]
35. Tosh, C.; Nagarajan, S.; Kumar, M.; Murugkar, H.V.; Venkatesh, G.; Shukla, S.; Mishra, A.; Mishra, P.; Agarwal, S.; Singh, B.; et al. Multiple Introductions of a Reassortant H5N1 Avian Influenza Virus of Clade 2.3.2.1c with PB2 Gene of H9N2 Subtype into Indian Poultry. *Infect. Genet. Evol.* **2016**, *43*, 173–178. [[CrossRef](#)]
36. Seiler, P.; Kercher, L.; Feeroz, M.M.; Shanmuganatham, K.; Jones-Engel, L.; Turner, J.; Walker, D.; Alam, S.M.R.; Hasan, M.K.; Akhtar, S.; et al. H9N2 Influenza Viruses from Bangladesh: Transmission in Chicken and New World Quail. *Influenza Other Respir. Viruses* **2018**, *12*, 814–817. [[CrossRef](#)] [[PubMed](#)]
37. Ge, Z.; Xu, L.; Hu, X.; Zhu, S.; Zhao, Y.; Li, Y.; Liu, K.; Gao, R.; Wang, X.; Hu, J.; et al. Phylogenetic and Phenotypic Characterization of Two Novel Clade 2.3.2.1 H5N2 Subtype Avian Influenza Viruses from Chickens in China. *Infect. Genet. Evol.* **2022**, *98*, 105205. [[CrossRef](#)]
38. FAO Global AIV with Zoonotic Potential Situation Update—FAO Emergency Prevention System for Animal Health (EMPRES-AH). Available online: https://www.fao.org/ag/againfo/programmes/en/empres/Global_AIV_Zoonotic_Update/situation_update.html (accessed on 22 February 2022).
39. Lee, D.-H.; Song, C.-S. H9N2 Avian Influenza Virus in Korea: Evolution and Vaccination. *Clin. Exp. Vaccine Res.* **2013**, *2*, 26–33. [[CrossRef](#)]
40. EL Houadfi, M.; Fellahi, S.; Nassik, S.; Guérin, J.-L.; Ducatez, M.F. First Outbreaks and Phylogenetic Analyses of Avian Influenza H9N2 Viruses Isolated from Poultry Flocks in Morocco. *Virol. J.* **2016**, *13*, 140. [[CrossRef](#)]
41. Park, K.J.; Kwon, H.-i.; Song, M.-S.; Pascua, P.N.Q.; Baek, Y.H.; Lee, J.H.; Jang, H.-L.; Lim, J.-Y.; Mo, I.-P.; Moon, H.-J.; et al. Rapid Evolution of Low-Pathogenic H9N2 Avian Influenza Viruses Following Poultry Vaccination Programmes. *J. Gen. Virol.* **2011**, *92 Pt 1*, 36–50. [[CrossRef](#)]
42. Bahari, P.; Pourbakhsh, S.A.; Shoushtari, H.; Bahmaninejad, M.A. Molecular Characterization of H9N2 Avian Influenza Viruses Isolated from Vaccinated Broiler Chickens in Northeast Iran. *Trop. Anim. Health Prod.* **2015**, *47*, 1195–1201. [[CrossRef](#)]
43. El Mellouli, F.; Mouahid, M.; Fusaro, A.; Zecchin, B.; Zekhnini, H.; El Khantour, A.; Giussani, E.; Palumbo, E.; Rguibi Idrissi, H.; Monne, I.; et al. Spatiotemporal Dynamics, Evolutionary History and Zoonotic Potential of Moroccan H9N2 Avian Influenza Viruses from 2016 to 2021. *Viruses* **2022**, *14*, 509. [[CrossRef](#)] [[PubMed](#)]
44. Ben Shabat, M.; Meir, R.; Haddas, R.; Lapin, E.; Shkoda, I.; Raibstein, I.; Perk, S.; Davidson, I. Development of a Real-Time TaqMan RT-PCR Assay for the Detection of H9N2 Avian Influenza Viruses. *J. Virol. Methods* **2010**, *168*, 72–77. [[CrossRef](#)] [[PubMed](#)]
45. Lv, J.; Wei, B.; Chai, T.; Xia, X.; Miao, Z.; Yao, M.; Gao, Y.; Huang, R.; Yang, H.; Roesler, U. Development of a Real-Time RT-PCR Method for Rapid Detection of H9 Avian Influenza Virus in the Air. *Arch. Virol.* **2011**, *156*, 1795–1801. [[CrossRef](#)] [[PubMed](#)]
46. Liu, J.; Yao, L.; Zhai, F.; Chen, Y.; Lei, J.; Bi, Z.; Hu, J.; Xiao, Q.; Song, S.; Yan, L.; et al. Development and Application of a Triplex Real-Time PCR Assay for the Simultaneous Detection of Avian Influenza Virus Subtype H5, H7 and H9. *J. Virol. Methods* **2018**, *252*, 49–56. [[CrossRef](#)]
47. Mirzaei, S.G.; Shoushtari, A.; Nouri, A. Development and Evaluation of Real-Time RT-PCR Test for Quantitative and Qualitative Recognition of Current H9N2 Subtype Avian Influenza Viruses in Iran. *Arch. Razi Inst.* **2018**, *73*, 177–182. [[CrossRef](#)]
48. Monne, I.; Ormelli, S.; Salviato, A.; De Battisti, C.; Bettini, F.; Salomoni, A.; Drago, A.; Zecchin, B.; Capua, I.; Cattoli, G. Development and Validation of a One-Step Real-Time PCR Assay for Simultaneous Detection of Subtype H5, H7, and H9 Avian Influenza Viruses. *J. Clin. Microbiol.* **2008**, *46*, 1769–1773. [[CrossRef](#)]
49. Hoffmann, B.; Hoffmann, D.; Henritzi, D.; Beer, M.; Harder, T.C. Riems Influenza a Typing Array (RITA): An RT-QPCR-Based Low Density Array for Subtyping Avian and Mammalian Influenza a Viruses. *Sci Rep.* **2016**, *6*, 27211. [[CrossRef](#)]
50. Slomka, M.J.; Hanna, A.; Mahmood, S.; Govil, J.; Krill, D.; Manvell, R.J.; Shell, W.; Arnold, M.E.; Banks, J.; Brown, I.H. Phylogenetic and Molecular Characteristics of Eurasian H9 Avian Influenza Viruses and Their Detection by Two Different H9-Specific RealTime Reverse Transcriptase Polymerase Chain Reaction Tests. *Vet. Microbiol.* **2013**, *162*, 530–542. [[CrossRef](#)]
51. Khantour, A.E.; Soulaymani, A.; Salek, M.; Maltouf, A.F.; Darkaoui, S.; Mellouli, F.E.; Ducatez, M.; Fellahi, S. Molecular Characterization of the Hemagglutinin Gene of H9N2 Avian Influenza Viruses Isolated from Broiler Flocks in Morocco from 2016 to 2018. *Vet. Arh.* **2020**, *90*, 477. [[CrossRef](#)]
52. Saito, S.; Takayama, I.; Nakauchi, M.; Nagata, S.; Oba, K.; Odagiri, T.; Kageyama, T. Development and Evaluation of a New Real-Time RT-PCR Assay for Detecting the Latest H9N2 Influenza Viruses Capable of Causing Human Infection. *Microbiol. Immunol.* **2019**, *63*, 21–31. [[CrossRef](#)]
53. Shu, Y.; McCauley, J. GISAID: Global initiative on sharing all influenza data—From vision to reality. *Eurosurveillance* **2017**, *22*, 30494. [[CrossRef](#)]
54. Kuraku, S.; Zmasek, C.M.; Nishimura, O.; Katoh, K. aLeaves Facilitates On-Demand Exploration of Metazoan Gene Family Trees on MAFFT Sequence Alignment Server with Enhanced Interactivity. *Nucleic Acids Res.* **2013**, *41*, W22–W28. [[CrossRef](#)] [[PubMed](#)]

55. Katoh, K.; Rozewicki, J.; Yamada, K.D. MAFFT Online Service: Multiple Sequence Alignment, Interactive Sequence Choice and Visualization. *Brief. Bioinform.* **2019**, *20*, 1160–1166. [CrossRef] [PubMed]
56. Geneious Prime 2020.1.2. Available online: <https://www.geneious.com> (accessed on 19 January 2019).
57. Nagy, A.; Jiřinec, T.; Černíková, L.; Jiřincová, H.; Havlíčková, M. Large-scale nucleotide sequence alignment and sequence variability assessment to identify the evolutionarily highly conserved regions for universal screening PCR assay design: An example of influenza A virus. *Methods Mol. Biol.* **2015**, *1275*, 57–72. [CrossRef] [PubMed]
58. Nagy, A.; Jiřinec, T.; Jiřincová, H.; Černíková, L.; Havlíčková, M. In Silico Re-Assessment of a Diagnostic RT-QPCR Assay for Universal Detection of Influenza A Viruses. *Sci. Rep.* **2019**, *9*, 1630. [CrossRef]
59. Integrated DNA Technologies OligoAnalyzer. Available online: <https://eu.idtdna.com/calc/analyzer> (accessed on 20 May 2021).
60. Heine, H.G.; Foord, A.J.; Wang, J.; Valdeter, S.; Walker, S.; Morrissy, C.; Wong, F.Y.K.; Meehan, B. Detection of Highly Pathogenic Zoonotic Influenza Virus H5N6 by Reverse-Transcriptase Quantitative Polymerase Chain Reaction. *Viol. J.* **2015**, *12*, 18. [CrossRef]
61. Laconi, A.; Fortin, A.; Bedendo, G.; Shibata, A.; Sakoda, Y.; Awuni, J.A.; Go-Maró, E.; Arafa, A.; Maken Ali, A.S.; Terregino, C.; et al. Detection of Avian Influenza Virus: A Comparative Study of the In Silico and In Vitro Performances of Current RT-QPCR Assays. *Sci. Rep.* **2020**, *10*, 8441. [CrossRef]
62. OIE. Principles and Methods of Validation of Diagnostic Assays for Infectious Disease (Version Adopted in May 2013). In *Manual of Diagnostic Tests and Vaccines for Terrestrial Animals*; OIE: Paris, France, 2021. Available online: https://www.oie.int/fileadmin/Home/eng/Health_standards/tahm/1.01.06_VALIDATION.pdf (accessed on 13 July 2021).
63. Waugh, C.M.; Clark, G.A.; Hollier, J.; Watson, J. *FAO/OIE Global Network of Expertise on Animal Influenzas (OFFLU)*; CSIRO-ACDP: East Geelong, Australia, 2022.
64. Hassan, K.E.; Ahrens, A.K.; Ali, A.; El-Kady, M.F.; Hafez, H.M.; Mettenleiter, T.C.; Beer, M.; Harder, T. Improved Subtyping of Avian Influenza Viruses Using an RT-QPCR-Based Low Density Array: ‘Riems Influenza a Typing Array’, Version 2 (RITA-2). *Viruses* **2022**, *14*, 415. [CrossRef]
65. Suttie, A.; Tok, S.; Yann, S.; Keo, P.; Horm, S.V.; Roe, M.; Kaye, M.; Sorn, S.; Holl, D.; Tum, S.; et al. The Evolution and Genetic Diversity of Avian Influenza A (H9N2) Viruses in Cambodia, 2015–2016. *PLoS ONE* **2019**, *14*, e0225428. [CrossRef]
66. Yan, W.; Cui, H.; Engelsma, M.; Beerens, N.; van Oers, M.M.; de Jong, M.C.M.; Li, X.; Liu, Q.; Yang, J.; Teng, Q.; et al. Molecular and Antigenic Characterization of Avian H9N2 Viruses in Southern China. *Microbiol. Spectr.* **2022**, *10*, e00822-21. [CrossRef]
67. Van Borm, S.; Belák, S.; Freimanis, G.; Fusaro, A.; Granberg, F.; Höper, D.; King, D.P.; Monne, I.; Orton, R.; Rosseel, T. Next-Generation Sequencing in Veterinary Medicine: How Can the Massive Amount of Information Arising from High-Throughput Technologies Improve Diagnosis, Control, and Management of Infectious Diseases? In *Veterinary Infection Biology: Molecular Diagnostics and High-Throughput Strategies*; Cunha, M.V., Inácio, J., Eds.; Methods in Molecular Biology; Springer: New York, NY, USA, 2015; Volume 1247, pp. 415–436, ISBN 978-1-4939-2003-7.

CHAPTER 4:

EFFECT OF ASSAY CHOICE, VIRAL CONCENTRATION AND OPERATOR INTERPRETATION ON INFECTIOUS BRONCHITIS VIRUS DETECTION AND CHARACTERIZATION

Tucciarone, C.M., Franzo, G., Legnardi, M, Fortin, A, Valastro, V., Lazzaro, E., Terregino, C. and Cecchinato, M.

Avian pathology, 2021

Effect of assay choice, viral concentration and operator interpretation on infectious bronchitis virus detection and characterization

Claudia Maria Tucciarone^a, Giovanni Franzo^a, Matteo Legnardi^a, Andrea Fortin^b, Viviana Valastro^b, Elena Lazzaro^a, Calogero Terregino^b and Mattia Cecchinato^a

^aDepartment of Animal Medicine, Production and Health (MAPS), Università degli Studi di Padova, Viale dell'Università, Legnaro PD, Italy;
^bIstituto Zooprofilattico Sperimentale delle Venezie, Viale dell'Università, Legnaro PD, Italy

ABSTRACT

Despite the efforts to achieve a consistent classification scheme based on the complete S1 gene, the genetic characterization of infectious bronchitis virus (IBV) is often performed on partial S1 regions due to economic and time constraints in the diagnostic routine. Sanger sequencing remains the most common and cost-effective option even if the analysis of samples where multiple field and vaccine strain populations coexist can lead to partial or misleading results. The present study aimed to evaluate the different diagnostic outcomes of three commonly used RT–PCR methods targeting two regions of the S1 gene. A possible bias in IBV detection and characterization was investigated in relation to the adopted method, the strain concentration as well as their ratio in mixed samples. Thirty samples were prepared by artificially mixing two vaccine strains, combined at different ratios and selected among four different IBV lineages, i.e. GI-1 (Mass), GI-13 (793/B), GI-19 (QX), GI-23 (Israeli Variant 2). Sequence analysis was conducted both manually and with bioinformatic methods. The result agreement among methods, replicates and analysis approaches was statistically evaluated. Consistent results emerged among the three assays, with a few discrepancies likely caused by primer affinity and target amount. This study confirms the complexity of IBV strain identification and highlights the importance of evaluating and updating the available diagnostic assays for a reliable detection of all circulating IBV strains.

ARTICLE HISTORY

Received 4 February 2021
Accepted 20 July 2021

KEYWORDS

Infectious bronchitis virus; diagnosis; RT–PCR; sequencing; assay comparison; genotyping; bioinformatics

Introduction


Infectious bronchitis virus (IBV), classified within the avian coronavirus species, is the cause of infectious bronchitis (IB), which is still one of the most burdensome and frequent diseases in poultry, affecting both bird health and management costs (Jackwood *et al.*, 2012). The clinical manifestations are generally characterized by respiratory signs, and a reduction in growth and egg-laying, and they are commonly controlled by biosecurity measures and vaccination (Jackwood & De Wit, 2020). To achieve the widest cross-protection levels, different vaccine strains have historically been associated and administered together (Cook *et al.*, 1999; Terregino *et al.*, 2008; Awad *et al.*, 2016), at least in Europe, where Mass-based (GI-1) vaccines are commonly combined with either a 793/B-based (GI-13) vaccine or a vaccine based on locally circulating strains (Franzo *et al.*, 2016) to provide homologous protection.

Nonetheless, this well-known strategy based on the association of different strains and/or multiple administrations (Jordan, 2017) presents some drawbacks other than the direct costs. Typically, IBV vaccines are attenuated and can replicate and persist for a

long time in birds (Tucciarone *et al.*, 2018). Since the induced immunity is not sterilizing, coinfection with field strains can occur, increasing the likelihood of recombination events (Jackwood, 2012). Moreover, it has been proven that some vaccines can persist at the population level as long as they are administered to the flocks (Franzo *et al.*, 2014). Therefore, the simultaneous presence of several strains confuses both the epidemiological picture (Legnardi *et al.*, 2019) and the diagnostic process.

The coinfection issue is particularly challenging considering that routine diagnostic assays are typically unable to identify more than one strain at the same time. The identification of multiple strains within one sample can be obtained only by screening with several genotype-specific molecular assays or by using deep sequencing techniques, the costs of which often make them unviable options for everyday use. For IBV characterization, routine diagnosis mainly relies on RT–PCR and Sanger sequencing, making the best of costs, rapidity and efficiency of the assays. However, no standardized protocol has been defined, and each laboratory adopts different assays in the attempt to keep up with local epidemiology, IBV

CONTACT Giovanni Franzo  giovanni.franzo@unipd.it

 Supplemental data for this article can be accessed at <https://doi.org/10.1080/03079457.2021.1959897>.

© 2021 Houghton Trust Ltd

evolution and technological progress (De Wit, 2000). In fact, due to the extreme genetic variability of IBV (Valastro *et al.*, 2016), the selection of a single assay able to identify every strain appears impossible and requires the careful evaluation and update of current methods, accounting for the virus propensity to evolve rapidly, the local epidemiological situation and administered vaccines. While a relevant amount of information can still be achieved by RT-PCR followed by sequencing, this technique is not free from limitations, primarily the inability to identify minor viral sub-populations and coinfections, and can also be affected by possible flaws in the RT-PCR process, such as poor sensitivity and specificity.

In an attempt to evaluate the influence of the diagnostic method and operator interpretation on the diagnostic outcome, this study was designed to compare (both manually, and with a bioinformatic approach) the results of three common RT-PCR assays followed by Sanger sequencing, on artificially coinfecting samples.

Materials and methods

Sample preparation, amplification and sequencing

Four common vaccines based on GI-1 (Mass), GI-13 (793/B), GI-19 (QX), and GI-23 (Israeli Variant 2) lineages were selected and RNA was extracted using High Pure Viral RNA Kit (Roche, Basel, Switzerland) following the manufacturer's instructions.

Samples were tested with a real-time RT-PCR targeting the UTR region (Callison *et al.*, 2006), and diluted in order to achieve a comparable initial concentration (C_T value ~ 18) for each vaccine. These were considered as starting samples (SD, starting dilution) for the artificial coinfection reproduction. Each SD was diluted again at 1:100 (-2) and 1:10,000 (-4) and mixed with another vaccine dilution, to produce 30 samples (Supplementary Table 1).

Samples were then amplified in triplicate with the following RT-PCR assays:

- Method A, a one-step RT-PCR performed with primers XCE1+ and XCE2- (Cavanagh *et al.*, 1999);
- Method B, a two-step nested RT-PCR performed with primers SX1+ and SX2-, SX3+ and SX4- (Worthington *et al.*, 2008);
- Method C, a one-step RT-PCR performed with primers IBV260+ and IBV548- (Valastro *et al.*, 2010).

Assay A was performed using the SuperScript™ III One-Step RT-PCR System with Platinum™ Taq DNA Polymerase kit (Invitrogen™, Waltham, MA, USA), assay C with the QIAGEN OneStep RT-PCR Kit

(QIAGEN, Hilden, Germany), whereas the retrotranscription phase of assay B was performed separately with the High-Capacity cDNA Reverse Transcription Kit (Applied Biosystems™, Waltham, MA, USA) and the following PCRs were performed with the Platinum™ Taq DNA Polymerase Kit (Invitrogen, USA).

Products were visualized by capillary gel electrophoresis. Amplicons were Sanger sequenced in both directions with the same primers that were also used in the amplification. Chromatograms were both manually inspected and automatically analysed with bioinformatic means.

Operator-driven analysis and lineage classification

For the manual analysis, chromatograms were visually inspected for a preliminary quality check, and trimmed to remove the primer sequence using FinchTV software (Geospiza, Inc., Seattle, WA, US). Sequences were copied in FASTA format before and after the consensus assembly with ChromasPro 2.1.8 (Technelysium Pty Ltd, Brisbane, QLD, Australia). Consensus, forward and reverse sequences were aligned to the vaccine reference sequences, and a phylogenetic tree was reconstructed within assay to allow a comparison of the characterization outcome.

Read quality evaluation and automatic lineage classification

The operator-independent chromatogram analysis was performed in R using the sangeranalyseR library. Briefly, chromatograms were automatically trimmed in the regions with a Phred quality score lower than 20. Since coinfection can lead to double peaks, the occurrence of these events was annotated. A ratio of 0.2 of the height of the secondary peak to the primary peak was selected to differentiate random noise from actual sub-population presence.

A database was created including the following features for each chromatogram: raw read length, trimmed read length, mean raw read quality, mean trimmed read quality, number of secondary peaks in the raw and trimmed sequences. Additionally, composite measures were created describing the percentage of information lost after trimming compared to the expected read length. Similarly, the percentage of nucleotide positions with double peak evidence was calculated.

The effect of different methods, vaccine and dilution combination on mean trimmed quality, secondary peaks and percentage of information lost were statistically evaluated using a mixed linear model, accounting for the same samples being tested in multiple runs for different methods. All models

were fitted using the nlme (Pinheiro *et al.*, 2019) library in R 3.4.4, and the statistical significance of each model improvement over simpler ones was assessed by the likelihood-ratio test.

When forward and reverse chromatograms of adequate quality were available, the respective FASTA files were generated as well as consensus sequences. For each method, the obtained sequences were aligned with the respective references and a neighbor-joining phylogenetic tree based on the p-distance was reconstructed using MEGA X (Kumar *et al.*, 2018) to classify them. The agreement between runs, methods, manual and automatic classification was assessed by calculating the Fleiss' kappa (K) using the irr library in R. The statistical significance level was set to P -value < 0.05 for all mentioned tests.

Results

All 30 combinations tested positive by every RT-PCR method and run, and therefore a total of 270 amplicons was obtained and then Sanger sequenced.

Operator-driven analysis and lineage classification

Overall, 212 out of 270 (78.5%) forward, 209 reverse (77.4%) and 197 (72.9%) consensus sequences of adequate quality were obtained. In detail, 21, 26, 22 consensus sequences were assembled in the three runs for method A; 24, 24, 24 for method B; and 18, 18, 20 for method C (Table 1). Method B globally yielded the highest number of sequences and appeared the most reproducible method. Forward and reverse sequences were always concordant, although, in some cases, only the forward or reverse sequence was obtained, hence preventing the consensus assembly. Generally, samples with a low and similar amount of vaccines were sequenced with difficulty, especially with methods A and C, whereas method B seemed affected by a more prominent within-run variability (Table 2). A substantial agreement ($K = 0.645$; P -value < 0.001) was observed among methods and among runs, within the method, while the agreement among forward and reverse reads was almost perfect ($K = 0.860$).

Read quality evaluation and automatic lineage classification

Overall, 192 out of 270 (71.1%) forward sequences, 190 (70.4%) reverse sequences, and 190 (70.4%) consensus sequences of adequate quality were obtained. In detail, 19, 23, 20 consensus sequences in the three runs for method A; 23, 24, 24 for method B; and 19, 16, 22 for method C were assembled (Table 1).

A moderate agreement ($K = 0.410$; P -value < 0.001) was observed among methods, although it was

significantly depressed by the disagreement among N.S. reads. On the other hand, the agreement among runs within method was substantial ($K = 0.68$; P -value < 0.001), whereas the agreement among forward and reverse reads was almost perfect ($K = 0.99$; P -value < 0.001) (Table 2).

Finally, the overall agreement between operator-driven and automatic classification was almost perfect ($K = 0.892$; P -value < 0.001) (Table 2).

Additionally, the following features were selected to evaluate the effect of different experimental conditions on the read quality:

- (1) average Phred score after trimming;
- (2) % of information lost due to poor quality region trimming;
- (3) % of secondary peaks in the read after trimming.

Independently of the considered outcome, the effect of RT-PCR method, lineage and dilution combinations was proven to be statistically significant, as well as their interaction (Table 3).

While the significant effect of so many independent variables makes a point by point dissertation challenging, some main trends can be identified. Independently of the method, the most challenging reads were obtained when both lineages were present at low viral titre (Figures 1 and 2). On the contrary, the combination of high and low viral titres for different lineages guaranteed the overall best performances. Besides, different methods revealed different performances depending on the tested lineage combination. The presence of double peaks appears more influenced by the ratio of the two lineages rather than the absolute titre. However, an effect of the particular combination of method and lineage was also clear in this case (Figure 3).

Discussion

The present study systematically evaluated the effect of co-infection, at variable ratios, with different IBV lineages on commonly applied diagnostic assays, followed by Sanger sequencing, thus simulating a regular scenario of the everyday diagnostic process. For this reason, four vaccines were selected to represent the most frequently encountered genotypes in the routine diagnostic activity, at least in Europe. The use of vaccines rather than isolated field strains was necessary to ensure the presence of a single population in the specimen.

An undeniable impact of all tested variables on the chromatogram quality was observed (Figure 1), thus leading to an extremely complex pattern and poor outcome predictability. Each method performed differently based on the combination of lineages involved and their ratio, as demonstrated by the statistical

Table 1. Summary of sample classification into lineages based on forward and reverse reads and consensus sequences obtained from the 270 amplicons.

	Method	Lineage	Consensus per run			Forward per run			Reverse per run			
			1	2	3	1	2	3	1	2	3	
Operator-driven analysis	A	GI-1 (Mass)	4	5	4	5	6	4	4	6	4	
		GI-13 (793/B)	8	11	9	8	11	9	9	11	9	
		GI-19 (QX)	4	3	3	4	3	3	4	3	3	
		GI-23 (Var2)	5	7	6	6	7	7	5	7	6	
		Total	21	26	22	23	27	23	22	27	22	
	B	N.S.	9	4	8	7	3	7	8	3	8	
		GI-1 (Mass)	8	8	10	8	8	10	10	8	10	
		GI-13 (793/B)	12	13	10	12	13	10	12	13	11	
		GI-19 (QX)	–	–	–	–	–	–	–	–	–	
		GI-23 (Var2)	4	3	4	4	3	5	5	3	5	
	C	Total	24	24	24	24	24	25	27	24	26	
		N.S.	6	6	5	6	6	5	3	6	4	
		GI-1 (Mass)	4	3	4	4	4	5	6	3	5	
		GI-13 (793/B)	6	9	9	7	9	11	6	9	9	
		GI-19 (QX)	6	3	4	8	3	5	6	4	5	
	All	GI-23 (Var2)	2	3	3	3	4	3	2	3	3	
		Total	18	18	29	22	20	24	20	19	22	
		N.S.	12	12	10	8	10	6	10	11	8	
		Total	197/270 (72.9%)			212/270 (78.5%)			209/270 (77.4%)			
		Total	197/270 (72.9%)			212/270 (78.5%)			209/270 (77.4%)			
	Automatic genotype classification	A	GI-1 (Mass)	4	4	4	4	4	4	4	4	4
			GI-13 (793/B)	8	11	9	8	11	9	8	11	9
			GI-19 (QX)	3	3	3	3	3	3	3	3	3
			GI-23 (Var2)	4	5	4	4	5	4	4	5	4
Total			19	23	20	19	23	20	19	23	20	
B		N.S.	11	7	10	11	7	10	11	7	10	
		GI-1 (Mass)	9	8	10	9	8	10	9	8	10	
		GI-13 (793/B)	11	13	10	12	13	10	11	13	10	
		GI-19 (QX)	–	–	–	–	–	–	–	–	–	
		GI-23 (Var2)	3	3	4	3	3	5	3	3	4	
C		Total	23	24	24	24	24	25	23	24	24	
		N.S.	6	6	5	6	6	5	7	6	6	
		GI-1 (Mass)	5	2	5	5	2	5	5	2	5	
		GI-13 (793/B)	6	8	10	6	8	10	6	8	10	
		GI-19 (QX)	6	3	4	6	3	4	6	3	4	
All		GI-23 (Var2)	2	3	3	2	3	3	2	3	3	
		Total	19	16	22	19	16	22	19	16	22	
		N.S.	11	14	8	11	14	8	11	14	8	
		Total	190/270 (70.4%)			192/270 (71.1%)			190/270 (70.4%)			
		Total	190/270 (70.4%)			192/270 (71.1%)			190/270 (70.4%)			

Note: The count has been divided according to the diagnostic method, run replicate and analytical approach (operator-driven/automatic classification). N.S. = not sequencable. Method A: (Cavanagh *et al.*, 1999); B (Worthington *et al.*, 2008); C (Valastro *et al.*, 2010).

significance of interactions for all considered outcomes (i.e. read quality, information loss and double peak presence) (Figures 1–3). Despite this, some general patterns could still be highlighted.

The presence of an equal template amount was definitely the most challenging scenario, leading to an average lower read quality and the presence of a higher percentage of double peaks, with the partial exception of method B (Figure 3). A comparable template amount can, in fact, lead to a similar ratio of amplicons and comparable fluorescence during

Sanger sequencing. The percentage of lost information was also affected (Figure 2), since a more intensive trimming was requested in case of a similar template amount. However, this was particularly severe at the lowest dilutions, suggesting a limit of the RT-PCR process rather than sequencing. The lineage effect is likely due to the differential primer affinity, and the overall outcome was further magnified by the interaction between these factors (Table 3, Figures 1–3).

In addition to a decreasing sequence quality, sequence exclusion due to mixed templates also

Table 2. Summary of *K* values of agreement among methods, runs and sequencing direction within analytic approach (operator-driven and automatic genotype classification) and between the two analytic approaches (*P*-value < 0.001).

Agreement K	Operator-driven analysis			Automatic genotype classification			Between operator-driven and automatic genotype classification
	Among methods	Among runs	Among forward and reverse	Among methods	Among runs	Among forward and reverse	
Overall	0.645	0.654	0.860	0.410	0.680	0.990	0.892
GI-13 (793/B)	0.773	0.798	0.958	0.659	0.784	0.991	0.969
GI-1 (Mass)	0.743	0.751	0.863	0.492	0.782	1.000	0.909
GI-19 (QX)	0.777	0.777	0.892	0.307	0.802	1.000	0.937
GI-23 (Var2)	0.736	0.722	0.898	0.574	0.750	0.982	0.865
N.S.	0.266	0.290	0.687	0.052	0.415	0.982	0.788

Note: Var 2: Israeli Variant 2; N.S.: not sequencable.

Table 3. Summary of the statistical significance of independent variables (i.e. diagnostic method, vaccine and dilution combination) for the considered outcome of interest.

	Variable	Chisq	Df	P-value
Average quality	Method	25.5173	2	<2.2e-16
	Dilution Combination	1.7882	4	0.002877
	Vaccine Combination	20.2766	5	0.001109
	Method:Dilution Combination	34.5755	8	0.0003194
	Method:Vaccine Combination	65.6222	10	3.081E-07
	Dilution Combination: Vaccine Combination	39.2442	20	0.006216
	Method:Dilution Combination: Vaccine Combination	119.6775	40	7.1E-07
	Percentage of lost information	Method	25.7565	2
Dilution Combination		0.1348	4	0.997827
Vaccine Combination		19.6651	5	0.001444
Method:Dilution Combination		18.6311	8	0.016962
Method:Vaccine Combination		67.8230	10	<0.001
Dilution Combination: Vaccine Combination		29.5777	20	0.076991
Method:Dilution Combination: Vaccine Combination		72.4347	40	0.001276
Percentage of secondary peaks		Method	30.8671	2
	Dilution Combination	1.4068	4	0.8430049
	Vaccine Combination	21.8664	5	0.0005551
	Method:Dilution Combination	38.7083	8	5.567E-05
	Method:Vaccine Combination	65.4242	10	3.362E-07
	Dilution Combination: Vaccine Combination	42.2161	20	0.0025917
	Method:Dilution Combination: Vaccine Combination	102.8153	40	0.0001957

Note: Both main effects and interactions (coded by “:”) are reported.

occurred, just as it can happen during the diagnostic activity when a confident characterization cannot be achieved. In this framework, the subjective evaluation of the operator could significantly discern if the reads can be retained or excluded, or affect the length of the trimmed regions, potentially leading to a different percentage of reads that were not sequencable (N.S. reads) or lineage classification. Even if understandable from a technical perspective, this last circumstance can cause misleading results, complicating the interpretation of the epidemiological scenario or leading to a decrease in clients’ trust. For this reason, the common operator-dependent approach was compared to an automatic approach, and the agreement between them was assessed, as well as the agreement among methods, runs and sequencing direction (i.e. forward or reverse).

The agreement among methods in lineage classification was substantial in most instances, although lower for the automatic approach. However, the main source of disagreement was represented by the N.S. reads, where a much higher variability was

observed. This evidence was particularly clear for the automatic approach, where the presence of fixed cut-offs for exclusion led to the discordant exclusion of “borderline” reads. Conversely, a well-trained operator was able to preserve a higher number of reads and therefore of consensus sequences.

The inability to achieve a sequence can have serious implications under field conditions, including false-negative results if the diagnostic protocol requires sequencing confirmation, costs for sample retesting, or at least the lack of a proper classification of the detected strains (i.e. field/vaccine strain, lineage, historical or emerging/recently introduced strain), severely hampering our control capabilities.

Although much less marked, the imperfect agreement among methods in the final lineage outcome can also lead to misleading results. The primer affinity for different templates clearly plays a role in this sense. For example, the genotype detected with method A corresponded mainly to the most abundant strain in the sample, with the sole exception of one sample composed by low concentration of GI-19 (QX) and GI-23 (Israeli Variant 2) vaccines, which was identified as GI-19 (QX) in the first run and as GI-23 (Israeli Variant 2) in the second (data not shown). This inconsistency could come from the randomness in primer annealing when the target templates have a similar concentration and from the rapid excess of amplification of one strain over the other. With method B, the most frequently detected strain was GI-13 (793/B), reflecting a primer affinity that was probably intensified by the three-phased process (cDNA synthesis and double amplification). Remarkably, the GI-19 (QX) vaccine was never identified by this method. A more focused analysis highlighted that the primers of the first PCR round presented the highest number of mismatches with GI-19 (QX) lineage (up to five mismatches in the forward primers, up to six in the reverse primers) (data not shown), thus supporting the primer-affinity hypothesis. On the contrary, method C was particularly efficient in detecting GI-19 (QX), since this assay was expressly validated for this purpose (Valastro *et al.*, 2010). Method C appeared heavily affected by the presence of multiple strains in the samples though, resulting in low-quality to unreadable sequences.

Even so, a generally high agreement was observed among different runs, suggesting that the final output is the result of a deterministic process, influenced by template concentration and primer affinity, rather than a stochastic one. Also in this case, the most common discrepancies were related to discarded reads. Unfortunately, the complexity of the observed patterns makes this process hardly predictable. Additionally, it must be stressed that the observed results were obtained with reference vaccine strains, leaving out the evaluation of how the within-lineage heterogeneity

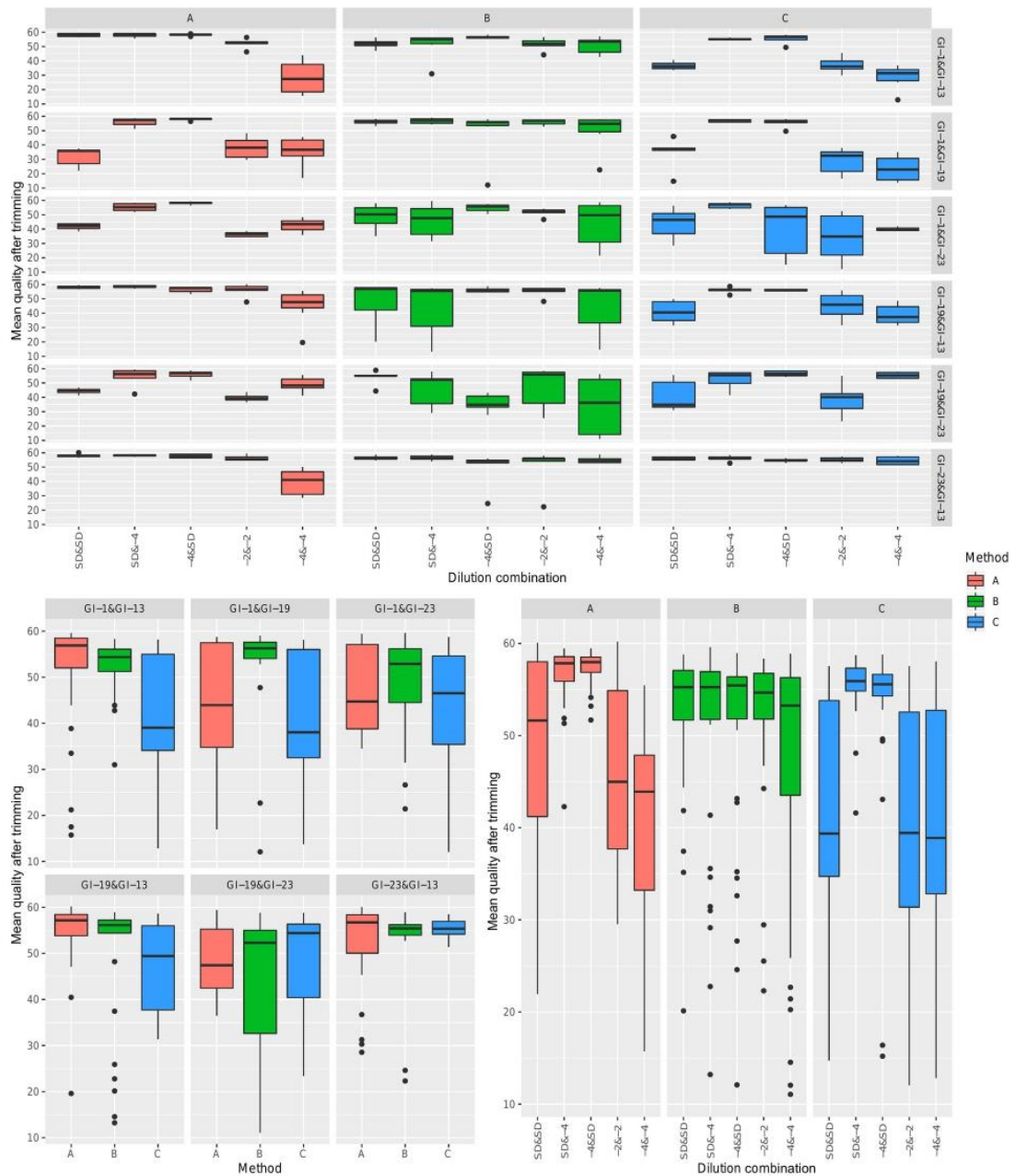


Figure 1. Boxplot reporting the distribution of average read quality after automatic trimming. Different diagnostic methods have been colour-coded. In the upper figure, score values have been faceted based on both vaccine and dilution combination. The overall effect of vaccine combination or dilution has been reported in the lower left and right panels, respectively.

could affect primer affinity and the relative sequencing results. Finally, an almost perfect agreement was proven between forward and reverse reads, testifying that the strain classification is determined by RT-PCR reaction dynamics rather than sequencing dynamics.

Overall, the present study discloses how a standardized laboratory process could still influence the results when working on tricky samples. Although Sanger sequencing can give some hints of mixed populations, such as by the presence of a strong background

signal or double peaks, the method itself is not suited for detecting more than one strain. Therefore, while an expert laboratory worker can inform field veterinarians of such evidence, further insights into the actual coinfection composition are prevented. Neither the automatic nor the operator-driven approach was able to effectively deal with the presence of coinfections in the achievement of a confident characterization, which was significantly determined by the selected diagnostic method. Human operators are

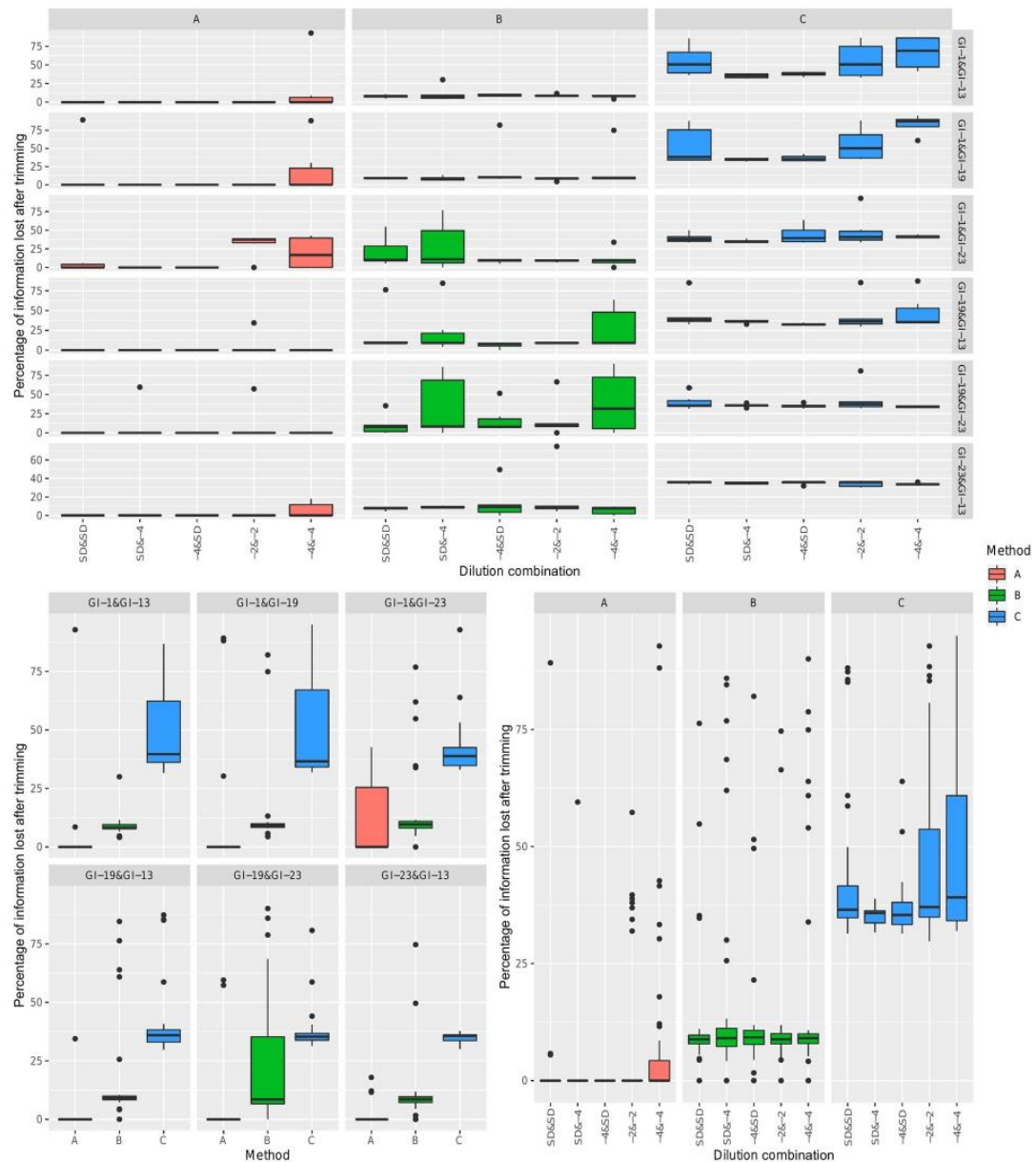


Figure 2. Boxplot reporting the distribution of percentage of information lost due to trimming. Different diagnostic methods have been colour-coded. In the upper figure, values have been faceted based on both vaccine and dilution combination. The overall effect of vaccine combination or dilution has been reported in the lower left and right panels, respectively.

generally able to more efficiently retain and interpret poor quality sequences, which are typically excluded by automatic approaches. While this could represent an economical and practical advantage for the veterinarians in everyday diagnostic activity, the effect of such subjective, operator-based, sequence evaluation should be carefully evaluated and accounted for when more precise epidemiological studies are the final target.

It cannot be underemphasized that, although some “general” rules were identified in the specific cases, the complexity of the interactions among the considered

variables, including specific lineage pairs and their concentration, prevents any inference or prevision on the method performances in unknown field samples. Additionally, the experimental conditions poorly represent the field conditions, where samples are frequently coinfecting but rarely contain equally concentrated strains, further complicating the diagnostic scenario.

Even if the evaluation of the different outcome and possible determinants of this variability aimed to assist in the choice of the diagnostic assay, a decisive answer is impossible to obtain and different assays exhibited

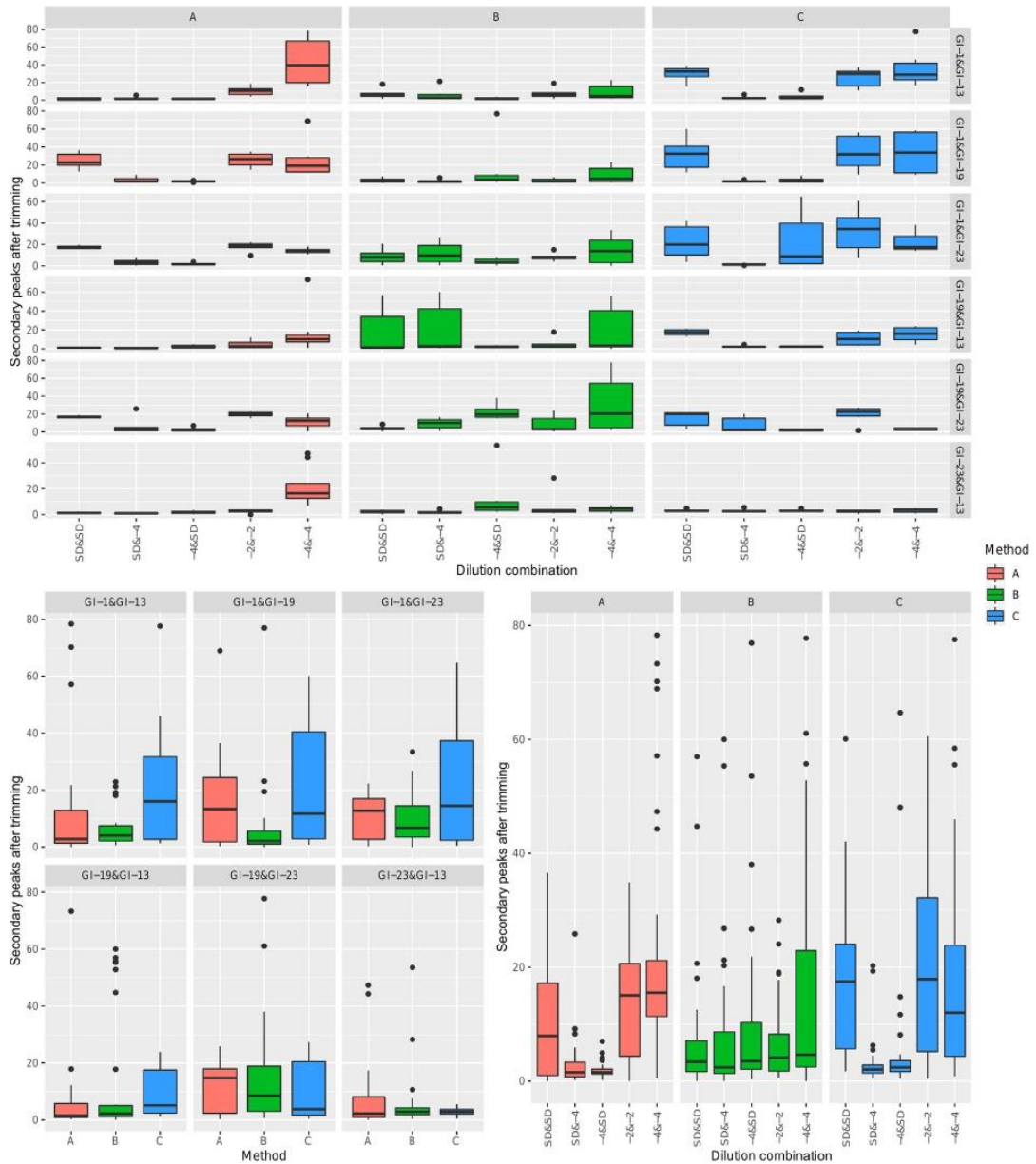


Figure 3. Boxplot reporting the distribution of the percentage of secondary peaks in the read after trimming. Different diagnostic methods have been colour-coded. In the upper figure, values have been faceted based on both vaccine and dilution combination. The overall effect of vaccine combination or dilution has been reported in the lower left and right panels, respectively.

pros and cons. The variability of the target region, the primer design and assay update including the emerging strains are only a few of the elements that can influence the performances of the diagnostic process.

The choice of the diagnostic assay should be based on the specific diagnostic purpose and consider all available elements indicating the presence of multiple strains, such as recent vaccination, clinical symptoms and epidemiological data. Information about the vaccination protocol could facilitate the interpretation of the results or suggest the use of a strain-specific assay to specifically detect, in light of a particular clinical

suspicion, the most likely field strain rather than a co-infecting vaccine one. Otherwise, in complete absence of indications, the least biased assay should be preferred, aiming to identify the prevalent strain, still acknowledging the possibility of other undetected strains, and being aware of potentially misleading results, the occurrence of which is largely unpredictable *a priori*.

Based on these considerations, a diagnostic algorithm combining several assays with different designs and features, should be developed to process difficult samples and assist in the achievement of a truthful

characterization of the strain composition of the samples.

Disclosure statement

No potential conflict of interest was reported by the authors.

References

- Awad, F., Hutton, S., Forrester, A., Baylis, M. & Ganapathy, K. (2016). Heterologous live infectious bronchitis virus vaccination in day-old commercial broiler chicks: clinical signs, ciliary health, immune responses and protection against variant infectious bronchitis viruses. *Avian Pathology*, 45, 169–177.
- Callison, S.A., Hilt, D.A., Boynton, T.O., Sample, B.F., Robison, R., Swayne, D.E. & Jackwood, M.W. (2006). Development and evaluation of a real-time Taqman RT-PCR assay for the detection of infectious bronchitis virus from infected chickens. *Journal of Virological Methods*, 138, 60–65.
- Cavanagh, D., Mawditt, K., Britton, P. & Naylor, C.J. (1999). Longitudinal field studies of infectious bronchitis virus and avian pneumovirus in broilers using type-specific polymerase chain reactions. *Avian Pathology*, 28, 593–605.
- Cook, J.K.A., Orbell, S.J., Woods, M.A. & Huggins, M.B. (1999). Breadth of protection of the respiratory tract provided by different live-attenuated infectious bronchitis vaccines against challenge with infectious bronchitis viruses of heterologous serotypes. *Avian Pathology*, 28, 477–485.
- De Wit, J.J. (2000). Detection of infectious bronchitis virus. *Avian Pathology*, 29, 71–93.
- Franzo, G., Naylor, C.J., Lupini, C., Drigo, M., Catelli, E., Listorti, V., Pesente, P., Giovanardi, D., Morandini, E. & Cecchinato, M. (2014). Continued use of IBV 793B vaccine needs reassessment after its withdrawal led to the genotype's disappearance. *Vaccine*, 32, 6765–6767.
- Franzo, G., Tucciarone, C.M., Blanco, A., Nofrarías, M., Biarnés, M., Cortey, M., Majó, N., Catelli, E. & Cecchinato, M. (2016). Effect of different vaccination strategies on IBV QX population dynamics and clinical outbreaks. *Vaccine*, 34, 5670–5676.
- Jackwood, M.W. (2012). Review of infectious bronchitis virus around the world. *Avian Diseases*, 56, 634–641.
- Jackwood, M.W. & De Wit, S. (2020). Infectious bronchitis. In David E. Swayne, Martine Boulianne, Catherine M. Logue, Larry R. McDougald, Venugopal Nair, David L. Suarez, Sjaak de Wit, Tom Grimes, Deirdre Johnson, Michelle Kromm, Teguh Yodiantara Prajitno, Ian Rubinoff & Guillermo Zavala (Eds.). *Diseases of Poultry*, 14th edn (pp. 167–188). Hoboken, NJ: Wiley.
- Jackwood, M.W., Hall, D. & Handel, A. (2012). Molecular evolution and emergence of avian gammacoronaviruses. *Infection, Genetics and Evolution*, 6, 1305–1311.
- Jordan, B. (2017). Vaccination against infectious bronchitis virus: a continuous challenge. *Veterinary Microbiology*, 206, 137–143.
- Kumar, S., Stecher, G., Li, M., Knyaz, C. & Tamura, K. (2018). MEGA x: molecular evolutionary genetics analysis across computing platforms. *Molecular Biology and Evolution*, 35, 1547–1549.
- Legnardi, M., Franzo, G., Koutoulis, K.C., Wiśniewski, M., Catelli, E., Tucciarone, C.M. & Cecchinato, M. (2019). Vaccine or field strains: the jigsaw pattern of infectious bronchitis virus molecular epidemiology in Poland. *Poultry Science*, 98, 6388–6392.
- Pinheiro, J., Bates, D., DebRoy, S., Sarkar, D. & Team, R.C. (2019). nlme: linear and nonlinear mixed effects models. *R Package*, 3, 1–117.
- Terregino, C., Toffan, A., Serena Beato, M., De Nardi, R., Vascellari, M., Meini, A., Ortali, G., Mancin, M. & Capua, I. (2008). Pathogenicity of a QX strain of infectious bronchitis virus in specific pathogen free and commercial broiler chickens, and evaluation of protection induced by a vaccination programme based on the Ma5 and 4/91 serotypes. *Avian Pathology*, 37, 487–493.
- Tucciarone, C.M., Franzo, G., Berto, G., Drigo, M., Ramon, G., Koutoulis, K.C., Catelli, E. & Cecchinato, M. (2018). Evaluation of 793/B-like and mass-like vaccine strain kinetics in experimental and field conditions by real-time RT-PCR quantification. *Poultry Science*, 97, 303–312.
- Valastro, V., Holmes, E.C., Britton, P., Fusaro, A., Jackwood, M.W., Cattoli, G. & Monne, I. (2016). S1 gene-based phylogeny of infectious bronchitis virus: an attempt to harmonize virus classification. *Infection, Genetics and Evolution*, 39, 349–364.
- Valastro, V., Monne, I., Fasolato, M., Cecchetti, K., Parker, D., Terregino, C. & Cattoli, G. (2010). QX-type infectious bronchitis virus in commercial flocks in the UK. *Veterinary Record*, 167, 865–866.
- Worthington, K.J., Currie, R.J.W. & Jones, R.C. (2008). A reverse transcriptase-polymerase chain reaction survey of infectious bronchitis virus genotypes in Western Europe from 2002 to 2006. *Avian Pathology*, 37, 247–257.

CHAPTER 5:

A NOVEL ARRAY OF REAL-TIME RT-PCR ASSAYS FOR THE RAPID PATHOTYPING OF TYPE I AVIAN PARAMYXOVIRUS (APMV-1)

Fortin, A., Laconi, A., Monne, M., Zohar, S., Andersson, K., Grund, C., Cecchinato, M., Crimardo, M., Valastro, V., D'Amico, V. et al

Journal of Virological Methods 2023, accepted in press

A novel array of real-time RT-PCR assays for the rapid pathotyping of type I avian paramyxovirus (APMV-1)

Andrea Fortin^{1,5}, Andrea Laconi², Isabella Monne¹, Siamak Zohari³, Kristofer Andersson³, Christian Grund⁴, Mattia Cecchinato⁵, Marika Crimauo¹, Viviana Valastro¹, Valeria D'Amico¹, Alessio Bortolami¹, Michele Gastaldelli¹, Maria Varotto¹, Newcastle Disease Collaborating Diagnostic Group[†], Calogero Terregino¹, Valentina Panzarin^{1,*}

¹ EU/WOAH/National Reference Laboratory for Avian Influenza and Newcastle Disease, FAO Reference Centre for Animal Influenza and Newcastle Disease, Division of Comparative Biomedical Sciences, Istituto Zooprofilattico Sperimentale delle Venezie (IZSve), 35020 Legnaro, Italy; afortin@izsvenezie.it; imonne@izsvenezie.it; mcrimauo@izsvenezie.it; vvalastro@izsvenezie.it; vdamico@izsvenezie.it; abortolami@izsvenezie.it; mgastaldelli@izsvenezie.it; mvarotto@izsvenezie.it; cterregino@izsvenezie.it; ypanzarin@izsvenezie.it

² Department of Comparative Biomedicine and Food Science, University of Padua (Unipd), 35020 Legnaro, Italy; andrea.laconi@unipd.it

³ Department of Microbiology, Swedish National Veterinary Institute (SVA), SE751 89 Uppsala, Sweden; siamak.zohari@sva.se; kristofer.andersson@sva.se

⁴ Institute of Diagnostic Virology, Federal Research Institute for Animal Health, Friedrich-Loeffler-Institut (FLI), 17493 Greifswald Insel-Riems, Germany; Christian.Grund@fli.de

⁵ Department of Animal Medicine, Production and Health, University of Padua (Unipd), 35020 Legnaro, Italy; mattia.cecchinato@unipd.it

[†] The Newcastle Disease Collaborating Diagnostic Group members are listed in Appendix A.

* Corresponding author: ypanzarin@izsvenezie.it (V. Panzarin).

Abstract

Newcastle disease (ND) caused by virulent avian paramyxovirus type I (APMV-1) is a WOAH and EU listed disease affecting poultry worldwide. ND exhibits different clinical manifestations that may either be neurological, respiratory and/or gastrointestinal, accompanied by high mortality. In contrast, mild or subclinical forms are generally caused by lentogenic APMV-1 and are not subject to notification. The rapid discrimination of virulent and avirulent viruses is paramount to limit the spread of virulent APMV-1. The appropriateness of molecular methods for APMV-1 pathotyping is often hampered by the high genetic variability of these viruses that affects sensitivity and inclusivity. This work presents a new array of real-time RT-PCR (RT-qPCR) assays that enable the identification of virulent and avirulent viruses in dual mode, i.e., through pathotype-specific probes and subsequent Sanger sequencing of the amplification product. Validation

was performed according to the WOAHP recommendations. Performance indicators on sensitivity, specificity, repeatability and reproducibility yielded favourable results. Reproducibility highlighted the need for assays optimization whenever major changes are made to the procedure. Overall, the new RT-qPCRs showed its ability to detect and pathotype all tested APMV-1 genotypes and its suitability for routine use in clinical samples.

Keywords: avian paramyxovirus type I (APMV-1); Newcastle disease; molecular pathotyping; virulent; avirulent.

1. Introduction

Avian paramyxoviruses type 1 (APMV-1) of the *genus* Avian orthoavulavirus 1 (AOaV-1) (ICTV, 2017) have been reported in over 240 domestic and wild bird species worldwide (Barbezange and Jestin, 2003; Jindal et al., 2009; Hoque et al., 2012; Snoeck et al., 2013; Dodovski et al., 2017; Napp et al., 2017; Absalón et al., 2019; Hicks et al., 2019; Mansour et al., 2021; Steensels et al., 2021; Mngumi et al., 2022; Nooruzzaman et al., 2022; Sun et al., 2022; Wang et al., 2022; Goraichuk et al., 2023) and display considerable variation in their pathogenicity, i.e., from subclinical infections to acute disease with high mortality, depending on the strain and host factors (Suarez et al., 2020). The severity of clinical signs triggered by viral intracerebral inoculation of 1-day-old SPF chickens (intracerebral pathogenicity index, ICPI) is used as a starting ground to define a harmonized categorization of APMV-1 pathotype as velogenic (i.e., highly virulent strains, viscerotropic or neurotropic), mesogenic (viruses of intermediate virulence producing respiratory and nervous disorders) or lentogenic (i.e., avirulent and low pathogenic viruses causing mild/subclinical signs) (WOAH, 2021). Velogenic and mesogenic APMV-1 strains are formally recognized as causative agents of Newcastle disease (ND), a World Organisation for Animal Health (WOAH) and European Union (EU) listed disease which has become a global economic burden given i) the high mortality in affected poultry and ii) the impact of control measures applied to curtail the spread of the infection. As an alternative to *in vivo* pathogenicity testing, the WOAHP and the EU have accepted sequencing of the cleavage site (CS) of the fusion protein gene precursor (F0) for ND case definition (*Commission Delegated Regulation (EU) 2020/689*, 2019; WOAHP, 2022a). As a matter of fact, the presence of multiple basic amino acids that permit fusion protein cleavability by ubiquitous host proteases (furin-like) and subsequent systemic infection is a predictor of high pathogenicity in chickens. Contrarily, avirulent and low pathogenic viruses are characterized by monobasic CS that limits their intra-host spread (Toyoda et al., 1987; Pritzer et al., 1990; Alexander, 2000; WOAHP, 2021).

The variety of virulence profiles of APMV-1 is accompanied by great genetic diversity, most likely resulting from the extensive viral circulation in poultry and wild birds and from vaccine-induced immune pressure (Ramey et al., 2017). In 2019, the joint effort of a network of experts led to a unified classification of APMV-1 in 2 classes and 21 genotypes, based on the phylogeny of the complete fusion protein gene (F). Class I consists of genotype 1, and three subgenotypes mostly referable to lentogenic viruses detected in wild birds. Class II envisages the highest genetic variability comprising velogenic, mesogenic and lentogenic viruses of

20 genotypes (I-XIV, XVI-XXI) detected in domestic and wild birds, as well as a plethora of subgenotypes and variants with different hierarchical levels (Dimitrov et al., 2019; Twabela et al., 2021). Genotype VI shows the highest genetic diversity and includes the widespread APMV-1 pigeon variant (PPMV-1) (Akhtar et al., 2016; Napp et al., 2017; He et al., 2018; Zhan et al., 2021; Rogers et al., 2021; Ramsubeik et al., 2023). Most of the live vaccine strains used worldwide for the immunization of flocks also derive from class II viruses, more specifically from lentogenic and mesogenic viruses of genotypes I-III (Hu et al., 2022; Mayers et al., 2017).

The rapid recognition of a ND case is of utmost importance so that health authorities may timely establish control measures to prevent the spread of the disease. By far, diagnosticians prefer using molecular methods rather than *in vivo* pathogenicity tests, both for ethical reasons related to animal welfare and for a rapid reporting of laboratory results. However, the sensitivity of such methods is hampered by the high genetic variability among different APMV-1 strains. This complexity is well represented by the variety of assays for APMV-1 characterization ($n \geq 15$) reported by laboratories taking part to the annual proficiency test organized by the EURL for avian influenza (AI) and ND, that highlights the lack of a universal test for APMV-1 pathotyping (data source: EURL Proficiency test AQUA IN 2022 for Avian Influenza and Newcastle Disease, Final Report). The majority of the reported protocols are based on RT-PCR followed by Sanger sequencing of the amplification product, which significantly increases time-to-results. To improve sensitivity, an isolation step in embryonated SPF chicken eggs prior genome amplification might also be performed, further rising turnaround time.

Real-time RT-PCR (RT-qPCR) based on hydrolysis probes would enable faster APMV-1 pathotyping with a higher level of sensitivity and specificity, although their design is challenged by the identification of APMV-1 genome regions discriminative of virulent and avirulent viruses and, at the same time, conserved among genotypes to guarantee assay inclusivity and sensitivity. In the past, several attempts were made to accomplish this ambitious goal (Wise et al., 2004; Kim et al., 2006; Fuller et al., 2009), but the routine use of these methods on newly emerged variants highlighted poor performance. Sabra et al., 2017 modified the assay developed by Kim et al., 2006 to improve detection of pigeon-derived virulent APMV-1 of genotypes VI and XXI from Egypt, Pakistan, South Korea, Ukraine and Bulgaria. More recently, Bhande et al., 2023 have modified the F gene RT-qPCR by Wise et al., 2004 to detect current APMV-1, using a multi sequence alignment (MSA) of genotypes V, VI, VII, XIII, XIX and XXI. These methods base their pathotyping strategy on the detection of virulent strains only and do not foresee a crosscheck with the simultaneous use of oligonucleotide sets targeting lentogenic viruses. This approach may have potential limitations and lead to false negatives, considering the observation of mismatches of these oligonucleotides sets against targeted genotypes currently circulating in Europe (i.e., VI, VII, XIII, XXI) and the poor coverage with respect to untargeted genotypes that might be introduced by migratory birds (Hicks et al., 2019). In addition, as virulent-specific assays do not foresee the detection of lentogenic and avirulent strains in the sample (including live vaccines), the probability of diagnostic dropouts of such pathotype-specific assays increases as a result of the limited replication and lower viral load of virulent strains in infected or vaccinated birds.

This study intends to address the need for a rapid and updated pathotyping system for APMV-1 by developing an array of three RT-qPCRs capable of distinguishing virulent and avirulent viruses, putatively of any current genotype. Discrimination is first accomplished with pathotype specific probes that match the CS sequence of virulent (i.e., velogenic and mesogenic APMV-1 with polybasic CS, hereafter referred as “Vir”) and avirulent (i.e., lentogenic and low pathogenic APMV-1 with monobasic CS, hereafter referred as “Avir”) viruses. For further downstream confirmation, amplification products can undergo Sanger sequencing to determine the F protein CS sequence.

2. Material and methods

2.1. Assays design

The nucleotide sequence of the F gene of APMV-1 strains detected worldwide in different bird species was downloaded from the Virus Pathogen Resource (ViPR) (Pickett et al., 2012) on 4th July 2019.

MAFFT version 7 (Multiple Alignment with Fast Fourier Transform) online server set with default parameters (Kato et al., 2019; Kuraku et al., 2013) was employed to align sequences against class I and class II pilot datasets developed by Dimitrov et al., 2019. Geneious Prime 2020.1.2 (<https://www.geneious.com>) (Biomatters Ltd., Auckland, New Zealand) was used to visualize the MSAs and remove low quality scores yielding datasets of 284 (class I) and 1489 (class II) sequences.

Maximum likelihood phylogenetic trees were generated in IQTREE v1.6.12 (Nguyen et al., 2015) performing an ultrafast bootstrap resampling analysis (1000 replications) (Hoang et al., 2018) and visualized in FigTree v1.4.4 (<http://tree.bio.ed.ac.uk/software/figtree/>). Monophyletic groups within tree topologies were used as a guide to identify conserved regions among different genotypes encompassing the F gene CS.

The Entropy-One online tool freely accessible at the HIV Sequence Database (https://www.hiv.lanl.gov/content/sequence/ENTROPY/entropy_one.html) was used to calculate Shannon entropy $H(i)$ within genotype and amongst different genotypes, in order to assess the level of nucleotide variation within the identified target regions.

The find-duplicates option available in Geneious Prime 2020.1.2 (Biomatters Ltd., Auckland, New Zealand) was employed to collapse the MSAs. Unique sequences were used to develop three independent oligonucleotides sets (i.e., A, B, C) with pathotype-specific probes, to be employed in simultaneous RT-qPCR reactions to cover the entire APMV-1 variability. In detail, SET A targets virulent and avirulent class II viruses of genotypes I-IV, IX-XI; SET B matches virulent and avirulent class II viruses of genotypes V-VIII, XII-XXI; SET C identifies class I lentogenic APMV-1 (Table 1). PCR products length (149-218 bp) covering APMV-1 CS permits Sanger sequencing to further confirm pathotype assignment. Physical properties of primers and probes were determined with the IDT OligoAnalyzer online tool (<https://eu.idtdna.com>) (Leuven, Belgium). Finally, their specificity was cross-checked against lentogenic, mesogenic and velogenic APMV-1 comprised in the datasets with Geneious Prime 2020.1.2 (Biomatters Ltd., Auckland, New Zealand).

Upon completion of the validation process, *in silico* specificity was re-assessed on 24th October 2022, using unpublished sequences newly made available at the IZSvE during routine diagnostic activities.

Table 1. Primers and pathotype-specific probes for class I and class II APMV-1 pathotyping by RT-qPCR.

Set	Oligonucleotide	Sequence 5' → 3'	Nt. position in F gene
A	Class II A for	CTC ACC CCY CTT GGT GA	274-457 ^a
	Class II A rev	GGA GRA TGT TGG CAG CAT T	
	Class II A avir MGB probe	FAM-CCT ATA AGG CGY CCC TGT YTC-MGB	
	Class II A vir MGB probe	CY5-CCT AYA AAG CGT YTC TGY CTC C-MGB	
B	Class II B for	GAR GCA TAY AAC AGA ACA	244-392 ^b
	Class II B rev	GTY GCA ACC CCR AGA GCT A	
	Class II B avir MGB probe	FAM-GAR ACA GGG ACG YCT TAT AGG-MGB	
	Class II B vir MGBa probe	CY5-ARA CGC TTY ATA GGT GC-MGB	
	Class II B vir MGBb probe	CY5-AAR CGY TTT RTA GGT GC -MGB	
C	Class I C for	CMG GGA CAA TTA TCA TCA A	173-390 ^c
	Class I C rev	GGC TAC ACC TAA TGC GA	
	Class I C MGB probe	FAM-CAG GAG CGK TTG RTA GG-MGB	

^a Nucleotide positions refer to strain LaSota (II) with ViPR accession number AF077761.

^b Nucleotide positions refer to strain PPMV-1/02VIR1875/turtledove/Italy/2002 (VI) with ViPR accession number KU377529.

^c Nucleotide positions refer to strain DE-R49/99 (class I) with ViPR accession number DQ097393.

2.2. Experimental settings and optimization of RT-qPCR assays

Pulmonary tissue was obtained from SPF chickens, placed in phosphate buffered saline with antibiotics and antimycotics (10,000 IU/ml penicillin, 10 mg/ml streptomycin, 0.25 mg/ml gentamycin, and 5,000 IU/ml nystatin) (PBSa) in a ratio 1:4 w/v, and homogenized with a stainless steel bead for 3 min at 30 Hz using a TissueLyser II (Qiagen, Hilden, Germany). Supernatant was collected after centrifugation for 2 min at 15000 × g, and artificially contaminated with representative APMV-1 viruses (SET A: APMV-1/turkey/Italy/14VIR7742/2014 (II); SET B: PPMV/peacock/Italy/13VIR1895/2013 (VI.2.1.1.1); SET C: APMV-1/chicken/Bulgaria/11VIR1897/2011 (class I)) at medium and low concentration. Total nucleic acids were purified from spiked samples using the QIASymphony DSP Virus/Pathogen Midi kit (Qiagen, Hilden, Germany) on a QIASymphony SP instrument (Qiagen, Hilden, Germany) (sample volume 300 µl; custom protocol). All the lysates were added with the Intype IC-RNA (Indical Bioscience GmbH, Leipzig, Germany) as foreseen by the upstream APMV-1 screening assay in place at the IZSve (Sutton et al., 2019).

The performance of different RT-qPCR kits (i.e., AgPath-ID One-Step RT-PCR Reagents, Applied Biosystems, Waltham, MA, USA; GoTaq 1-Step RT-qPCR System, Promega Corporation, Madison, WI, USA; QuantiNova Multiplex RT-PCR Kit, (Qiagen, Hilden, Germany); QuantiTect Multiplex RT-PCR Kit, (Qiagen, Hilden, Germany); TaqMan Fast Virus 1-Step Master Mix, Applied Biosystems, Waltham, MA, USA; SuperScript III One-Step RT-PCR System with Platinum Taq DNA Polymerase, Invitrogen, Waltham, MA, USA) was preliminarily evaluated using the above material. The TaqMan Fast Virus 1-Step Master Mix (Applied Biosystems, Waltham, MA, USA) exhibited higher sensitivity and lower quantification cycle (Cq) values and was thus selected for subsequent optimization steps. A multi-parametric grid encompassing different combinations of testing conditions (i.e., annealing temperature, magnesium concentration and oligonucleotides concentration) was developed to determine optimal settings for each assay, as assessed by

clear amplification plots with the lowest C_q values. Samples were analyzed in duplicate under the different parameters combinations employing 5 µl template in a 25 µl reaction mix. Runs were performed on a QuantStudio 5 Real-Time PCR System (Applied Biosystems, Waltham, MA, USA) equipped with VeriFlex blocks allowing different temperature zones, with a ramp/rate of 1.6°C/s. Data were analyzed using the Design & Analysis Software Version 2.6.2 (Applied Biosystems, Waltham, MA, USA), with auto adjustment of the baseline and single threshold manually set at 0.04 ΔRN. Table 2 outlines optimal RT-qPCR conditions for each assay. PCR products were subject to electrophoresis using the QIAxcel Advanced system (Qiagen, Hilden, Germany) to verify their size. Amplicons pre-diluted 1:5 v/v with molecular grade water were sequenced with a 3130xl Genetic Analyzer (Applied Biosystems, Waltham, MA, USA). The above protocol was employed for the entire validation process, except otherwise specified.

Table 2. Optimal experimental settings for the RT-qPCRs array. Primers and probes concentration refers to each oligonucleotide employed in the reaction.

Set	Oligonucleotides concentration	Thermal cycle
A	1 µM primers, 300 nM probes	50°C 5 min; 95°C 20 sec; 45 × [95°C 30 sec, 60°C 45 sec]
B	1 µM primers, 250 nM probes	50°C 5 min; 95°C 20 sec; 45 × [95°C 30 sec, 55°C 45 sec]
C	900 nM primers, 250 nM probe	

2.3. Analytical specificity (ASp)

A wide panel of virulent and avirulent APMV-1 isolates representing different genotypes of class I and II ($n = 66$) and previously characterized by the IZSVe and SVA, was tested to assess the inclusivity of the RT-qPCR array and to verify the correct pathotype definition. The simultaneous testing of all the samples with the three assays allowed a thorough evaluation of their capacity to discriminate between virulent and avirulent viruses. Exclusivity was verified by testing non-target bacteria and viruses of avian species, including different APMV subtypes and avian influenza viruses (AIV). The absence of cross reactivity with sample matrix components was checked by testing APMV-1 negative specimens from birds (swabs, tissue homogenates and PBSa). All samples were tested in duplicate (Supplementary Table S1 – sheet ASp) as reported in paragraph 2.2. Alternatively, samples were processed with the IndiMag Pathogen Kit (Indical Bioscience GmbH, Leipzig, Germany) on a Maelstrom 9600 Nucleic Acid Extractor (TANBead Taiwan Advanced Nanotech Inc., Taoyuan City, Taiwan) and run on a 7500 Fast Real-Time PCR System (ThermoFisher Scientific, Waltham, MA, USA) with a ramp/rate of 3.5°C/s. For these samples, Sanger sequencing of the RT-qPCR products was not performed.

2.4. Limit of detection (LOD) and repeatability

Lung homogenate prepared as described previously was used to serially dilute titrated APMV-1 isolates representing different genotypes ($n = 10$) with diverse levels of match against the oligonucleotide sets developed in the study (Table 3). Spiked samples were analyzed with the respective RT-qPCR assay, based on

the targeted genotype, employing the experimental conditions reported in paragraph 2.2. Each dilution was tested in triplicate in order to determine the LOD (i.e., the highest dilution testing positive by RT-qPCR and yielding the CS sequence). To compare the sensitivity of the pathotyping RT-qPCRs with that of a screening method, the assay by Sutton et al., 2019 was performed in parallel.

Repeatability was tested for APMV-1 showing different analytical sensitivity in lung homogenate and representing either virulent and avirulent strains. In detail, dilutions corresponding to high (i.e., the LOD + $1\log_{10}$) and low (i.e., the LOD) viral titres were analyzed in triplicate on three different days by two operators. Repeatability was expressed as the percent coefficient of variation (%CV) of the C_q values recorded within and between days. Only higher dilutions were subject to Sanger sequencing, as described above.

2.5. Diagnostic performance

Clinical samples with known reactivity as per previous testing performed by the IZS_{Ve} and SVA were used to evaluate the diagnostic performance of the RT-qPCRs array. The panel comprised 59 APMV-1 samples of different genotypes originating from Europe, Asia, Africa and the Middle East and representing a variety of avian species and matrices, as well as 67 APMV-1 negative samples from experimentally challenged chickens (Bortolami et al., 2022; Zamperin et al., 2021) and wild birds (Supplementary Table S1 – sheet DP). Samples were tested with the three RT-qPCR assays followed by Sanger sequencing as described above, in parallel with the screening protocol by Sutton et al., 2019.

2.6. Reproducibility

To assess the reproducibility of the RT-qPCR assays and their capacity to yield consistent results, an inter-laboratory exercise was organized involving the IZS_{Ve}, SVA and FLI. For this purpose, a panel of 11 blind samples (both virulent and avirulent) prepared in PrimeStore MTM (Longhorn Vaccines and Diagnostics, Bethesda, MD, USA) were provided (Supplementary Table S1 – sheet ILR) together with the necessary amplification reagents. The quality standards foreseen by the ISO/IEC 17043:2010 were applied for samples preparation. Each laboratory employed the nucleic acids extraction method (i.e., QIASymphony DSP Virus/Pathogen Midi kit, Qiagen, Hilden, Germany; IndiMag Pathogen Kit, Indical Bioscience GmbH, Leipzig, Germany; QIAamp Viral RNA Mini Kit, Qiagen, Hilden, Germany) and the real-time platforms (i.e., QuantStudio 5 Real-Time PCR System, Applied Biosystems, Waltham, MA, USA with ramp/rate 1.6°C/s; 7500 Fast Real-Time PCR System, ThermoFisher Scientific, Waltham, MA, USA with ramp/rate 3.5 or 1.6°C/s; CFX96 Deep Well Real-Time PCR System, Biorad, Hercules, CA, USA with ramp/rate 3.2°C/s) in place at their facilities. Fleiss' kappa was calculated to measure the agreement among the three laboratories according to the method proposed by (Falotico and Quatto, 2015) and implemented in the package raters (Quatto and Ripamonti, 2022) under the R environment (R Core Team, 2020). Kappa's confidence interval was calculated using the percentile bootstrap ($n = 1000$). Paired t-tests were conducted on the C_q values recorded by three laboratories to reveal significant differences in the mean values. The resulting *p* values were adjusted according to Holm's method (Holm, 1979).

To further verify the precision of the pathotyping protocols, the IZSVE tested an additional panel of blind lyophilized samples ($n = 14$) (Supplementary Table S1 – sheet EQA) provided by the FLI, as part of the German external quality assessment (EQA) program. Agreement with the expected results was assessed by Cohen's kappa.

For both the reproducibility exercises, Sanger sequencing of the amplification products was not performed.

3. Results

3.1. Analytical performance

As part of the Stage 1 validation workflow set by the WOH (2022b), specificity, sensitivity and repeatability were determined for the RT-qPCR array developed in this study.

The assays proved to be specific, with no evidence of cross reaction against matrix components or non-target avian microorganisms. In contrast, all APMV-1 isolates of classes I and II representing genotypes 1, I, II, VI, VII, XIII, XIV, XVIII, XXI were detected and correctly pathotyped (Supplementary Table S1 – sheet ASp). A few class II isolates reacted both with SET A and SET B regardless of the assays target genotypes, but notably this did not lead to incorrect pathotyping. Being unavailable, additional genotypes could not be tested in this phase.

Analytical sensitivity was assessed for a variety of virulent or avirulent genotypes spiked in lung homogenates to mimic clinical samples, and all but one yielded a $\text{LOD} \leq 10^{2.83} \text{ EID}_{50}/100\mu\text{l}$ (Table 3). Efficiency and R^2 were within acceptable values (Bustin et al., 2009). All samples employed for analytical sensitivity were correctly pathotyped at any tested dilution. Overall, the LOD of the screening RT-qPCR run for comparison (Sutton et al., 2019) was lower by 1 log₁₀, except for the VG/GA vaccine strain that was detected with a higher sensitivity by SET A (data not shown). Expectedly, only strain APMV-1/chicken/California/18-016505-1/2018 yielded a LOD of $10^{4.62} \text{ EID}_{50}/100\mu\text{l}$. This sample represents genotype V.1 that is circulating almost exclusively in North and Latin America (Absalón et al., 2019) and shows 1 mismatch at the hybridization region of the forward primer of SET A. An *in silico* verification of the impact of this mismatch resulted in a sharp drop of the primer's melting temperature that most likely affected assay sensitivity.

All the replicates and repeats analyzed for repeatability assessment tested positive and yielded the correct pathotype. At the highest virus concentration, the overall %CV intra- and inter-assay was ≥ 3.2 and 4.9, respectively. Under challenging conditions (i.e., at the LOD), repeatability was slightly lower (%CV between 2.9 and 6.7), although pathotyping was neither impaired by probes' recognition nor by Sanger sequencing of the amplification product.

Table 3. Analytical sensitivity and repeatability of different APMV-1 genotypes spiked in lung homogenates. The LOD is expressed as $\text{EID}_{50}/100\mu\text{l}$. The amplification efficiency %*E* and the correlation coefficient are also reported. For each strain, intra- and inter-assay repeatability was expressed as percent coefficient of variation

of Cq values. Vir = velogenic and mesogenic APMV-1 with polybasic CS; Avir = lentogenic and low pathogenic APMV-1 with monobasic CS. n.a. = not available; * = vaccine strain.

Strain spiked in lung homogenate	Genotype	Set	LoD EID ₅₀ /100 µl	%E	R ²	%CV
APMV-1 Ulster*	I	A (Avir)	10 ^{1.5}	95.67	0.996	n.a.
APMV-1 V4 like*	I	A (Avir)	10 ^{1.5}	98.50	0.986	≤ 4.2
APMV-1 VG/GA*	I.1.1	A (Avir)	10 ^{1.83}	105.10	0.982	n.a.
APMV-1 B1*	II	A (Avir)	10 ^{1.5}	103.68	0.982	n.a.
APMV-1 LaSota*	II	A (Avir)	10 ^{2.83}	108.30	0.981	n.a.
APMV-1 Herts	IV	A (Vir)	10 ^{1.62}	95.24	0.889	≤ 4.4
APMV-1/chicken/California/18-016505-1/2018	V.1	A (Vir)	10 ^{4.62}	80.83	0.872	≤ 6.5
PPMV-1/pigeon/Italy/19vir8321/2019	VI.2.1.1.2.2	B (Vir)	10 ¹	100.60	0.892	≤ 6.7
APMV-1/bassette chicken/Belgium/4096/2018	VII	B (Vir)	10 ^{1.62}	108.41	0.972	n.a.
APMV-1/chicken/rus/Krasnodar/9.1/2019	VII.1.1	B (Vir)	10 ^{2.62}	92.81	0.996	n.a.
APMV-1/Macedonia/20VIR1984-1/2020	VII.2	B (Vir)	10 ^{1.5}	108.30	0.996	n.a.
APMV-1/chicken/Nigeria/4TACK15-18T_21RS744-46/2020	XIV.2	B (Vir)	10 ^{2.62}	80.15	0.960	n.a.
APMV-1/chicken/Camerun/3490-168/2008	XVII	B (Vir)	10 ^{2.83}	90.65	0.969	n.a.
PPMV-1/pigeon/Luxembourg/18175752/2018	XXI.1.1	B (Vir)	10 ^{2.62}	88.50	0.942	n.a.
APMV-1/avian/Bulgaria/11VIR1897/2011	1	C (Avir)	10 ^{1.7}	81.07	0.990	≤ 2.9

3.2. Assays application on clinical samples

All APMV-1 positive specimens collected from poultry and wild birds were detected with the RT-qPCRs array and correctly pathotyped (Table 4; Supplementary Table S1 – sheet DP). The samples represent genotypes I, II, VI, VII, XIII, XIV, XVIII and XXI from different countries in the European, Asian and African continents, thus confirming data previously obtained during analytical specificity assessment. Due to the lack of samples from the Americas and from Asian countries other than Jordan and Bangladesh, it was not possible to validate the RT-qPCR assays on the genotypes circulating in these areas. As observed during analytical validation, several samples cross reacted both with SET A and SET B while achieving correct pathotyping with both assays. A few cases showed high Cq values (≥ 40), although the assays led to correct virulent/avirulent discrimination by probes. The absence of a linear relationship with Cq values yielded by the screening protocol by Sutton et al., 2019 suggests that sensitivity of SET A and SET B appeared mostly strain-dependent and only in part determined by the viral load in the sample (Supplementary Table S1 – sheet DP). The amplification products of 8 samples out of 59 APMV-1 did not yield a clear sequence chromatogram. On the other hand, for 48 samples the CS sequence could also be obtained, further confirming the correct pathotype assignment by probes. Notably, 4 clinical samples of genotype VI that could not be directly pathotyped with the RT-PCR protocols developed by Kant et al., 1997 and De Battisti et al., 2013, were recognized by SET A and SET B (Supplementary Table S1 – sheet DP). Of these, 3 were successfully sequenced downstream the RT-qPCR.

No cross reaction was observed with APMV-1 negative samples, i.e., SPF chickens challenged with H9N2 or H7N1 as well as wild birds collected in Italy in 2022 (Supplementary Table S1 – sheet DP).

Table 4. Diagnostic performance of the RT-qPCRs array on APMV-1 positive samples. For each specimen, the type of matrix, the genotype and the reactivity with the different oligonucleotide sets are reported, with specification of the pathotype interpretation (Vir = velogenic and mesogenic APMV-1 with polybasic CS; Avir = lentogenic and low pathogenic APMV-1 with monobasic CS) according to the reactive probe. The CS sequence (aa 113-118) obtained from the RT-qPCR product is also reported, when available.

Sample	Source	Genotype	SET A	SET B	SET C	CS
APMV1_PPMV_pigeon_Sweden_SVA29_03_NGS46_2003	Intestine	VI	Vir	Vir	Neg	Not performed
APMV-1/dove/Italy/11VIR7110-9/2011	Intestine	VI	Vir	Vir	Neg	RRQKR*F
APMV-1/chicken/Bangladesh/11VIR1915-19/2011	Trachea	XIII	Neg	Vir	Neg	RRQKR*F
PPMV-1/pigeon/Italy/12VIR5499/2012	Stomach	VI.2.1.1.1	Vir	Vir	Neg	RRQKR*F
APMV-1/turkey/Italy/13VIR4184/2013	Trachea	I	Avir	Neg	Neg	Unsuccessful
APMV-1/chicken/Egypt/13VIR5009-21/2013	Lung/Trachea	II	Avir	Avir	Neg	GRQGR*L
PPMV-1/peacock/Italy/13VIR1895/2013	Organ	VI.2.1.1.2	Vir	Vir	Neg	RRQKR*F
APMV-1/chicken/Jordan/13VIR2720-2/2013	Organ	VII.1.1	Neg	Vir	Neg	RRQKR*F
APMV-1/chicken/Jordan/13VIR2720-4/2013	Organ	VII.1.1	Neg	Vir	Neg	RRQKR*F
APMV-1/chicken/Egypt/13VIR2962-116/2013	Trachea	VII.1.1	Neg	Vir	Neg	RRQKR*F
APMV-1/chicken/Ivory Coast/17RS804-26/2013	Organ	XVIII.2	Neg	Vir	Neg	RRQKR*F
PPMV-1/avian/Ethiopia/14VIR4296-4/2014	Intestine	VI.2.1.2	Neg	Vir	Neg	RRRKR*F
APMV-1/chicken/Italy/15VIR2663-3/2015	Lung	II	Avir	Neg	Neg	GRQGR*L
APMV-1/avian/Libya/15VIR5368/2015	FTA card	VII.2	Vir	Vir	Neg	RRQKR*F
APMV-1/avian/Libya/15VIR5371/2015	FTA card	VII.2	Neg	Vir	Neg	RRQKR*F
APMV-1/chicken/Nigeria/15VIR1737-3/2015	Organ	XIV.2	Neg	Vir	Neg	Unsuccessful
APMV-1/chicken/Nigeria/15VIR1737-4/2015	Organ	XIV.2	Neg	Vir	Neg	Unsuccessful
APMV-1/avian/Burkina Faso/15VIR2488-8/2015	Swab	XVIII	Neg	Vir	Neg	RRRKR*F
APMV-1/avian/Libya/15VIR5369/2015	Swab	XXI.1.1	Neg	Vir	Neg	KKRKR*F
APMV-1/turkey/Italy/16VIR3537/2016	Trachea	I.1	Avir	Neg	Neg	Unsuccessful
PPMV-1/pigeon/Italy/16VIR276-2/2016	Organ	VI.2.1.1.2	Vir	Vir	Neg	RRQKR*F
APMV-1/pigeon/Italy/16VIR1463-7/2016	Organ	VI	Neg	Vir	Neg	RRRKR*F
APMV-1/chicken/Sudan/16VIR4763-1/2016	Organ	VII.1.1	Neg	Vir	Neg	Unsuccessful
APMV-1/chicken/Sudan/16VIR4763-2/2016	Organ	VII.1.1	Neg	Vir	Neg	RRQKR*F
APMV-1/turkey/Italy/17VIR4141-1/2017	Trachea	I.1	Avir	Avir	Neg	GKQGR*L
APMV-1/turkey/Italy/17VIR7229-1/2017	Trachea	I.1	Avir	Avir	Neg	GKQGR*L
APMV-1/turkey/Italy/17VIR10741-2/2017	Trachea	I.1	Avir	Neg	Neg	GKQGR*L
APMV-1/turkey/Italy/17VIR10741-6/2017	Trachea	II	Avir	Neg	Neg	GKQGR*L
PPMV-1/pigeon/Italy/17VIR2719/2017	Organ	VI.2.1.1.2.2	Vir	Vir	Neg	RRQKR*F
PPMV-1/dove/Italy/17VIR7677-1/2017	Organ	VI.2.1.1.2.2	Vir	Vir	Neg	RRQKR*F
APMV-1/pigeon/Italy/17VIR7739/2017	Organ	VI	Neg	Vir	Neg	Unsuccessful
APMV-1/pigeon/Italy/17VIR8019/2017	Brain	VI	Vir	Vir	Neg	RRQKR*F
APMV-1/showeler/Italy/18VIR1199/2018	Organ	I.2	Avir	Neg	Neg	Unsuccessful
APMV-1/Eurasian teal/Italy/18VIR1279-1/2018	Organ	I.2	Avir	Neg	Neg	Unsuccessful
PPMV-1/pigeon/Italy/18VIR9029-1/2018	Cloacal swab	VI.2.1.1.2	Vir	Vir	Neg	RRRKR*F
PPMV-1/pigeon/Italy/18VIR1275/2018	Organ	VI.2.1.1.2.2	Neg	Vir	Neg	RRQKR*F
PPMV-1/pigeon/Italy/18VIR3373-1/2018	Cloacal swab	VI.2.1.1.2.2	Vir	Vir	Neg	RRQKR*F
PPMV-1/pigeon/Italy/18VIR3373-3/2018	Cloacal swab	VI.2.1.1.2.2	Vir	Vir	Neg	RRQKR*F
PPMV-1/pigeon/Italy/18VIR9028-1/2018	Cloacal swab	VI.2.1.1.2.2	Vir	Vir	Neg	RRRKR*F
PPMV-1/pigeon/Italy/18VIR9028-2/2018	Cloacal swab	VI.2.1.1.2.2	Vir	Vir	Neg	RRRKR*F
PPMV-1/pigeon/Italy/18VIR9028-3/2018	Cloacal swab	VI.2.1.1.2.2	Vir	Vir	Neg	RRRKR*F
APMV-1/pigeon/Italy/18VIR7466-1/2018	Brain	VI	Neg	Vir	Neg	RRQKR*F
APMV-1/pigeon/Italy/18VIR7466-2/2018	Intestine	VI	Vir	Vir	Neg	RRQKR*F
APMV-1/avian/Congo/18VIR3696-2/2018	Cloacal swab	XIII	Neg	Vir	Neg	RRQKR*F
APMV-1/dove/Italy/19VIR8422-3/2019	Organ	XXI.2	Vir	Vir	Neg	RRQKR*F
PPMV-1/pigeon/Italy/20VIR3033-1/2020	Trachea	VI.2.1.1.2.2	Neg	Vir	Neg	RRQKR*F
APMV-1/pigeon/Cyprus/20VIR3543-3/2020	Intestine	VI.2.1.1.2.2	Neg	Vir	Neg	RRQKR*F
PPMV-1/pigeon/Italy/20VIR7088/2020	Organ	VI.2.1.1.2.2	Vir	Vir	Neg	RRQKR*F
APMV-1/chicken/North Macedonia/20VIR1984-1/2020	Lung	VII.2	Neg	Vir	Neg	RRQKR*F
APMV-1/pigeon/Cyprus/20VIR3543-9/2020	Intestine	XXI.1.1	Vir	Neg	Neg	RRQKR*F
APMV-1/dove/Italy/20VIR7750-9/2020	Organ	XXI.2	Vir	Vir	Neg	RRQKR*F
APMV-1/chicken/Italy/21VIR407-17/2021	Intestine	I.1.1	Avir	Avir	Neg	GKQGR*L
APMV-1/chicken/Italy/21VIR2608-16/2021	Organ	I.1.1	Avir	Avir	Neg	GKQGR*L
PPMV-1/avian/Italy/21VIR138-1/2021	Brain	VI.2.1.1.2	Vir	Vir	Neg	RRQKR*F
PPMV-1/avian/Italy/21VIR750-1/2021	Organ	VI.2.1.1.2.2	Vir	Vir	Neg	RRQKR*F
PPMV-1/dove/Italy/21VIR72-1/2021	Lung	VI.2.1.2.2	Vir	Vir	Neg	RRQKR*F
APMV-1/pigeon/Italy/21VIR1109-8/2021	Intestine	VII	Avir	Vir	Neg	RRQKR*F/GKQGR*L
APMV-1_chicken_Sweden_SVA230302SZ0005_M-2023	Cloacal swab	I	Avir	Avir	Neg	Not performed
APMV-1_PPMV_Pigeon_Sweden_SVA1469	Intestine	VI	Neg	Vir	Neg	Not performed

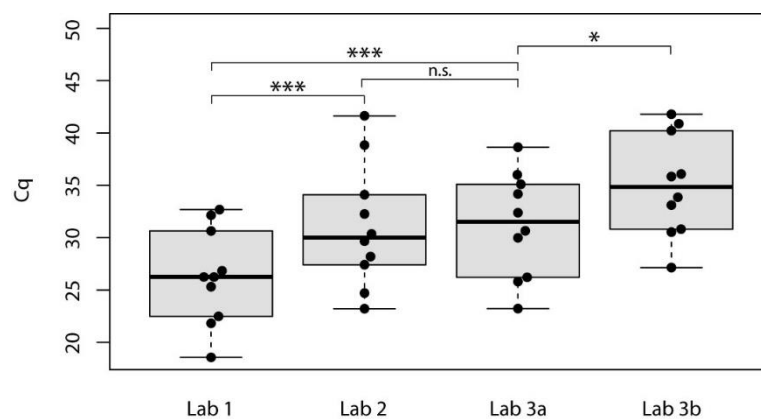
3.3. Reproducibility

The parallel testing of APMV-1 samples revealed an almost perfect agreement among laboratories (Fleiss kappa = 0.88; 95% CI: 0.64 - 1) (Nichols et al., 2010). Only one specimen was missed by Lab 2, while the

remaining samples were detected and correctly pathotyped by all participants. Notably, Cq values varied significantly between laboratories. In detail, Lab 1 showed Cq values systematically lower than Lab 2 and Lab 3 (with $p < 0.001$) (Figure 1; Supplementary Table S1 – sheet ILR). Lab 3 performed the exercise applying different ramp/rate during thermal cycling (i.e., 1.6 and 3.5°C/s). Four out of 11 (4/11) samples yielded Cq > 40 and irregular amplification curves with the highest ramp/rate. Decreasing the speed of temperature change down to 1.6°C/s resulted in an improved detection and lower Cq values.

All the samples included in the panel for the APMV-1 EQA program were detected and properly categorized as virulent or avirulent, yielding a Cohen’s kappa of 1.

Figure 1. Reproducibility study involving three different diagnostic laboratories (Lab1, Lab2, Lab3). Cq values are reported as dots along the y-axis. All laboratories employed the same batch of reagents and amplification conditions, while nucleic acids purification systems and real-time PCR instruments are reported in Supplementary Table S1 (sheet ILR) for each participant. Results obtained by Lab3 are reported for both the ramp/rates utilized: (a) = 1.6°C/s and (b) = 3.5°C/s. Asterisks indicate different levels of statistical significance of paired t-tests (***) = $p < 0.001$; * = $p < 0.05$; n.s. = not significant.



4. Discussion

For the initial assessment of APMV-1 pathotype, sequence determination of the cleavage site of the F protein gene is largely preferred over ICPI determination, as it reduces the use of live animals and costs, and shortens the time-to-results. However, this task is rather demanding for veterinary diagnosticians due the high genetic variability of APMV-1 that hampers effectiveness of existing molecular methods (Bhande et al., 2023; Sabra et al., 2017). Consequently, laboratories often decide to use multiple protocols to compensate for the lack of sensitivity and inclusivity of individual methods. In compliance with the WOAHA recommendations (WOAHA, 2021) this choice should carefully consider the genotypes that circulate locally, but also contemplate the possible introduction of viruses conveyed by wild birds. The constant threat for poultry species posed by *Columbiformes* as reservoirs of virulent PPMV-1 (Brown and Bevins, 2017; Hicks et al., 2019; Annaheim et al., 2022; Goraichuk et al., 2023) and the increasing number of ND outbreaks linked to the introduction of class II velogenic genotypes from wild birds (data source: <https://www.izsvenezie.com/reference->

[laboratories/avian-influenza-newcastle-disease/workshops/](#)) are issues of great concern, which would require the availability of widely inclusive molecular tools capable of distinguishing virulent and avirulent viruses with specificity.

The aim of this study was to develop and validate a reliable and widely inclusive array of RT-qPCRs for the determination of APMV-1 pathotype in clinical samples, in dual mode. Specific probes targeting the F gene CS and labeled with diverse dyes enable the discrimination of virulent and avirulent viruses. The size of the amplification product offers the chance to further confirm the pathotype assignment through Sanger sequencing and determination of the CS sequence. The design of the array consisting of one reaction for class I viruses, and two reactions for class II strains, allows the use of less degenerated oligonucleotides with higher affinity for the target region of different genotypes. However, mutations in primers and probes hybridization regions might result in a decrease of sensitivity, as demonstrated during LOD determination for strain APMV-1/chicken/California/18-016505-1/2018. Consistently with this observation, laboratory tests on clinical samples showed a certain variation in the biases of Cq values with respect to the screening RT-qPCR by Sutton et al., 2019, without however affecting the correct discrimination of virulent and avirulent viruses by pathotype-specific probes, even at high Cq. As a result, this prevented the identification of an unambiguous diagnostic cut-off value. Notably, the CS sequence was also determined for samples yielding high Cq values (i.e., 35 – 39). This is of great utility to confirm the pathotype for doubtful samples with a low viral load, and allows laboratories to perform pathotyping in dual mode or by RT-qPCR only, based on the equipment available at their facility and on the existing knowledge of the epidemiological situation and the reporting times required. As a matter of fact, remote areas where APMV-1 is endemic in poultry and domestic birds (Alexander et al., 2004) most often do not have sequencing facilities and could take advantage from this possibility. While leaving these considerations to end-users, the authors recommend Sanger sequencing of the array RT-qPCRs amplification products for samples with $Cq \geq 35$; in absence of CS determination, such samples should be considered not typeable. Contrarily, for specimens with lower Cq values, CS sequencing downstream RT-qPCR can be optional.

Another key feature of the array of RT-qPCRs developed in this study is the possibility to detect co-infections of virulent and avirulent viruses. Sample APMV-1/pigeon/Italy/21VIR1109-8/2021 well exemplifies this casuistry. As a matter of fact, the application of the RT-qPCR assays revealed the presence of both mesogenic and lentogenic strains in the intestine of a domestic pigeon. The same sample produced no amplification product with the RT-PCR by De Battisti et al., 2013, while it tested positive by Kant et al., 1997 yielding a CS sequence typical of virulent PPMV-1. Upon isolation and re-testing with the protocol by De Battisti et al., 2013, the sample was successfully amplified and typed as avirulent (vaccine strain of genotype I). Notably, the RT-qPCRs array applied to samples collected from SPF chickens subject to intracerebral inoculation, confirmed the co-presence of virulent and avirulent viruses. The deep investigation of this case highlights the potential of the RT-qPCRs array to detect co-infections in clinical samples without introducing biases. In contrast, APMV-1 pathotyping based on sequencing only, might yield inconsistent results with respect to ICPI, as the consensus sequence obtained rather frequently reflects the most abundant virus in the

sample (Naguib et al., 2022). In addition, the RT-qPCRs array represents an attractive opportunity as DIVA (Differentiating Infected from Vaccinate Animals) strategy to monitor the circulation of virulent APMV-1 in vaccinated animals. Such a principle was employed by Moharam et al., 2019 who succeeded in detecting virulent APMV-1 in vaccinated flocks farmed in Egypt under low biosecurity standards, through the application of assays targeting genotype VII-b and LaSota clone 30.

During the validation process, the reproducibility of the RT-qPCR assays and their transferability to other laboratories were also evaluated through a collaborative study. Although the three participants correctly pathotyped all the detected samples, the bias of Cq values recorded among laboratories was indeed striking. The exercise envisaged the use of diverse nucleic acids systems and PCR platforms. It can be assumed that the different ramp/rates applied during thermal cycling might have affected the kinetics of the reaction, as previously demonstrated by other authors (Derendinger et al., 2018). Indeed, the comparison of laboratory data obtained by Lab3 with different ramp/rates confirms this hypothesis. In addition to ramp/rate, other major changes are known to influence molecular assays performance (e.g., nucleic acids system, amplification kit, temperature and duration of amplification steps, magnesium concentration, etc.). Thus, upon modification of the protocol herein described, it is recommended to optimize amplification settings based on the reagents and instruments employed and to verify the protocol under each laboratory specific conditions.

In short, the array of RT-qPCRs proposed in this study proved to be fit for APMV-1 molecular pathotyping both in the isolates and clinical samples herein analyzed. An evaluation of the array performance would be required also for genotypes not included in the study, although primers and probes were designed to maximize their coverage. However, as repeatedly remarked, the high genetic variability of APMV-1 is a threat for the effectiveness of molecular tools employed either for screening or typing, and the newly developed array of RT-qPCRs is not exempt from this issue. For this reason, in order to exploit its best potential, we recommend making a periodic *in silico* re-assessment of its performance as new sequences become available; in addition, laboratories are required to evaluate its use based on the genotypes and variants circulating in the target population. Importantly, molecular pathotyping may not always be predictive of the real pathogenic power of APMV-1 and PPMV-1 in poultry, thus *in vivo* tests should not be completely dismissed.

Funding

This work was supported by the European Union within the framework of the activities foreseen by the EURL for AI/ND. The research was also partially funded by a grant from the European Commission (Development Cooperation Instruments) awarded to the project “EU Support to Livestock Disease Surveillance Knowledge Integration - LIDISKI” (FOOD/2019/410-957) within the frame of the Development of Smart Innovation through Research in Agriculture (DeSIRa) program and by the Italian Ministry of Health (Grant number RC IZSVe 05/2020).

Author Contributions: Conceptualization, I.M. and V.P.; data curation, A.F., V.V., A.B., M.G. and V.P.; formal analysis, A.F., S.Z., K.A., C.G., M.Cr., V.V., V.D. and A.B.; funding acquisition, I.M., M.Ce. and C.T.;

investigation, A.F., I.M., A.B., C.T. and V.P.; methodology, A.F., A.L., and V.P.; project administration, I.M., A.L. and V.P.; resources, S.Z., K.A., C.G, I.M., V.V., A.B., N.D.C.D.G. and C.T.; software, A.F., A.L., M.G. and V.P.; supervision, C.T. and V.P.; validation, A.F., S.Z., K.A., C.G., M.Cr., V.V., V.D., M.V. and A.B.; visualization, A.F. and V.P.; writing—original draft, A.F. and V.P.; writing—review and editing, all the authors; all authors have read and agreed to the published version of the manuscript.

Declaration of Competing Interest

The authors declare no conflict of interest.

Supplementary Materials: Table S1: Validation data (Analytical specificity (ASp); Diagnostic performance (DP); Inter-laboratory reproducibility (ILR); External quality assessment (EQA)).

Data Availability Statement: The data presented in this study are reported in the main text and Supplementary or available upon request.

Acknowledgments

The authors warmly thank state veterinarians from Italy and from collaborating countries for submitting clinical samples to ND diagnostic laboratories. The LIDISKI team members at the National Veterinary Research Institute (NVRI) of Vom (Nigeria) are well appreciated. Sabrina Marciano, Alessandra Drago, Silvia Ormelli, Silvia Maniero and Erika Quaranta provided technical support. Francesca Ellero assisted the authors with manuscript editing.

Appendix A. Newcastle Disease Collaborating Diagnostic Group

Amgad Abdelrahman, Nadim Amarin, Mustapha Bala Abubakar, Redeat Belayneh, Yapi Bokpè Cyprien, Vasiliki Christodoulou, Ilya Chvala, Aleksandar Dodovski, Seyed Ali Ghafouri, Mohammed Giasuddin, Magdy Hassan, Abdulwahab Kammon, Ismaila Shittu, Chantal J. Snoeck, Mieke Steensel, David Suarez, Mia Kim Torchetti, Serge Mpiana Tshipambe, Lamouni Habibata Ouermi Zerbo. Samples shared by the Newcastle Disease Collaborating Diagnostic Group were sent to the IZSVE before February 2022.

References

- Absalón, A.E., Cortés-Espinosa, D.V., Lucio, E., Miller, P.J., Afonso, C.L., 2019. Epidemiology, control, and prevention of Newcastle disease in endemic regions: Latin America. *Trop Anim Health Prod* 51, 1033–1048. <https://doi.org/10.1007/s11250-019-01843-z>
- Akhtar, S., Muneer, M.A., Muhammad, K., Tipu, M.Y., Rabbani, M., ul-Rahman, A., Shabbir, M.Z., 2016. Genetic characterization and phylogeny of pigeon paramyxovirus isolate (PPMV-1) from Pakistan. *SpringerPlus* 5, 1295. <https://doi.org/10.1186/s40064-016-2939-1>

Alexander, D.J., 2000. Newcastle disease and other avian paramyxoviruses. *Rev Sci Tech OIE* 19. <http://dx.doi.org/10.20506/rst.issue.19.2.14>

Alexander, D.J., Bell, J.G., Alders, R.G., 2004. Newcastle disease virology and epidemiology, in: *A Technology Review: Newcastle Disease*. Food and Agriculture Organization of the United Nations, Rome.

Annaheim, D., Vogler, B.R., Sigrist, B., Vöggtlin, A., Hüssy, D., Breitler, C., Hartnack, S., Grund, C., King, J., Wolfrum, N., Albini, S., 2022. Screening of healthy feral pigeons (*Columba livia domestica*) in the city of Zurich reveals continuous circulation of Pigeon Paramyxovirus-1 and a serious threat of transmission to domestic poultry. *Microorganisms* 10, 1656. <https://doi.org/10.3390/microorganisms10081656>

Barbezange, C., Jestin, V., 2003. Molecular characterisation of three avian paramyxovirus type 1 isolated from pigeons in France. *Virus Genes* 26, 175–183. <https://doi.org/10.1023/a:1023439530750>

Bhande, P., Sigrist, B., Balke, L., Albini, S., Wolfrum, N., 2023. Improvement of a real-time reverse transcription–polymerase chain reaction assay for the sensitive detection of the F gene of avian orthoavulavirus-1 (AOAV-1). *Vet Sci.* 10, 223. <https://doi.org/10.3390/vetsci10030223>

Bortolami, A., Mazzetto, E., Kangethe, R.T., Wijewardana, V., Barbato, M., Porfiri, L., Maniero, S., Mazzacan, E., Budai, J., Marciano, S., Panzarin, V., Terregino, C., Bonfante, F., Cattoli, G., 2022. Protective efficacy of H9N2 avian influenza vaccines inactivated by ionizing radiation methods administered by the parenteral or mucosal routes. *Front Vet Sci* 9, 916108. <https://doi.org/10.3389/fvets.2022.916108>

Brown, V.R., Bevins, S.N., 2017. A review of virulent Newcastle disease viruses in the United States and the role of wild birds in viral persistence and spread. *Vet Res* 48, 68. <https://doi.org/10.1186/s13567-017-0475-9>

Bustin, S.A., Benes, V., Garson, J.A., Hellemans, J., Huggett, J., Kubista, M., Mueller, R., Nolan, T., Pfaffl, M.W., Shipley, G.L., Vandesompele, J., Wittwer, C.T., 2009. The MIQE guidelines: minimum information for publication of quantitative real-time PCR experiments. *Clin Chem* 55, 611–622. <https://doi.org/10.1373/clinchem.2008.112797>

Commission Delegated Regulation (EU) 2020/689, 2019. Official Journal of the European Union.

De Battisti, C., Salomoni, A., Ormelli, S., Monne, I., Capua, I., Cattoli, G., 2013. Rapid pathotyping of Newcastle Disease Virus by pyrosequencing. *J Virol Meth* 188, 13–20. <https://doi.org/10.1016/j.jviromet.2012.11.021>

Derendinger, B., de Vos, M., Nathavitharana, R.R., Dolby, T., Simpson, J.A., van Helden, P.D., Warren, R.M., Theron, G., 2018. Widespread use of incorrect PCR ramp rate negatively impacts multidrug-resistant tuberculosis diagnosis (MTBDRplus). *Sci Rep* 8, 3206. <https://doi.org/10.1038/s41598-018-21458-y>

Dimitrov, K.M., Abolnik, C., Afonso, C.L., Albina, E., Bahl, J., Berg, M., Briand, F.-X., Brown, I.H., Choi, K.-S., Chvala, I., Diel, D.G., Durr, P.A., Ferreira, H.L., Fusaro, A., Gil, P., Goujgoulova, G.V., Grund, C., Hicks, J.T., Joannis, T.M., Torchetti, M.K., Kolosov, S., Lambrecht, B., Lewis, N.S., Liu, Haijin, Liu, Hualei, McCullough, S., Miller, P.J., Monne, I., Muller, C.P., Munir, M., Reischak, D., Sabra, M., Samal, S.K., Servan de Almeida, R., Shittu, I., Snoeck, C.J., Suarez, D.L., Van Borm, S., Wang, Z., Wong, F.Y.K., 2019. Updated

unified phylogenetic classification system and revised nomenclature for Newcastle disease virus. *Infect Genet Evol* 74, 103917. <https://doi.org/10.1016/j.meegid.2019.103917>

Dodovski, A., Cvetkovikj, I., Krstevski, K., Naletoski, I., Savić, V., 2017. Characterization and epidemiology of Pigeon Paramyxovirus Type-1 Viruses (PPMV-1) Isolated in Macedonia. *Avian Dis* 61, 146–152. <https://doi.org/10.1637/11517-101816-Reg.1>

Falotico, R., Quatto, P., 2015. Fleiss' kappa statistic without paradoxes. *Qual Quant* 49, 463–470. <https://doi.org/10.1007/s11135-014-0003-1>

Fuller, C.M., Collins, M.S., Alexander, D.J., 2009. Development of a real-time reverse-transcription PCR for the detection and simultaneous pathotyping of Newcastle disease virus isolates using a novel probe. *Arch Virol* 154, 929–937. <https://doi.org/10.1007/s00705-009-0391-z>

Goraichuk, I.V., Gerilovych, A., Bolotin, V., Solodiankin, O., Dimitrov, K.M., Rula, O., Muzyka, N., Mezinov, O., Stegnyy, B., Kolesnyk, O., Pantin-Jackwood, M.J., Miller, P.J., Afonso, C.L., Muzyka, D., 2023. Genetic diversity of Newcastle disease viruses circulating in wild and synanthropic birds in Ukraine between 2006 and 2015. *Front Vet Sci* 10. <https://doi.org/10.3389/fvets.2023.1026296>

He, Y., Taylor, T.L., Dimitrov, K.M., Butt, S.L., Stanton, J.B., Goraichuk, I.V., Fenton, H., Poulson, R., Zhang, J., Brown, C.C., Ip, H.S., Isidoro-Ayza, M., Afonso, C.L., 2018. Whole-genome sequencing of genotype VI Newcastle disease viruses from formalin-fixed paraffin-embedded tissues from wild pigeons reveals continuous evolution and previously unrecognized genetic diversity in the U.S. *Virol J* 15, 9. <https://doi.org/10.1186/s12985-017-0914-2>

Hicks, J.T., Dimitrov, K.M., Afonso, C.L., Ramey, A.M., Bahl, J., 2019. Global phylodynamic analysis of avian paramyxovirus-1 provides evidence of inter-host transmission and intercontinental spatial diffusion. *BMC Evol Biol* 19, 108. <https://doi.org/10.1186/s12862-019-1431-2>

Hoang, D.T., Chernomor, O., von Haeseler, A., Minh, B.Q., Vinh, L.S., 2018. UFBoot2: Improving the Ultrafast Bootstrap Approximation. *Mol Biol Evol* 35, 518–522. <https://doi.org/10.1093/molbev/msx281>

Holm, S., 1979. A Simple Sequentially Rejective Multiple Test Procedure. *Scandinavian Journal of Statistics* 6, 65–70.

Hoque, M.A., Burgess, G.W., Karo-Karo, D., Cheam, A.L., Skerratt, L.F., 2012. Monitoring of wild birds for Newcastle disease virus in north Queensland, Australia. *Prev Vet Med* 103, 49–62. <https://doi.org/10.1016/j.prevetmed.2011.08.013>

Hu, Z., He, X., Deng, J., Hu, J., Liu, X., 2022. Current situation and future direction of Newcastle disease vaccines. *Vet Res* 53, 99. <https://doi.org/10.1186/s13567-022-01118-w>

ICTV, 2017. International Committee on Taxonomy of Viruses. URL https://ictv.global/taxonomy/taxondetails?taxnode_id=202101591 (accessed 7.6.19).

ISO/IEC 17043:2010 Conformity assessment — General requirements for proficiency testing, 2010.

Jindal, N., Chander, Y., Chockalingam, A.K., de Abin, M., Redig, P.T., Goyal, S.M., 2009. Phylogenetic analysis of Newcastle disease viruses isolated from waterfowl in the upper midwest region of the United States. *Virol J* 6, 191. <https://doi.org/10.1186/1743-422X-6-191>

Kant, A., Koch, G., Van Roozelaar, D.J., Balk, F., Huurne, A.T., 1997. Differentiation of virulent and non-virulent strains of Newcastle disease virus within 24 hours by polymerase chain reaction. *Avian Pathol* 26, 837–849. <https://doi.org/10.1080/03079459708419257>

Katoh, K., Rozewicki, J., Yamada, K.D., 2019. MAFFT online service: multiple sequence alignment, interactive sequence choice and visualization. *Brief Bioinform* 20, 1160–1166. <https://doi.org/10.1093/bib/bbx108>

Kim, L.M., Afonso, C.L., Suarez, D.L., 2006. Effect of probe-site mismatches on detection of virulent Newcastle disease viruses using a fusion-gene real-time reverse transcription polymerase chain reaction test. *J Vet Diagn Invest* 18, 519–528. <https://doi.org/10.1177/104063870601800601>

Kuraku, S., Zmasek, C.M., Nishimura, O., Katoh, K., 2013. aLeaves facilitates on-demand exploration of metazoan gene family trees on MAFFT sequence alignment server with enhanced interactivity. *Nucleic Acids Res* 41, W22–W28. <https://doi.org/10.1093/nar/gkt389>

Mansour, S.M.G., ElBakrey, R.M., Mohamed, F.F., Hamouda, E.E., Abdallah, M.S., Elbestawy, A.R., Ismail, M.M., Abdien, H.M.F., Eid, A.A.M., 2021. Avian Paramyxovirus type 1 in Egypt: epidemiology, evolutionary perspective, and vaccine approach. *Front Vet Sci* 8, 647–462. <https://doi.org/10.3389/fvets.2021.647462>

Mayers, J., Mansfield, K.L., Brown, I.H., 2017. The role of vaccination in risk mitigation and control of Newcastle disease in poultry. *Vaccine* 35, 5974–5980. <https://doi.org/10.1016/j.vaccine.2017.09.008>

Mngumi, E.B., Mpenda, F.N., Buza, J., 2022. Epidemiology of Newcastle disease in poultry in Africa: systematic review and meta-analysis. *Trop Anim Health Prod* 54, 214. <https://doi.org/10.1007/s11250-022-03198-4>

Moharam, I., Razik, A.A. el, Sultan, H., Ghezlan, M., Meseko, C., Franzke, K., Harder, T., Beer, M., Grund, C., 2019. Investigation of suspected Newcastle disease (ND) outbreaks in Egypt uncovers a high virus velogenic ND virus burden in small-scale holdings and the presence of multiple pathogens. *Avian Pathol* 48, 406–415. <https://doi.org/10.1080/03079457.2019.1612852>

Naguib, M.M., Höper, D., Elkady, M.F., Afifi, M.A., Erfan, A., Abozeid, H.H., Hasan, W.M., Arafa, A.-S., Shahein, M., Beer, M., Harder, T.C., Grund, C., 2022. Comparison of genomic and antigenic properties of Newcastle Disease virus genotypes II, XXI and VII from Egypt do not point to antigenic drift as selection marker. *Transbound Emerg Dis* 69, 849–863. <https://doi.org/10.1111/tbed.14121>

Napp, S., Alba, A., Rocha, A.I., Sánchez, A., Rivas, R., Majó, N., Perarnau, M., Massot, C., Miguel, E.S., Soler, M., Busquets, N., 2017. Six-year surveillance of Newcastle disease virus in wild birds in north-eastern Spain (Catalonia). *Avian Pathol* 46, 59–67. <https://doi.org/10.1080/03079457.2016.1206177>

Nguyen, L.-T., Schmidt, H.A., von Haeseler, A., Minh, B.Q., 2015. IQ-TREE: A fast and effective stochastic algorithm for estimating maximum-likelihood phylogenies. *Mol Biol Evol* 32, 268–274. <https://doi.org/10.1093/molbev/msu300>

Nichols, T.R., Wisner, P.M., Cripe, G., Gulabchand, L., 2010. Putting the Kappa statistic to use. *Qual Assur J* 13, 57–61. <https://doi.org/10.1002/qaj.481>

- Nooruzzaman, M., Hossain, I., Begum, J.A., Moula, M., Khaled, S.A., Parvin, R., Chowdhury, E.H., Islam, M.R., Diel, D.G., Dimitrov, K.M., 2022. The first report of a virulent Newcastle Disease virus of genotype VII.2 causing outbreaks in chickens in Bangladesh. *Viruses* 14, 2627. <https://doi.org/10.3390/v14122627>
- Pickett, B.E., Greer, D.S., Zhang, Y., Stewart, L., Zhou, L., Sun, G., Gu, Z., Kumar, S., Zaremba, S., Larsen, C.N., Jen, W., Klem, E.B., Scheuermann, R.H., 2012. Virus pathogen database and analysis resource (ViPR): a comprehensive bioinformatics database and analysis resource for the coronavirus research community. *Viruses* 4, 3209–3226. <https://doi.org/10.3390/v4113209>
- Pritzer, E., Kuroda, K., Garten, W., Nagai, Y., Klenk, H.-D., 1990. A host range mutant of Newcastle disease virus with an altered cleavage site for proteolytic activation of the F protein. *Virus Res* 15, 237–242. [https://doi.org/10.1016/0168-1702\(90\)90031-6](https://doi.org/10.1016/0168-1702(90)90031-6)
- Quatto, P., Ripamonti, E., 2022. raters: A modification of Fleiss' Kappa in case of nominal and ordinal variables. R version 2.0.2 from CRAN. URL <https://rdr.io/cran/raters/> (accessed 6.9.23).
- R Core Team, 2020. R: A Language and Environment for Statistical Computing. R Foundation for Statistical Computing, Vienna, Austria. <https://www.r-project.org/>
- Ramey, A.M., Goraichuk, I.V., Hicks, J.T., Dimitrov, K.M., Poulson, R.L., Stallknecht, D.E., Bahl, J., Afonso, C.L., 2017. Assessment of contemporary genetic diversity and inter-taxa/inter-region exchange of avian paramyxovirus serotype 1 in wild birds sampled in North America. *Virology* 14, 43. <https://doi.org/10.1186/s12985-017-0714-8>
- Ramsubeik, S., Crossley, B., Jerry, C., Bland, M., Rejmanek, D., Shivaprasad, H.L., Stoute, S., 2023. Molecular and retrospective analysis of pigeon paramyxovirus type 1 infections in confinement-reared pigeons (*Columba livia*); 2010–2020. *J Appl Poult Res* 32, 100343. <https://doi.org/10.1016/j.japr.2023.100343>
- Rogers, K.H., Mete, A., Ip, H.S., Torchetti, M.K., Killian, M.L., Crossley, B., 2021. Emergence and molecular characterization of pigeon Paramyxovirus-1 in non-native Eurasian collared doves (*Streptopelia decaocto*) in California, USA. *Infect Genet Evol* 91, 104809. <https://doi.org/10.1016/j.meegid.2021.104809>
- Sabra, M., Dimitrov, K.M., Goraichuk, I.V., Wajid, A., Sharma, P., Williams-Coplin, D., Basharat, A., Rehmani, S.F., Muzyka, D.V., Miller, P.J., Afonso, C.L., 2017. Phylogenetic assessment reveals continuous evolution and circulation of pigeon-derived virulent avian avulaviruses 1 in Eastern Europe, Asia, and Africa. *BMC Vet Res* 13, 291. <https://doi.org/10.1186/s12917-017-1211-4>
- Snoeck, C.J., Adeyanju, A.T., Owoade, A.A., Couacy-Hymann, E., Alkali, B.R., Ottosson, U., Muller, C.P., 2013. Genetic diversity of Newcastle disease virus in wild birds and pigeons in West Africa. *Appl Environ Microbiol* 79, 7867–7874. <https://doi.org/10.1128/AEM.02716-13>
- Steensels, M., Van Borm, S., Mertens, I., Houdart, P., Rauw, F., Roupie, V., Snoeck, C.J., Bourg, M., Losch, S., Beerens, N., van den Berg, T., Lambrecht, B., 2021. Molecular and virological characterization of the first poultry outbreaks of Genotype VII.2 velogenic avian orthoavulavirus type 1 (NDV) in North-West Europe, BeNeLux, 2018. *Transbound Emerg Dis* 68, 2147–2160. <https://doi.org/10.1111/tbed.13863>

Suarez, D.L., Miller, P.J., Koch, G., Mundt, E., Rautenschlein, S., 2020. Newcastle Disease, other Avian Paramyxoviruses, and Avian Metapneumovirus infections, in: *Diseases of Poultry*. John Wiley & Sons, Ltd, pp. 109–166. <https://doi.org/10.1002/9781119371199.ch3>

Sun, J., Ai, H., Chen, L., Li, L., Shi, Q., Liu, T., Zhao, R., Zhang, C., Han, Z., Liu, S., 2022. Surveillance of class I Newcastle Disease virus at live bird markets in China and identification of variants with increased virulence and replication capacity. *J Virol* 96, e0024122. <https://doi.org/10.1128/jvi.00241-22>

Sutton, D.A., Allen, D.P., Fuller, C.M., Mayers, J., Mollett, B.C., Londt, B.Z., Reid, S.M., Mansfield, K.L., Brown, I.H., 2019. Development of an avian avulavirus 1 (AAvV-1) L-gene real-time RT-PCR assay using minor groove binding probes for application as a routine diagnostic tool. *J Virol Meth* 265, 9–14. <https://doi.org/10.1016/j.jviromet.2018.12.001>

Toyoda, T., Sakaguchi, T., Imai, K., Inocencio, N.M., Gotoh, B., Hamaguchi, M., Nagai, Y., 1987. Structural comparison of the cleavage-activation site of the fusion glycoprotein between virulent and avirulent strains of Newcastle disease virus. *Virology* 158, 242–247. [https://doi.org/10.1016/0042-6822\(87\)90261-3](https://doi.org/10.1016/0042-6822(87)90261-3)

Twabela, A.T., Nguyen, L.T., Masumu, J., Mpoyo, P., Mpiana, S., Sumbu, J., Okamatsu, M., Matsuno, K., Isoda, N., Zecchin, B., Monne, I., Sakoda, Y., 2021. A new variant among Newcastle Disease Viruses isolated in the Democratic Republic of the Congo in 2018 and 2019. *Viruses* 13, 151. <https://doi.org/10.3390/v13020151>

Wang, J., Yu, X., Zheng, D., Zhao, Y., Lv, Y., Shu, B., Jiang, W., Liu, S., Li, J., Hou, G., Peng, C., Wang, S., Yu, J., Li, Y., Liu, H., 2022. Continuous surveillance revealing a wide distribution of class I Newcastle disease viruses in China from 2011 to 2020. *PLoS One* 17, e0264936. <https://doi.org/10.1371/journal.pone.0264936>

Wise, M.G., Suarez, D.L., Seal, B.S., Pedersen, J.C., Senne, D.A., King, D.J., Kapczynski, D.R., Spackman, E., 2004. Development of a real-time reverse-transcription PCR for detection of Newcastle Disease Virus RNA in clinical samples. *J Clin Microbiol* 42, 329–338. <https://doi.org/10.1128/JCM.42.1.329-338.2004>

WOAH, 2021. Newcastle disease (infection with Newcastle disease virus) (version adopted in May 2021), in: *Manual of Diagnostic Tests and Vaccines for Terrestrial Animals 2022*.

WOAH, 2022a. Chapter 10.9. Infection with Newcastle disease virus, in: *Terrestrial Animal Health Code*.

WOAH, 2022b. Principles and methods of validation of diagnostic assays for infectious diseases (version adopted in May 2013), in: *Manual of Diagnostic Tests and Vaccines for Terrestrial Animals 2022*.

Zamperin, G., Bianco, A., Smith, J., Bortolami, A., Vervelde, L., Schivo, A., Fortin, A., Marciano, S., Panzarin, V., Mazzetto, E., Milani, A., Berhane, Y., Digard, P., Bonfante, F., Monne, I., 2021. Heterogeneity of early host response to infection with four low-pathogenic H7 viruses with a different evolutionary history in the field. *Viruses* 13, 2323. <https://doi.org/10.3390/v13112323>

Zhan, T., He, D., Lu, X., Liao, T., Wang, W., Chen, Q., Liu, Xiaowen, Gu, M., Wang, X., Hu, S., Liu, Xiufan, 2021. Biological characterization and evolutionary dynamics of Pigeon Paramyxovirus type 1 in China. *Front Vet Sci* 8. <https://doi.org/10.3389/fvets.2021.721102>

CHAPTER 6:

GENERAL CONCLUSIONS

The results of the studies presented in this paper offer promising solutions to the common challenges faced during the routine application of biotechnology-based diagnostic methods in the field of avian virology.

First Challenge: Non-optimal characterisation of a pathogen

In the first case, addressed in Chapter 3 of this research, the main challenge revolved around the constant monitoring of the performance of molecular diagnostic methods, particularly in the context of avian virology. The specific case concerned the failure to accurately detect certain Middle Eastern viruses belonging to the avian influenza (AI) subtype H9.

Through an *in silico* analysis of the haemagglutinin (HA) gene, the research team discovered a nucleotide mutation responsible for the virus' failure to detect it. This mutation hindered the correct binding of the probe used in the previously established method. In addition, the analysis revealed further mutations in the primer recognition sites, which could potentially decrease the efficiency of virus identification.

Solutions: Adaptation of Diagnostic Protocol

The main solution to the challenge of suboptimal pathogen characterisation was to adapt the existing characterisation protocol, originally implemented in 2008. This protocol, as it already existed, did not take into account all the new mutations identified through *in silico* analysis.

The feasibility of updating the oligonucleotide sequences was made possible by the characteristics of the avian influenza H9 subtype genome. A comprehensive comparison of all deposited sequences showed that the specific genomic region chosen in 2008 by Monne et al. (Monne et al., 2008) remained sufficiently conserved to accurately identify all currently circulating H9 subtypes.

Adaptation of the oligonucleotide sequences following alignment with the newly identified virus gene sequences significantly improved the accuracy and reliability of H9 subtype characterisation. This targeted adaptation addressed the ongoing challenge of rapidly evolving pathogens and ensured that diagnostic methods remained effective in the identification and characterisation of the H9 subtype of avian influenza.

Second challenge: selecting the most efficient protocol

The second chapter of this thesis (Chapter 4) addresses the diagnostic challenge of determining the most suitable protocol to characterise a highly prevalent virus with different vaccination schedules, exemplified by the case of infectious bronchitis virus (IBV). In this scenario, numerous protocols are available, mainly using conventional PCR followed by Sanger sequencing. These protocols target a highly variable region within the IBV genome, allowing discrimination between different strains. However, the variability of this target region poses a particular problem with regard to the affinity of the oligonucleotides used. This affinity depends on the degree of binding between the oligonucleotides and the target. Consequently, in the event of co-infection or the presence of a vaccine strain and a pathogenic strain, a given protocol can only identify the strain for which it has a higher affinity, even if it is present in the minority.

Solution: Protocol affinity monitoring

To address this challenge, a systematic screening approach was implemented to assess the different affinities of the primary protocols in use. The screening involved applying these protocols to samples of known reactivity, specifically designed to simulate co-infection scenarios in which two IBV strains coexist at different relative concentrations.

The results of this screening provided crucial insights into the different affinities exhibited by the various protocols. These newly acquired data, combined with knowledge of the vaccine protocols used and an understanding of the prevalence of circulating strains, allow diagnosticians to make informed choices on the most appropriate protocol for their specific goals. By reducing turnaround times and minimising the likelihood of unsuccessful characterisations, this approach streamlines the diagnostic process and increases its effectiveness in dealing with complex scenarios involving highly variable viral strains such as IBV.

Third challenge: Difficulties in pathotyping

Chapter 5 of this thesis delves into the third challenge, which concerns the intricate task of pathotyping, a challenge commonly encountered in the diagnosis of various pathogens. Focusing on the characterisation of Newcastle disease virus (NDV), this study reveals a multifaceted problem:

First, the existing literature lacks protocols that consistently maintain high performance for all existing NDV genotypes. Variability within NDV strains is a substantial

obstacle, as one-size-fits-all approaches are ineffective. Secondly, NDV is listed by the World Organisation for Animal Health (WOAH) due to its potential for serious consequences. Consequently, it is imperative to quickly identify highly virulent velogenic strains. This urgency leaves no room for time-consuming traditional testing procedures such as egg isolation or *in vivo* testing. Finally, the unpredictable nature of potential circulating strains further complicates the scenario. NDV, like many pathogens, can evolve, leading to new variants that may not be covered by existing diagnostic methods.

Solutions: Adoption of a new real-time PCR array

In response to these challenges, the research team devised a comprehensive solution. Recognising the marked variability of NDV, the search for a single universally effective method was deemed unattainable. Instead, the strategy pursued for NDV pathotyping involved the development of a new array.

This array was designed by integrating distinct sets of oligos, identified through a thorough *in silico* analysis of available NDV sequences. Unlike the single approach, this array allowed the use of multiple PCR reactions, each optimised for specific genotypes. This approach allowed a high level of sensitivity to be maintained without sacrificing inclusivity.

To meet the need for a rapid response, real-time PCR technology was adopted. Real-time PCR offered several advantages. In particular, it made possible to discriminate, by means of probes labelled with different fluorophores, between velogenic and lentogenic strains within the time frame of the PCR reaction itself, without the need for additional steps.

Moreover, the real-time PCR approach made the array a versatile analytical algorithm. Besides discriminating between pathotypes using labelled probes, it offered an option for further investigation. The fragment amplified during real-time PCR could be sequenced directly to confirm the pathotype through genetic analysis. Furthermore, this approach eliminated the need for an additional conventional PCR step, simplifying the pathotyping process.

This solution therefore not only addressed the challenge of pathotyping in the context of highly variable pathogens such as NDV, but also produced an alternative and adaptable analytical algorithm. This algorithm was able to flexibly adapt to different run-time requirements, further highlighting the importance of adaptability and innovation in the field of diagnostic algorithms.

Conclusion: The power of adaptability in diagnostic algorithms

The studies presented in this thesis underline a fundamental fact in the field of diagnostic algorithms: there is no universal, one-size-fits-all approach to solving challenges. The optimal strategy to address diagnostic challenges varies depending on a multitude of contextual factors. These factors include the changing epidemiological landscape, the unique characteristics of the viral pathogens at play, the state of current diagnostic capabilities, and more. In response to these dynamic boundary conditions, various optimisation techniques emerge as effective means to address the challenges, including introducing new methods, updating existing ones or rationalising the selection of methods from a plethora of possibilities.

Adaptability, exemplified by the different strategies and approaches presented in these studies, emerges as the most powerful tool in the arsenal of testing laboratories. It enables these laboratories to keep pace with the dynamic evolution of pathogens and ensures their ability to provide efficient and timely responses to emerging challenges. The ability to change and adapt diagnostic methods to specific circumstances is crucial in the field of virology and disease control.

However, this adaptability depends on a critical component: a robust, reliable and reproducible validation process. The validation process of methods is not just a formality, but it is the foundation on which adaptability is based. It ensures that diagnostic methods, whether newly developed or improved, retain their effectiveness and reliability.

In the context of the studies presented here, validation takes on even greater significance. Even seemingly minor modifications, such as adjustments to oligonucleotide sequences, can have far-reaching implications for the overall performance of the protocol. Therefore, a thorough validation process becomes indispensable to safeguard the flexibility and adaptability that are so crucial in the dynamic landscape of avian virology.

In summary, these studies emphasise the need for a multifaceted and context-aware approach to the design and optimisation of diagnostic algorithms. They highlight the central role of adaptability and emphasise that such adaptability can only flourish within a rigorous validation process. By embracing this holistic perspective, virologists and diagnosticians can better navigate the complex and ever-changing world of avian viruses, ensuring the continued effectiveness of their diagnostic methods.

CHAPTER 7:

REFERENCES

- Christopherson, C., Sninsky, J., Kwok, S., 1997. The effects of internal primer-template mismatches on RT-PCR: HIV-1 model studies. *Nucleic Acids Res* 25, 654–658. <https://doi.org/10.1093/nar/25.3.654>
- Crossley, B.M., Bai, J., Glaser, A., Maes, R., Porter, E., Killian, M.L., Clement, T., Toohey-Kurth, K., 2020. Guidelines for Sanger sequencing and molecular assay monitoring. *J Vet Diagn Invest* 32, 767–775. <https://doi.org/10.1177/1040638720905833>
- Dimitrov, K.M., Abolnik, C., Afonso, C.L., Albina, E., Bahl, J., Berg, M., Briand, F.-X., Brown, I.H., Choi, K.-S., Chvala, I., Diel, D.G., Durr, P.A., Ferreira, H.L., Fusaro, A., Gil, P., Goujgoulova, G.V., Grund, C., Hicks, J.T., Joannis, T.M., Torchetti, M.K., Kolosov, S., Lambrecht, B., Lewis, N.S., Liu, Haijin, Liu, Hualei, McCullough, S., Miller, P.J., Monne, I., Muller, C.P., Munir, M., Reischak, D., Sabra, M., Samal, S.K., Servan de Almeida, R., Shittu, I., Snoeck, C.J., Suarez, D.L., Van Borm, S., Wang, Z., Wong, F.Y.K., 2019. Updated unified phylogenetic classification system and revised nomenclature for Newcastle disease virus. *Infect Genet Evol* 74, 103917. <https://doi.org/10.1016/j.meegid.2019.103917>
- European Parliament. Directorate General for Parliamentary Research Services., 2019. The EU poultry meat and egg sector: main features, challenges and prospects : in depth analysis. Publications Office, LU.
- FAOSTAT, 2023. URL <https://www.fao.org/faostat/en/#data/FBS> (accessed 7.5.23).
- Gilbert, M., Xiao, X., Robinson, T.P., 2017. Intensifying poultry production systems and the emergence of avian influenza in China: a ‘One Health/Ecohealth’ epitome. *Archives of Public Health* 75, 48. <https://doi.org/10.1186/s13690-017-0218-4>
- Hochachka, W.M., Dhondt, A.A., 2000. Density-dependent decline of host abundance resulting from a new infectious disease. *Proceedings of the National Academy of Sciences* 97, 5303–5306. <https://doi.org/10.1073/pnas.080551197>

- Hoffmann, B., Beer, M., Reid, S.M., Mertens, P., Oura, C.A.L., van Rijn, P.A., Slomka, M.J., Banks, J., Brown, I.H., Alexander, D.J., King, D.P., 2009. A review of RT-PCR technologies used in veterinary virology and disease control: Sensitive and specific diagnosis of five livestock diseases notifiable to the World Organisation for Animal Health. *Vet Microbiol* 139, 1–23. <https://doi.org/10.1016/j.vetmic.2009.04.034>
- Houta, M.H., Hassan, K.E., El-Sawah, A.A., Elkady, M.F., Kilany, W.H., Ali, A., Abdel-Moneim, A.S., 2021. The emergence, evolution and spread of infectious bronchitis virus genotype GI-23. *Arch Virol* 166, 9–26. <https://doi.org/10.1007/s00705-020-04920-z>
- Kim, L.M., Afonso, C.L., Suarez, D.L., 2006. Effect of probe-site mismatches on detection of virulent Newcastle disease viruses using a fusion-gene real-time reverse transcription polymerase chain reaction test. *J Vet Diagn Invest* 18, 519–528. <https://doi.org/10.1177/104063870601800601>
- Kwok, S., Kellogg, D.E., McKinney, N., Spasic, D., Goda, L., Levenson, C., Sninsky, J.J., 1990. Effects of primer-template mismatches on the polymerase chain reaction: human immunodeficiency virus type 1 model studies. *Nucleic Acids Res* 18, 999–1005. <https://doi.org/10.1093/nar/18.4.999>
- Monne, I., Ormelli, S., Salviato, A., De Battisti, C., Bettini, F., Salomoni, A., Drago, A., Zecchin, B., Capua, I., Cattoli, G., 2008. Development and validation of a one-step real-time PCR assay for simultaneous detection of subtype H5, H7, and H9 avian influenza viruses. *J Clin Microbiol* 46, 1769–1773. <https://doi.org/10.1128/JCM.02204-07>
- OFFLU, 2022. Influenza A Cleavage Sites. URL <https://www.offlu.org/wp-content/uploads/2022/01/Influenza-A-Cleavage-Sites-Final-04-01-2022.pdf>
- Plowright, R.K., Parrish, C.R., McCallum, H., Hudson, P.J., Ko, A.I., Graham, A.L., Lloyd-Smith, J.O., 2017. Pathways to zoonotic spillover. *Nat Rev Microbiol* 15, 502–510. <https://doi.org/10.1038/nrmicro.2017.45>
- Rohaim, M.A., El Naggar, R.F., Helal, A.M., Hussein, H.A., Munir, M., 2017. Reverse spillover of avian viral vaccine strains from domesticated poultry to wild birds. *Vaccine* 35, 3523–3527. <https://doi.org/10.1016/j.vaccine.2017.05.033>

- Smith, S., Vigilant, L., Morin, P.A., 2002. The effects of sequence length and oligonucleotide mismatches on 5' exonuclease assay efficiency. *Nucleic Acids Res* 30, e111. <https://doi.org/10.1093/nar/gnf110>
- Valastro, V., Holmes, E.C., Britton, P., Fusaro, A., Jackwood, M.W., Cattoli, G., Monne, I., 2016. S1 gene-based phylogeny of infectious bronchitis virus: An attempt to harmonize virus classification. *Infect Genet Evol* 39, 349–364. <https://doi.org/10.1016/j.meegid.2016.02.015>
- Waters, D.L.E., Shapter, F.M., 2014. The Polymerase Chain Reaction (PCR): General Methods, in: Henry, R.J., Furtado, A. (Eds.), *Cereal Genomics: Methods and Protocols*, *Methods Mol Biol.* Humana Press, Totowa, NJ, pp. 65–75. https://doi.org/10.1007/978-1-62703-715-0_7
- WOAH, 2023a. Chapter 3.3.2. Avian infectious bronchitis, in: *Manual of Diagnostic Tests and Vaccines for Terrestrial Animals*, Twelfth Edition 2023.
- WOAH, 2023b. Management of veterinary diagnostic laboratories (version adopted in May 2021), in: *Manual of Diagnostic Tests and Vaccines for Terrestrial Animals* 2023.
- WOAH, 2021. Biotechnology advances in the diagnosis of infectious diseases (version adopted in May 2021), in: *Manual of Diagnostic Tests and Vaccines for Terrestrial Animals* 2022.
- WOAH, 2022a. Chapter 10.9. Infection with Newcastle disease virus, in: *Terrestrial Animal Health Code*.